

11-2011

Chromosome malorientation precedes nondisjunction during female meiosis I

Shane Gillies

DePaul University, SHANE_GILLIES@HOTMAIL.COM

Follow this and additional works at: <https://via.library.depaul.edu/etd>

Recommended Citation

Gillies, Shane, "Chromosome malorientation precedes nondisjunction during female meiosis I" (2011).
College of Liberal Arts & Social Sciences Theses and Dissertations. 105.
<https://via.library.depaul.edu/etd/105>

This Thesis is brought to you for free and open access by the College of Liberal Arts and Social Sciences at Digital Commons@DePaul. It has been accepted for inclusion in College of Liberal Arts & Social Sciences Theses and Dissertations by an authorized administrator of Digital Commons@DePaul. For more information, please contact digitalservices@depaul.edu.

Chromosome malorientation precedes nondisjunction during female Meiosis I

A Thesis

Presented in

Partial Fulfillment of the
Requirements for the Degree of
Master of Science

November, 2011

BY

Shane Gillies

Department of Biological Sciences

College of Science and Health

DePaul University

Chicago, Illinois

CONTENTS

ILLUSTRATIONS.....	v
ABBREVIATIONS.....	vii
ACKNOWLEDGMENTS.....	viii
ABSTRACT.....	x
I. INTRODUCTION.....	1
II. BACKGROUND AND SIGNIFICANCE.....	3
Meiosis.....	3
Aneuploidy.....	6
The Fly System.....	7
Chromosome Congression.....	9
Female Meiosis in <i>D. melanogaster</i>	10
Prometaphase & Metaphase I - The "New" versus the "Old".....	12
Do Congression Defects Cause MI Nondisjunction?.....	15
<i>monopolar spindles 1(mps1)</i> --- <i>altered disjunction (ald)</i>	16
III. STATEMENT OF HYPOTHESIS.....	22
IV. MATERIALS & METHODS.....	23
Fly Crosses and Nondisjunction Assay.....	23
Probes for <i>in situ</i> hybridization.....	26
Ovary dissection and fixation.....	27
Immunofluorescent, Fluorescent <i>in situ</i> hybridization, and confocal microscopy.....	27
DNA Isolation.....	29
Primers.....	30
Polymerase Chain Reaction and Gel Electrophoresis.....	30
DNA Sequencing.....	31
Western Blot Analysis.....	32
Statistical Analysis.....	33
Excision 14 - <i>ald</i> ^{P{GS:13084}-excision 14}	33

V.	RESULTS	35
VI.	DISCUSSION	51
VII.	APPENDIX A: Fly Crosses & Visible Markers	61
VIII.	APPENDIX B: Supplementary Data	67
IX.	APPENDIX C: Cytology Images	73
X.	APPENDIX D: Consensus DNA Sequences of P{GS:13084} Excisions	78
XI.	APPENDIX E: DNA Sequence Analyses of P{GS:13084} Excisions	83
XII.	APPENDIX F: Excision 14	90
XIII.	APPENDIX G: Raw Data	93
XIV.	REFERENCES	95

ILLUSTRATIONS

Figures

1.	Key events of meiosis	4
2.	Cohesion during meiosis.....	5
3.	Congression in mice oocytes	9
4.	Life cycle of <i>Drosophila melanogaster</i>	11
5.	Ovariole structure and stages of meiosis	12
6.	The Theurkauf and Hawley model of Metaphase I Arrest	13
7.	Models of chromosome movement and metaphase arrest	14
8.	Presence of Mps1 kinase activity.....	18
9.	Absence of Mps1 kinase activity	19
10.	Map of <i>ald</i> locus	20
11.	Components of the P{GS:13084} <i>ald</i> allele	20
12.	Genomic sequences used as probes for <i>in situ</i> hybridization	26
13.	Interaction of <i>nosGal4</i> and <i>UAS</i> of P{GS:13084}.....	34
14.	Preliminary X and 4 nondisjunction rate assay.....	36
15.	<i>ald</i> ¹ vs. <i>Df(3R)AN6</i> nondisjunction assays	39
16.	Cytological examination scenarios	40
17.	Correlation of genetic and cytological NDJ rates for the X chromosome	42
18.	Correlation of genetic and cytological NDJ rates for the 4 chromosome	43
19.	Polymerase Chain Reaction amplification of excision DNA	45
20.	Components of the P{GS:13084}-excision 14 <i>ald</i> allele	49
21.	DNA sequence analyses of P{GS:13084} excision lines	50

A1.	X chromosome progeny outcomes	63
A2.	Chromosome 4 progeny outcomes.....	64
B1.	Percent Heterologous Doubles.....	70
B2.	Percent Non-heterologous Doubles	71
C1.	Cytological coorientation of X and 4 chromosomes	73
C2.	Cytological X-only NDJ	74
C3.	Cytological 4-only NDJ	75
C4.	Cytological heterologous segregation double NDJ.....	76
C5.	Cytological non-heterologous double NDJ.....	77
F1.	Absence of the <i>mini-white</i> gene of the P{GS:13084} allele.....	90
F2.	P{GS:13084} 5' and 3' ends PCR amplification.....	91
F3.	Heat-shocked GFP analysis of Excision 14	92

Tables

1.	X chromosome genetic NDJ and cytological malorientation rates	37
2.	4 chromosome genetic NDJ and cytological malorientation rates.....	37
B1.	Preliminary nondisjunction assay of excision lines	67
B2.	Statistical significance between broods	68
B3.	Heterologous and Non-heterologous doubles	69
B4.	Percent Heterologous and Non-heterologous doubles.....	69
B5.	95% Confidence Intervals for genetic and cytological assays	72
G1.	Raw counts for preliminary <i>ald</i> ¹ cross	93
G2.	Raw counts for secondary <i>Df(3R)AN6</i> cross	94

ABBREVIATIONS

AD1 - *attached-X-Y, v f B; C(4)RM, ci ey^R* (tester stock with vermilion eye color, forked bristles, Bar eyes, interrupted wing veins and reduced eyes)

ALD - altered disjunction

APC/C - anaphase-promoting complex/cyclosome

BSA - Bovine Serum Albumin

DAPI - 4',6-Diamidino-2-Phenylindole

DPE - days post eclosion

EDTA - Ethylenediaminetetraacetic acid (ethylenediaminetetraacetate)

EtOH - Ethanol (Ethyl alcohol)

FISH - Fluorescence *in situ* hybridization

FM7 - First Multiple 7, X chromosome balancer

GFP - Green Fluorescent Protein

GVBD - germinal vesicle breakdown

IUMMNO-FISH - Immunofluorescence and Fluorescence *in situ* hybridization

KAc - Potassium acetate

MI - Meiosis I

MII - Meiosis II

MPS1 - monopolar spindles1

NaAc - Sodium acetate

NEB - nuclear envelope breakdown

NDJ - nondisjunction

PBS - Phosphate buffered saline

PBST - Phosphate buffered saline with Tween 20

PBST-NGS - Phosphate buffered saline with Tween 20 and Normal Goat Serum

SAC - spindle assembly checkpoint

SC - synaptonemal complex

SCCT - Saline sodium citrate with Tween 20

SDS - Sodium dodecyl sulfate

TBS - Tris-Buffered Saline

TE - Tris-EDTA

TM3 - Third Multiple 3, 3rd chromosome balancer

UAS - Upstream activation sequence

UTR - untranslated region

ACKNOWLEDGMENTS

The completion of this project was the culmination of dedication and hard work of many individuals. First and foremost, I would like to thank my thesis advisor, Dr. William Gilliland. I would like to thank him for his long-lasting patience and all the time that he spent answering the thousands of questions that I had for him. I would like to thank him for his guidance during this stressful process, from start to finish. I have learned so much from him. I am very honored to have had him as my advisor and mentor throughout my graduate career. Future grad students, as well as undergraduates, will benefit from his knowledge.

I would also like to thank the faculty in the Department of Biological Sciences at DePaul University. They have provided me with an excellent education, and they have always been available to answer any question to answer any questions that I might have had during my graduate work. In particular, I would like to thank Dr. Margaret Silliker and Dr. Jingjing Kipp for their assistance on this project as thesis committee members. Their knowledge, availability, and guidance throughout my thesis process has been admirable. A special thank you to Dr. Margaret Silliker for her guidance throughout the two years and to her patience for answering the hundreds of emails from me.

I would also like to thank both Dr. Phil Funk and Dr. Windsor Aguirre for the help with completion of my project. Their willingness to help and lend materials to my project has been highly appreciated. I would also like to thank Ms. Rima Barkauskas for her support along the way. It was truly a pleasure to work with Rima during my graduate career. Her support and willingness to listen to me vent my frustrations when research

was not going as smoothly as I wanted was a great comfort and much needed asset during my journey. She is a valuable benefit to the Biology Department at DePaul.

In addition, I would like to thank the undergraduates in the Gilliland lab for their help along this journey of mine. First of all, I would like to thank Maria Uhler, Khateriaa Pytrek, and Nneka Wallace for their help getting the project started with completing the preliminary nondisjunction assay crosses. A special thank you to Won Paik for all of his hard work with helping me to collect the secondary data. I applaud his hard work and dedication for helping me count thousands of fruit flies during the project. It has been a truly wonderful experience working with each and every one of the members of the lab.

Finally, I would like to thank Dr. Scott Hawley and the members of his lab at Stowers Institute for Medical Research (Kansas City, MO) for their help and advice along the way. It was very much appreciated that Dr. Hawley both provided the FISH probes and the funding for the DNA sequencing. This project could not have been completed without their valued support.

ABSTRACT

Meiosis is a specialized form of cellular division in which the gametes are formed. During female meiosis I, homologous chromosomes must coorient to opposite poles to ensure proper segregation, otherwise nondisjunction can occur which would form aneuploid gametes. The recent discovery that chromosomes do in fact congress prior to metaphase I arrest in *Drosophila* requires a reexamination of the mechanisms behind nondisjunction. To do this, a series of *altered disjunction (ald)* mutant alleles generated by imprecise excision of a P element in the 5' UTR were compared through a genetic nondisjunction assay and cytological examinations for the chromosomes' coorientation. These excision mutants have been shown to be competent to complete congression, but produce varying levels of wildtype Ald protein, which results in varying nondisjunction rates, ranging from wildtype to near-random segregation, all within an isogenic background. The hypothesis was that if nondisjunction is set up by congression errors that result in maloriented homologs at metaphase arrest, then the predicted outcome would be that the rates of genetic nondisjunction and malorientation should be equal. To test this hypothesis, the nondisjunction rates were measured genetically and the chromosomes' coorientation at metaphase I arrest was measured by scoring Immuno-FISH probed oocytes. The data showed high correlation between the genetic and cytological nondisjunction rates. The sequence analysis showed that various components of the P-element, P{GS:13084}, sequence were inserted into each line. Further research of meiosis I and mechanisms by which nondisjunction occurs could potentially provide a better understanding of many medical problems.

I. INTRODUCTION

Drosophila melanogaster has helped scientists to make great advances in the field of genetics and developmental biology. One of those advances has been to further define female meiosis and oogenesis using *Drosophila*. It was first thought, through the first fluorescent cytology of the chromosomes, that the achiasmate (nonexchange) chromosomes anti-congressed, or moved out onto the spindle from the main chromosome mass, and arrested until fertilization [1]. However, it was later shown that congression did occur in *Drosophila*, similar to other species, such as mice. Both achiasmate (nonexchange) and chiasmate (exchange) chromosomes, were shown to congress to the spindle mid zone where they arrest in a compact, "lemon"-shaped mass at metaphase I until activation, fertilization and completion of meiosis II [2]. This recent discovery invites the reexamination of some basic questions in the field, such as what are the mechanisms behind meiosis I nondisjunction.

To investigate this, a series of *altered disjunction (ald)* mutant alleles generated by imprecise excision of a P element in the 5' UTR were compared through a genetic nondisjunction assay and cytological examinations for the chromosomes' coorientation. The progeny were genetically analyzed to observe chromosome mis-segregation utilizing visible markers. Confocal microscopy and a novel combined approach of immunofluorescence and fluorescence *in situ* hybridization (FISH) was used to cytologically observe the chromosomes' mis-orientation within the "lemon." If the proposed mechanism for malformation of the lemon-shaped mass seen at metaphase arrest in *Drosophila melanogaster* resulting in meiosis I nondisjunction was correct, then there should be a correlation between the genetic and cytological measurements.

This hopeful discovery will potentially have medical applications. Just like in flies, chromosome missegregation occurs in humans, especially chromosome 21. Down syndrome, Turner syndrome, and the majority of miscarriages are a result of nondisjunction with the majority of events occurring in the female germline during meiosis I [3-4]. Therefore, the study of meiosis in *Drosophila* is an important model system for human health. Better understanding the mechanism of how the oocyte deals with constructing the chromosomes into a compact mass will potentially provide a better understanding of the underlying causes of errors that occur during female meiosis and result in aneuploid gametes.

III. BACKGROUND AND SIGNIFICANCE

Meiosis:

Meiosis is a specialized form of cellular division used in the formation of gametes. Meiosis can functionally differ between organisms. For example, animals use meiosis to form the gametes (egg and sperm), whereas in other organisms, like fungi and some plants, meiosis is used to form spores. The process begins with the DNA replicating itself in the premeiotic S phase (Figure 1), giving rise to sister chromatids that are held together by cohesins. The cell contains two copies of each homolog from each parent, or a total of four chromatids of each type of chromosome. Once DNA replication has taken place, the cell undergoes two rounds of division, Meiosis I (MI) and Meiosis II (MII). The end result of meiosis is the formation of four daughter cells that are both genetically unique from one another as well as the parental cells [5-7].

Mitosis and meiosis have similar stages; however, meiosis is unique in the fact that it segregates (or disjoins) not only sister chromatids, but also homologous chromosomes during the process. The homologous chromosomes segregate during the first meiotic division and the sister chromatids segregate during the second meiotic division, much like in mitosis [5]. The separation of the homologs makes meiosis I a very unique process.

Premeiotic	Meiosis I				Meiosis II					
S Phase	Prophase I		Prometaphase I	Metaphase I	Anaphase I		Prophase II	Prometaph. II	Metaphase II	Anaphase II
DNA Replication	Pairing & Recombination			Oocyte Arrests	Homologs Segregate		Sister Chromatids Segregate			
	Nuclear Envelope Breakdown	Spindle Assembly	Kinetochores Attachment	Homolog Coorientation	Chromosome Congression					

Figure 1: Key events of meiosis During premeiotic S phase, DNA replication occurs, creating the sister chromatids. During Prophase I, homologous chromosomes pair and recombine, establishing chiasmata that lock homologs together. Prophase I ends and prometaphase begins with nuclear envelope breakdown. In early prometaphase, the tubulin spindle forms, establishing kinetochores attachments and homolog coorientation. Cooriented chromosomes then congress to the metaphase plate, ending prometaphase I. Homologs then separate during Anaphase I, and then sister chromatids separate during Meiosis II. In some species (such as *Drosophila melanogaster*) the oocyte arrests at metaphase I to await fertilization, while other species may arrest at different stages (such as mice, which arrest at metaphase II). (Gilliland, 2010).

Accurate segregation of the homologous chromosomes during MI is dependent on three processes: homologous chromosomes must pair, that pairing must then be maintained by locking homologs together, and finally, homologs must segregate away from each other at anaphase I of MI [5]. Prophase I is a crucial step for the proper segregation of the homologous chromosomes, since in most organisms the linkages between homologs are formed during the process known as homologous recombination. During prophase, homolog pairing occurs, in which the two homologs for each chromosome pair through the interactions between complementary DNA sequences on the two homologs [8-10]. After the homologs pair, synapsis occurs when the homologs are joined tightly along their entire length at sites of recombination by a protein scaffold called the synaptonemal complex (SC). The homologs are physically linked to each other through chiasmata, which are the physical linkages created between homologous chromosomes established by recombination, which ensures that the homologs remain paired until the chiasmata are resolved at anaphase. Chiasmata are normally sufficient to ensure proper segregation during the first meiotic division [8, 10, 11].

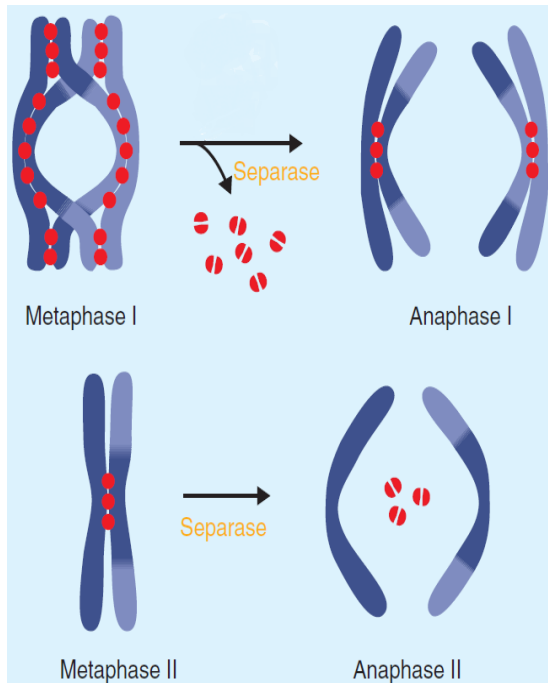


Figure 2. Cohesion during meiosis
 During meiosis, the breakdown of cohesins by separase allow the homologous chromosomes and sister chromatids to separate between the metaphase to anaphase transition [12].

After prophase I of meiosis I, the homologous chromosomes bi-orient themselves on the spindle through specialized mechanisms to make sure that the kinetochores of a sister-chromatid pair are attached to the same spindle pole and the homologs are attached to different poles [1, 6].

Cohesion keeps the chromosomes attached until the cohesin is dissolved by separase at the metaphase-to-anaphase transition.

The release of cohesion between the homologs and between the sister chromatids differ between MI and MII. During MI, the arm cohesin between the homologous chromosomes gets dissolved by separase, but the sister chromatids that comprise the homologs are still held together by centromere cohesin until MII (Figure 2). Shugoshin, or Mei-S322 in flies, is responsible for helping to maintain the centromeric cohesin between the sister chromatids. Through the interaction of multiple proteins, the proper segregation of the homologs during MI and the sister chromatids during MII can occur.

In order to proceed through meiosis, the sister chromatids must be under tension in order to segregate properly, and normally that tension is established by connection to

opposite spindle poles. The kinetochores sense the tension to ensure they are attached to both poles in order to segregate into four, genetically unique haploid daughter cells at the end of meiosis.

Aneuploidy:

Even though meiosis is a tightly regulated process, errors do occur during the creation of the gametes. These errors result in the chromosomes, whether it be the homologous chromosomes during meiosis I or sister chromatids during meiosis II, not segregating properly, a process called nondisjunction (NDJ). The resulting NDJ produces gametes with the incorrect number of chromosomes, known as aneuploid cells. This aneuploidy can either have minimal effects on the cell in which the organism can survive or it can cause irreversible defects and/or death [6, 7].

Nondisjunction occurs in most organisms, but is usually a rare occurrence. It is, however, more common in humans than other organisms. Aneuploidy is the main cause of birth defects as well as many other numerous human diseases, including Down syndrome, Turner syndrome, Klinefelter syndrome, and others. The meiotic NDJ rate in human males is only 1-2%, but the rate in females is approximately 20% [3, 4]. Nine out of 10 birth defects caused by NDJ occur in the female germline during meiosis I [4].

These meiotic nondisjunction events account for almost half of the miscarriages seen during the first trimester of pregnancy, since these aneuploid zygotes generally fail to survive. Sometimes, however, aneuploid zygotes actually give rise to viable, but partially defective, embryos [3]. For example, embryos with a third copy of chromosome 21 (trisomy 21) develop into offspring with Down syndrome, a condition associated with

mental retardation and altered physical appearance, and is the most common human birth defect. Indeed, studies of Down syndrome have found that the majority of the cases observed resulted from trisomy 21, with 88% of nondisjunction events coming from the female germline, according to the National Institute of Health [www.nichd.nih.gov]; thus, making the case for the studying of female meiotic nondisjunction a significant area of concern and future research [13].

The Fly System:

While in some systems, chiasmata are usually sufficient to ensure proper alignment and segregation during meiosis, in other systems chiasmata are not essential. One example of this phenomenon is in the fruit fly, *Drosophila melanogaster*. Chromosomes in *D. melanogaster* can either exchange, or chiasmate, or nonexchange, or achiasmate, during meiosis. The chiasmate chromosomes are those that exchange information by crossing over and forming chiasmata just like in the human model system, whereas the achiasmate chromosomes are those that do not cross over or form chiasmata [7, 14]. These achiasmate chromosomes are instead held together by heterochromatin threads until prometaphase, and yet they still segregate accurately even though they are not held together by chiasmata.

D. melanogaster is quite tolerant of nonexchange chromosomes. The X chromosomes spontaneously fail to recombine in approximately 6-10% of meioses, while the small 4 chromosomes never undergo meiotic recombination. This species also tolerates balancer chromosomes, which carry multiple rearrangements that prevent recombination with a normal sequence chromosome. In flies that are heterozygous for a

normal chromosome and a balancer, such as the *X* chromosome balancer *FM7*, 100% of meioses do not undergo meiotic recombination for the *X* [15]. This is beneficial for researchers, because it allows them to force these chromosomes to segregate by a different method of segregation, known as the distributive segregation system [7,16, 17].

The distributive segregation system is comprised of two fundamentally different systems: homologous achiasmate segregation and heterologous achiasmate segregation. Homologous achiasmate segregation depends on heterochromatic pairings ($X \leftrightarrow X \text{ Bal}$ or $4 \leftrightarrow 4$), whereas heterologous achiasmate segregation does not involve the physical association of segregational partners ($XX \leftrightarrow 44$) [17-19].

A number of mutants have been identified through mutant screens that specifically disrupt achiasmate segregation in *Drosophila*, while seemingly not impairing the segregation of exchange chromosomes. These mutants include *Axs*, *mtrm*, *nod*, *ald*, and others. [6, 7]. Some human homologs of these genes are known, and associated with disease phenotypes [14]. Other organisms, besides flies, have the ability to compensate and segregate achiasmate chromosomes; however, this system of segregation has only been studied at length in flies. For example, approximately 20% of human chromosome 21s are achiasmate, or do not undergo meiotic recombination, yet the rate of trisomy 21 for females under age 35 is only 1 in 2,500 births [4]. While it has not yet been demonstrated to be genuinely homologous to the *Drosophila* system, humans must have something analogous to a distributive segregation system as 20% of female meioses do not undergo recombination on chromosome 21, yet the rate of NDJ is much lower [13].

Chromosome Congression:

Most species have a step during mitosis and meiosis called congression. During congression, chromosomes are aligned at the spindle equator, prior to segregation of the chromosomes, with their centromeres oriented towards opposite spindle poles [20]. Poleward forces produced by kinetochores and the anti-poleward forces produced by the interactions between the tubulin spindle and chromosome arms balance and maintain this chromosome alignment during congression [21, 22]. In a study in mouse oocytes, increased rates of congression defects were found to correlate with subsequent meiotic NDJ which reinforces the importance of congression in studying how chromosomes segregate [25]. Studies have shown that congression occurs in most species, including mice (Figure 3) and *C. elegans* [23-25].

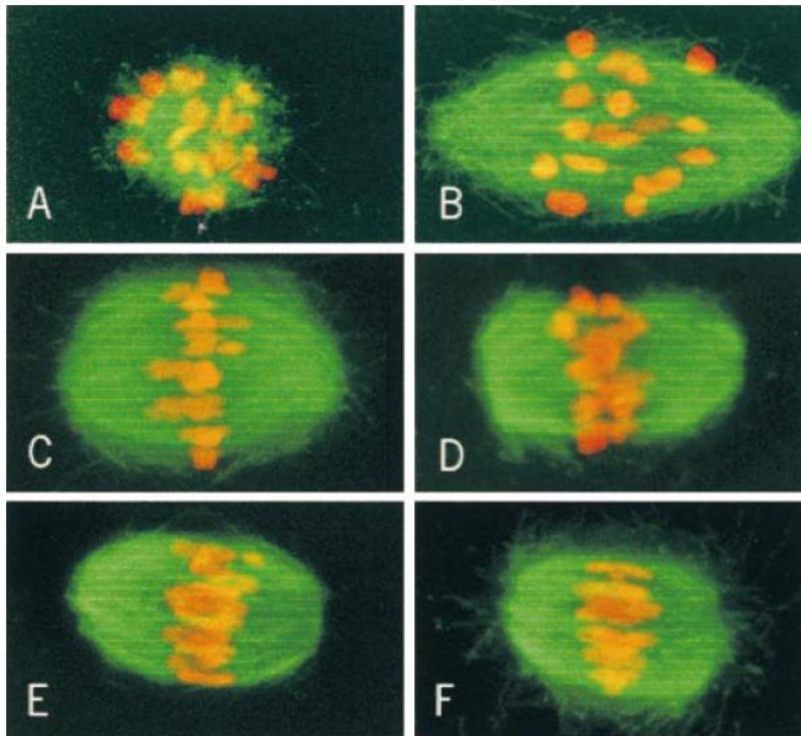


Figure 3.
Congression in mouse oocytes
Microtubules are seen in green and the chromosomes are in orange. A-F shows the progression of the chromosomes through meiosis from GVBD to the chromosomes congressing to the metaphase plate [23].

Through the multiple studies, genes have been identified that are required for congression and have been shown to be conserved among metazoans. These conserved genes, such as the Kinesin-8 family (Klp67a and Kip3 in flies and yeast, respectively), were recently demonstrated to cause mitotic congression defects [26, 29]. Most of the studies done have been in the budding yeast, *S. cerevisiae*, during mitosis and not meiosis [26-28].

Female Meiosis in *D. melanogaster*:

Drosophila melanogaster, the fruit fly, has proven to be a useful research model, especially in genetics and developmental biology. A few key traits which make this organism useful to scientists include a short generation time (Figure 4), large number of progeny, small number of chromosomes in the genome, and a well-annotated genome sequence. While these features would seem to make the fly ideal to study the process of congression, early cytological studies of female meiosis in this species suggested that congression did not take place [1]. Instead, the achiasmate chromosomes were thought to undergo a process of “anti-congression,” reaching metaphase arrest with the nonexchange chromosomes on opposite sides of the spindle. However, subsequent studies (described below) have shown that congression does in fact occur during female meiosis [30]. This means *D. melanogaster* can be used to study the process of congression. Furthermore, the revised model of prometaphase provides an opportunity to revisit basic questions about this process, such as what events are actually resulting in MI NDJ [29, 30].

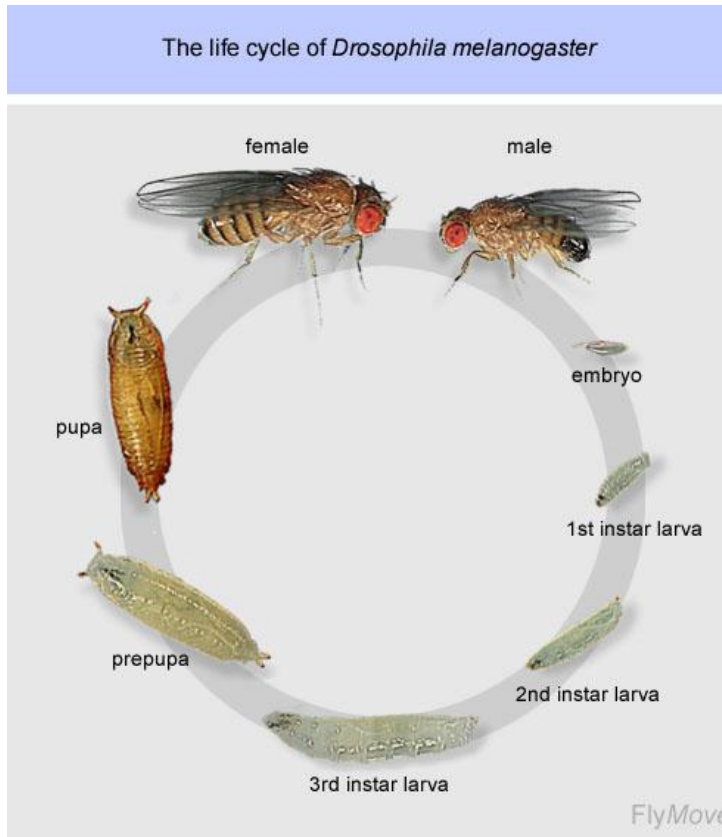


Figure 4. Life cycle of *Drosophila melanogaster*. A figure showing the life cycle of the *Drosophila melanogaster*. The cycle includes three instar larva stages, a pupa stage, and finally concludes with a mature fly. The life cycle takes approximately 10 days from egg to mature adult, depending on the temperature at which it is incubated. The optimal temperature for the generation time of 10 days is approximately 25°C. (http://flymove.uni-muenster.de/Genetics/Flies/LifeCycle/LifeCyclePict/life_cycle.jpg).

Oogenesis, the creation of the female egg, is a highly regulated process that is divided into 14 stages (as seen in Figure 5) based on developmental landmarks that correlate to the progression of the oocyte through the meiotic cell cycle [31, 32]. This makes it possible to identify oocytes in specific stages of the cell cycle based on gross morphology, although it is clear that meiotic mutants can modify this correlation [33, 34].

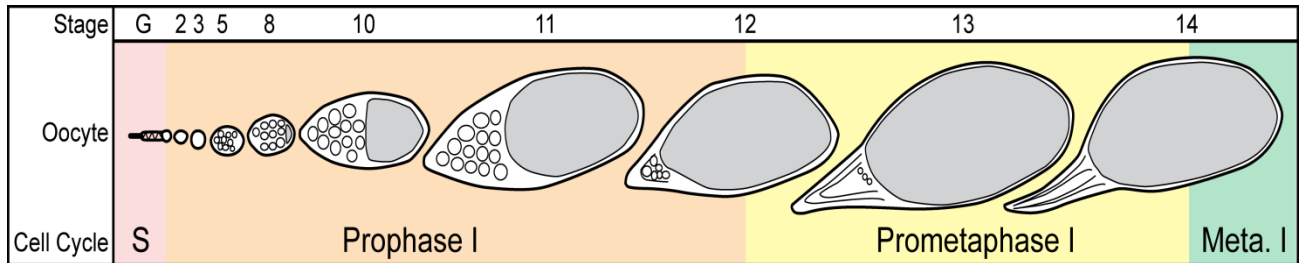


Figure 5: Ovariole structure and stages of oogenesis The ovariole is a string of developing cysts, divided into 14 stages (Stage; not all shown) based on oocyte morphology (Oocyte, gray), polytene nurse cells (white circles) and dorsal appendages (black lines). Stages correlate to progress through the meiotic cell cycle (Cell Cycle; colors), so Stage 12/13 is the transition from Prophase I to Prometaphase I, while Stage 14 oocytes are at Metaphase I arrest. This allows inference of cell cycle stage from morphology. Illustration adapted from [31].

A 16-cell cyst gives rise to the oocyte from one cell, with the remaining 15 cells becoming nurse cells [31]. During the early phases of oogenesis, DNA replication takes place. Along with DNA replication, the SC, the complex in which helps the chromosomes attach and separate, forms and recombination occurs between chiasmate chromosomes [1, 7, 11]. The nurse cells are very active during the middle stages of the process. They are producing the yolk, alongside the enlargement process of the oocyte. The follicle cells eventually produce the vitelline membrane and chorion. The oocyte progresses through additional stages, and starts to undergo germinal vesicle breakdown (GVBD), signaling stage 13 of oogenesis. The oocyte then enters prometaphase where the chromosomes congress to the metaphase plate. The meiotic spindle forms during this stage as well. Stage 14, with the dorsal appendages being fully formed, marks the end of oogenesis. The oocyte then arrests at metaphase I, until fertilization [30, 31, 36].

Prometaphase & Metaphase I - The "New" versus the "Old":

The beginning of prometaphase is earmarked by nuclear envelope breakdown (NEB). Theurkauf and Hawley (1992) showed that after NEB, microtubules nucleate

around the chromosomes and are soon bundled into a bipolar spindle. Once spindle formation is complete, the nonexchange chromosomes begin to separate from the main chromosome mass and move towards the spindle poles [1, 37, 38]. Using fixed images of the oocytes, Theurkauf and Hawley developed a model in which *D. melanogaster* female meiosis was thought to undergo a form of "anti-congression" where the exchange chromosomes stayed at the metaphase plate while the nonexchange chromosomes were in a balanced configuration on opposite sides of the spindle (Figures 6 and 7A) [1, 37-40].

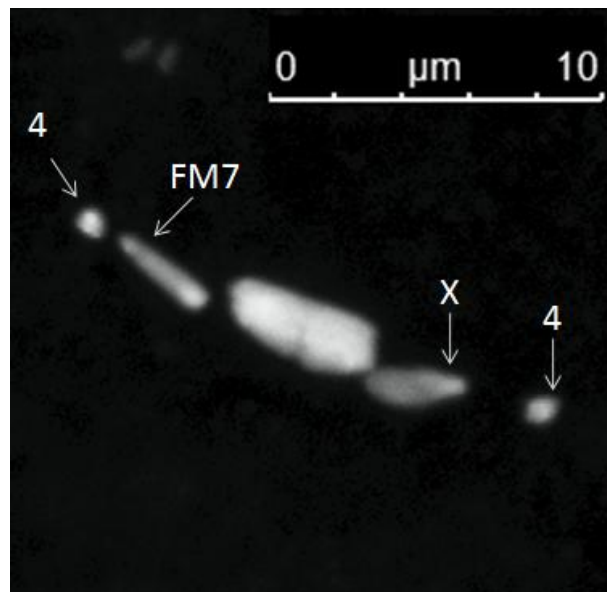


Figure 6. The Theurkauf and Hawley model of Metaphase I Arrest A confocal microscopic image representing the previously accepted model of metaphase I arrest proposed by that of Theurkauf and Hawley in 1992. The nonexchange chromosomes have moved out towards the spindle poles in a size dependent manner in which the small 4 chromosomes closer to the poles and the normal X and FM7 balancer chromosomes are in between the 4 chromosomes and the main chromosome mass containing the 2nd and 3rd chromosomes.

From this model, the explanation of how nonexchange chromosomes segregated was that they were believed to enter prometaphase physically paired and then moved directly to opposite sides of the spindle to arrest at metaphase. This model also predicted that

nondisjunction would result if both chromosomes moved onto the same arm of the spindle [1].

The Theurkauf and Hawley model was widely accepted until Gilliland, *et al.* (2009) overturned this model and proposed a new model. Their experiment examined fixed metaphase-arrested oocytes, looking for the nonexchange chromosomes out on the spindle as what was proposed by the fixed images of the previous model. To ensure that they were observing the correct stage, virgin females, without access to males, were aged for four days post eclosion (dpe). As virgin females hold their eggs for several days, this was predicted to enrich for eggs that are arrested at metaphase I awaiting fertilization to complete meiosis. However, when the mature oocytes were examined, they discovered almost no oocytes with chromosomes out on the spindle like in Figure 6. Instead, all of the chromosomes, both nonexchange and exchange, were condensed into a consistent "lemon" shaped configuration (Figure 7B, Stage 14). This configuration had been seen before, but those oocytes had been thought to be in early prometaphase, before the chromosomes had actually started to move out on the spindle [30].

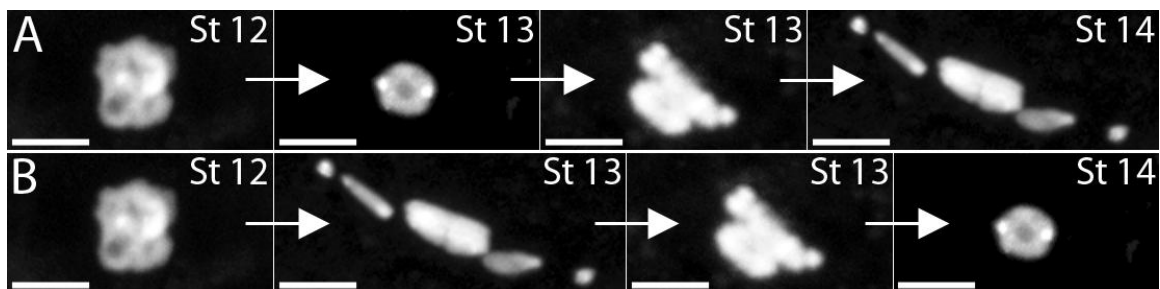


Figure 7: Models of chromosome movement and metaphase arrest. (A) The “anti-congression” model of prometaphase proposed in 1992 predicted that during prometaphase (Stage 13) the nonexchange chromosomes move out onto the spindle, and reach metaphase arrest (Stage 14) with the nonexchange chromosomes in a balanced configuration near the poles. (B) The new model of metaphase arrest shows that the balanced configuration actually occurs as part of prometaphase, and the nonexchange chromosomes subsequently congress into a single “lemon” shaped mass at metaphase arrest. (DAPI; Bars = 5 μ m) [30].

Through a series of experiments that showed the age of the females is correlated with the number of oocytes in a single DNA mass and that those oocytes with the longest dorsal appendages (gill-like structures, used as a breathing apparatus that begin to grow from the oocyte at NEB) also contain single DNA masses, Gilliland and his colleagues showed that the balanced configuration with the nonexchange chromosomes out on the spindle (Figure 6) was actually the midpoint of prometaphase. These chromosomes then subsequently congress back to the metaphase plate to rejoin the main chromosome mass (Figure 7B, Stage 14) [30].

Do Congression Defects Cause MI Nondisjunction?

With the old model of metaphase arrest, it was thought that pairing of nonexchange homologs was established during prophase I. The nonexchange homologs then simply moved out onto opposite spindle poles, and then to the closest pole at Anaphase I. Under this model, NDJ was caused when the homologs erroneously moved onto the same side of the spindle [1]. The cytological effects of meiotic mutants were interpreted under this framework, and it was assumed that NDJ was due to the fact that chromosomes were not properly coorientated, as well as not having time to adjust, before they had to segregate to opposite poles.

However, through recent experiments, there have been important revisions to the understanding of the prometaphase to metaphase I arrest transition [2, 41]. Until recently, chiasmata were considered to be the sole mechanism by which chromosomes were held together to ensure proper segregation. On the other hand, nonexchange chromosomes

were thought to not be physically associated with each other once they moved to opposite poles. However, nonexchange chromosomes were found to be reassociating themselves with their achiasmate homolog. Heterochromatin threads help to reestablish these associations during prometaphase [41]. Instead of simply moving directly towards the nearest spindle pole during mid-prometaphase, achiasmate homologs undergo cycles of detachment and reattachment until stable coorientation can be properly achieved. The observation that achiasmate homologs that are on the same side of the spindle can cross the metaphase plate and reorient themselves has prompted a reexamination of basic ideas of how this process occurs [41]. Along with this observation, the finding that congression of the nonexchange chromosomes to rejoin the main chromosome mass to form this compact, "lemon"-shaped mass invalidates the mechanism of nondisjunction proposed for the Theurkauf and Hawley model of metaphase I arrest [30].

This leads to the question: what is the mechanistic basis of meiosis I nondisjunction under the new model?

monopolar spindles 1 (mps1)/ altered disjunction (ald):

The *altered disjunction (ald)* locus was first discovered in a screen for mutants causing NDJ in female flies [42] and encodes the fly homolog of the widely-conserved spindle checkpoint gene, *mps1* [43, 44]. Mps1 is a multifunctional kinase involved in chromosome orientation, monitoring of kinetochore-spindle attachments and the response to hypoxia, and is present in most organisms, with the notable exception of the nematode, *C. elegans* [45-47]. Mps1 is a key component of the mitotic and meiotic spindle assembly checkpoint (SAC) in which it ensures the proper alignment of kinetochores on the spindle

to prevent precocious entry into anaphase until the chromosomes are under proper tension [48].

Acting in one step of a signaling cascade, when the chromosomes are not under proper tension, the Mps1 activates BubR1 and Mad2 to inhibit the activity of Cdc20 and the anaphase-promoting complex/cyclosome (APC/C). With the APC inhibited, separase cannot be activated to cleave the cohesins holding sister chromatids together, which prevents them from disjoining from one another and proceeding into anaphase I (Figure 8). On the other hand, without Mps1 kinase activity, the SAC cannot be activated in the presence of misaligned chromosomes. Therefore, the APC/C can then degrade Securin, allowing Separase to cleave Cohesin [46]. This ultimately allows the homologs to bypass normal arrest and enter anaphase I, even if the chromosomes are not properly aligned, or cooriented, on the spindle. This can result in chromosomes segregating prior to establishing proper coorientation, which results in aneuploid gametes (Figure 9) [7, 10, 42].

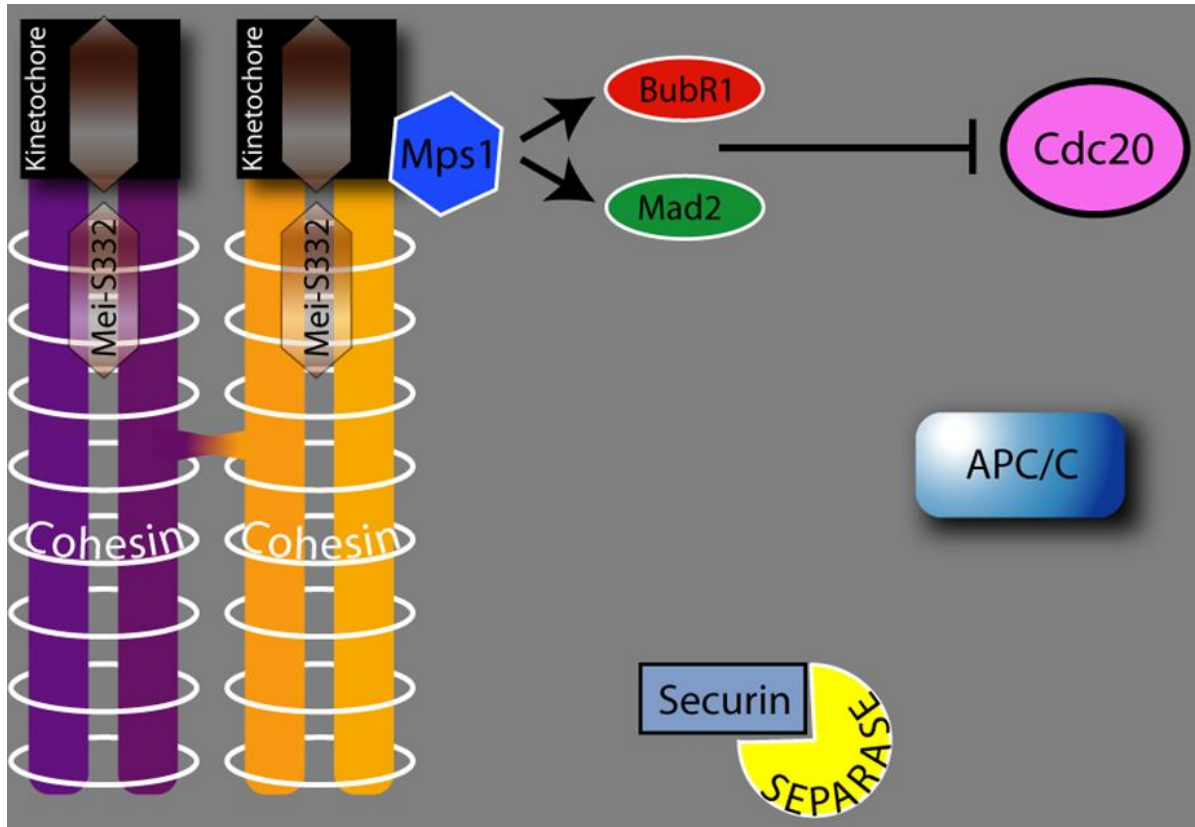


Figure 8. Presence of Mps1 kinase activity A systematic representation of the Mps1 signaling cascade when Mps1 is present. When Mps1 functions normally, it can activate BubR1 and Mad2 when the homologs and sister chromatids are not under proper tension. BubR1 and Mad2 act together to inhibit the activity of the anaphase-promoting complex, which prevents the cleavage of Securin from the Securin/Separase complex. As Separase inhibits Securin, the Cohesin holding the sister chromatids protected and the chromosomes cannot enter anaphase I. Illustration adapted from [10] (Gilliland).

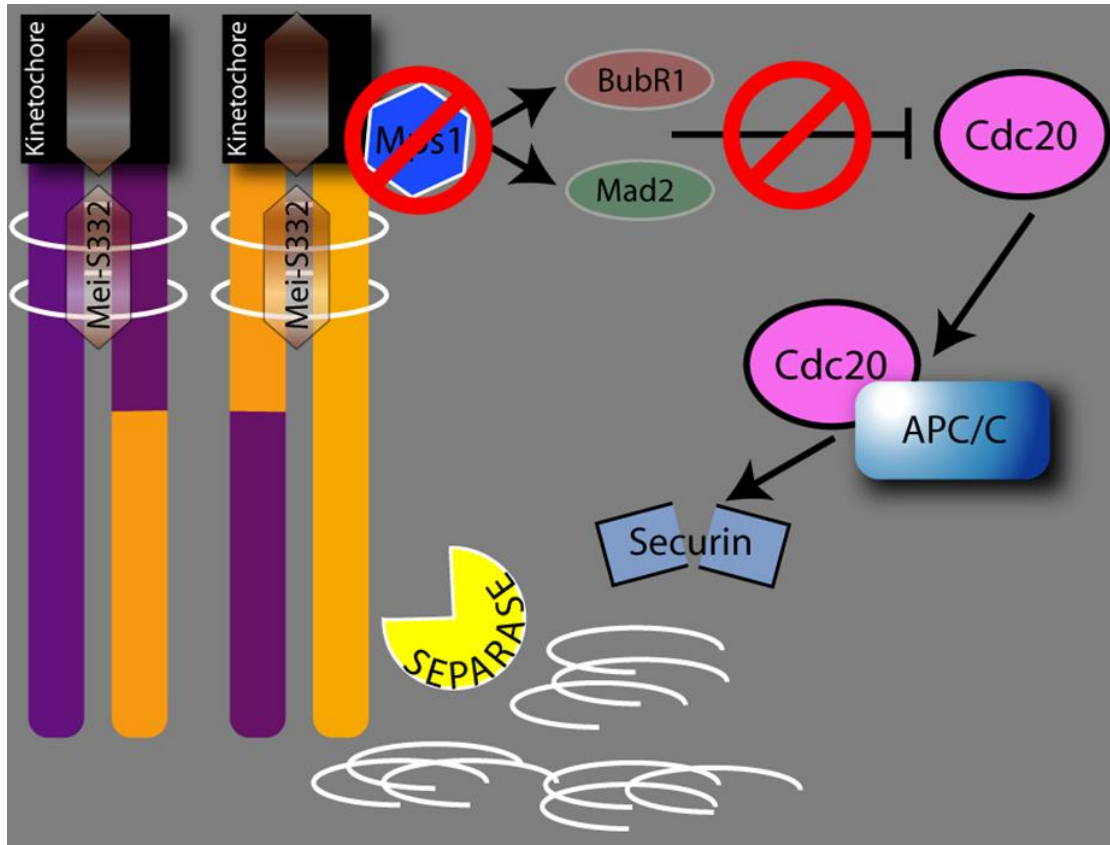


Figure 9. Absence of Mps1 kinase activity A systematic representation of the Mps1 signaling cascade when Mps1 is absent. When Mps1's function is absent, it cannot activate BubR1 and Mad2. BubR1 and Mad2 cannot then inhibit the activity of the complex of Cdc20 and APC/C, which releases Separase from the Securin/Separase complex. Separase then cleaves the Cohesin holding sister chromatids together, allowing the nuclei to bypass normal arrest and enter anaphase I, even without proper homolog coorientation. Illustration adapted from [10] (Gilliland).

Different *ald* alleles are available, ranging from point mutants to deletions, providing different characteristic NDJ rates in female meiosis from these mutants [2, 48]. The complete knockout of this gene is semi-lethal, but even a small amount of wildtype function is sufficient for full viability [2, 43, 48]. The *ald* gene has a low threshold of viability; however, the gene dosage needed for normal meiotic segregation is much higher. A single wildtype dose is sufficient to achieve wildtype NDJ rates, but if the dosage of the gene is reduced, an increase in the amount of NDJ occurring can be seen during female meiosis. The *ald* gene can cause increased levels of nonexchange

chromosomal nondisjunction, while not affecting exchange chromosomes to the same extent, since the nonexchange chromosomes are more sensitive to loss of *ald* function [7].

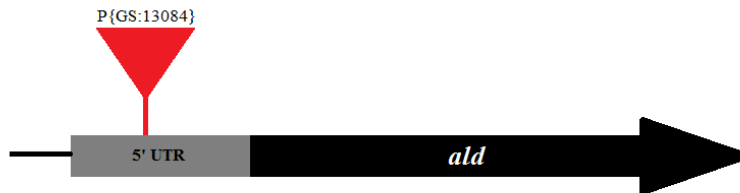


Figure 10. Map of *ald* locus

A representation of the *ald* gene locus. The transcript of the *ald* gene is preceded by a 5' UTR (untranslated region) in which the P-element (P{GS:13084}) is inserted after the 14th nucleotide. Illustration adapted from [2, 48].

One allele, *ald*^{P{GS:13084}}, is caused by a P element inserted after the 14th nucleotide in the 5'UTR (untranslated region) of the transcript (Figure 10). This allele was created in a genome-wide overexpression screen [49] and has an outward-facing *Hsp70Bb* core promoter in line with the *ald* protein coding sequence (Figure 11). A small amount of wildtype Ald protein can be produced from this promoter, even in the absence of heat shock, due to leaky transcription [2].



Figure 11. Components of the P{GS:13084} *ald* allele A systematic representation of the various components that compromise the 6.83 kb P-element, P{GS:13084}, that is inserted after the 14 nucleotide of the 5' UTR of the *ald* gene. The P-element has an outward facing heat shock promoter, *Hsp70Bb*, as well as another *Hsp70Bb*, upstream of the Green Fluorescent Protein (*GFP*). The *GFP* is under the control of the *Hsp70Bb* region of the gene. Within the P-element, the *mini-white* gene, if present, gives the flies peach color eyes. Finally, the P-element is flanked by a 5' and 3' region on either end (not shown), which is flanked by endogenous *ald* 5' UTR.

An allelic series was generated from this source chromosome by imprecise P element excision. These alleles range from precise excisions with wildtype levels of NDJ to hypomorphic alleles with intermediate levels of NDJ to semi-lethal alleles that appear to have no remaining *ald* function [48]. These mutant alleles are dosage-dependent alleles, which change the amount of protein produced; however, the protein produced appears to be wildtype. Using an allelic series like this avoids having different genetic background being present in an experiment. In previous experiments comparing both *ald*^{P{GS:13084}-excision25} and *ald*^{P{GS:13084}-excision23} using a Western Blot, the strongly hypomorphic allele (excision 23) showed a greatly reduced amount of protein as compared to a precise excision allele (excision 25). However in both cases, the protein produced seemed to be wildtype [2]. This minimizes the risk of allele-specific effects associated with protein variants.

These *ald* mutants have a wide range of NDJ rates, but are still competent to complete congression. Segregation in *FM7/yw; ald^l/Df(3R)AN6* hemizygous females is quite compromised, with ~39% X and ~28% 4 NDJ [30]. However, in 4 dpe aged virgin females of this genotype, 47 out of 50 oocytes (94%) had their chromosomes in a single DNA mass, a rate similar to wildtype oocytes at the same age, which had 149/164 (91%) of their oocytes with a single DNA mass. Similar results were obtained for, the previously characterized, *ald*^{P{GS:13084}Δ23} allele, which demonstrates these *ald* mutants are competent of carrying out congression. The fact that this allelic series was created from a single source chromosome allows the experiment to be done in a single genetic background and eliminates the possibility of protein variants. These mutants are suitable to study their effects on female meiosis by comparing them genetically and cytologically.

III. STATEMENT OF HYPOTHESIS

Given that mutant alleles are nondisjoining despite completing congression, one hypothesis is that the chromosome mis-segregation seen during meiosis I is the result of the homologous chromosomes being incorrectly cooriented when they congress to form the compact lemon-shaped mass.

This hypothesis predicts that if the "lemon" is being formed with maloriented chromosomes, and this orientation defect is causing nondisjunction, then the genetic nondisjunction rate should be equal to the cytological malorientation rate.

IV. MATERIALS AND METHODS

Fly Crosses and Nondisjunction Assay:

A series of fly crosses using different excisions of the P-element allele $ald^{P[GS:13084]}$, were done to test progeny of the various alleles of the *ald* gene. These excisions were generated in a previous study [48] and had been maintained by Dr. William Gilliland. Each line was first made homozygous for the chromosome 4 marker *poliert* (*pol*), which gives the flies eyes with the surface being glazed over and shiny like glass instead of individual eye facets, in order to test for 4 chromosome nondisjunction. The crosses used to create these stocks are detailed in Appendix A. Once the *yw*; $\Delta/TM3, sb$; *pol* stock for each line was crossed to $FM7/y+Y$; $ald^l/TM3, Sb$; *pol* males, virgin females, $FM7/yw$; ald^l/Δ ; *pol*, picked up from the previous cross for each excision were crossed individually to $C(1;Y), v f B; C(4)RM, ci ey^R$, (hereafter referred to as AD1) males, which have *X* and 4 phenotypic markers attached including the *X* markers: *vermillion* (*v*), *forked* (*f*), *Bar* (*B*); and the 4 markers: *cubitus interruptus* (*ci*) and *eyeless*, *Russian allele* (ey^R), to measure the frequency of nondisjunction. *FM7* is a balancer chromosome, and when heterozygous with a normal sequence *X*, will prevent the *X* chromosomes from recombining [50]. The AD1 tester stock males have a phenotype of *vermillion* eye color, *brown* body, *forked* bristles, *Bar* eyes, interrupted wing veins, as well as a more round and reduced to missing eye shape. All crosses are fully detailed in Appendix A.

Both 4 chromosome and *X* chromosome nondisjunction was measured through this cross. Nondisjunctional progeny were determined using visible markers, or phenotypic characteristics, located on the *X* and 4 chromosomes in order to classify their

genotype and whether nondisjunction had occurred in the female germline. Descriptions on each marker used in the nondisjunction assay, potential outcomes for the X and 4 chromosomes, and the nondisjunction progeny are detailed in Appendix A. This initial screening was done using *ald*^l as null alleles are semi-lethal. The *ald*^l allele was used so all alleles would be viable.

Once the initial screening of the nondisjunction rates was obtained, eight excisions from the first experiment (listed in Table 1 and 2) with well separated nondisjunction rates were selected. Females from each stock were crossed to *FM7/y+Y; Df(3R)AN6/TM3, Sb; pol* males to produce *FM7/yw; Δ/Df(3R)AN6; pol* experimental females. The *Df(3R)AN6* chromosome carries a small deletion on the 3rd chromosome that deletes the entire *ald* locus [2], making the females hemizygous for each *ald* excision allele. These females were crossed individually to AD1 males to measure nondisjunction. Females and males from each vial for each excision were transferred to another vial, or brooded, on the fifth day after setup to increase the total progeny sample size, and adults were discarded from the second vials after another five days. As with the previous experiment, both 4 and X nondisjunction was measured simultaneously.

As half of the X nondisjunctional progeny can only survive if fertilized with one of the two types of sperm, the rate of NDJ in meiosis is not equal to the rate of nondisjunctional progeny observed.

Nondisjunction rates were calculated using the following equations, with the nondisjunctional progeny defined as the *exceptions* [7, 16]:

$$\text{Adjusted Total} = \frac{2(X \text{ Exceptions}) + 2(X \& 4 \text{ Exceptions}) + (4 \text{ Exceptions}) + \text{Normal Progeny}}{}$$

$$X \text{ NDJ} = \frac{2(X \text{ Exceptions}) + 2(X \& 4 \text{ Exceptions})}{\text{Adjusted Total}}$$

$$4 \text{ NDJ} = \frac{2(X \& 4 \text{ Exceptions}) + 4 \text{ Exceptions}}{\text{Adjusted Total}}$$

Nondisjunctional gametes from the maternal line contain diplo-X (XX) or nullo-X (00) ova. These gametes, when combined with sperm, affect the progeny just like in humans. After fertilization, nondisjunctional ova would be one of four possibilities: XXY, XXX, X0, or Y0 zygotes. The XXX and Y0 progeny die; however, the XXY and X0 progeny survive. The X0 males are completely sterile and the XXY females seem relatively normal but show an increased level of nondisjunction due to secondary nondisjunction [7, 50]. So the X chromosome nondisjunction progeny are doubled in the equations above to account for the progeny that do not survive into adulthood, but still count towards the nondisjunction events occurring in the female germline. The 4 chromosome nondisjunction progeny do not have to be doubled, since both NDJ and normal progeny have the same chance of survival into adulthood. Flies with 3 chromosome 4s survive, unlike flies that have 3 X chromosomes which do not survive.

Flies with only 1 chromosome 4 can survive and can be identified as having the phenotype *minute*. As *minute* flies are very sick, they are recorded in the experiment but are excluded from analysis.

Probes for *in situ* hybridization:

The following sequences were used for FISH probes (Figure 12): (TTT-TCC-AAA-TTT-CGG-TCA-TCA-AAT-AAT-CAT) recognizing the 359-bp satellite block on the X chromosome; and (AAT-AT)₆ recognizing the 4 chromosome as well as a small region on the X chromosome. Each probe had a fluorescent dye attached. Alexa Fluor 488 was used for the X chromosome and Alexa Fluor 560 was used for the 4 chromosome. The probes were prepared as described in [52] and generously provided by Scott Hawley and his lab at Stowers Medical Research Institute (Kansas City, MO).

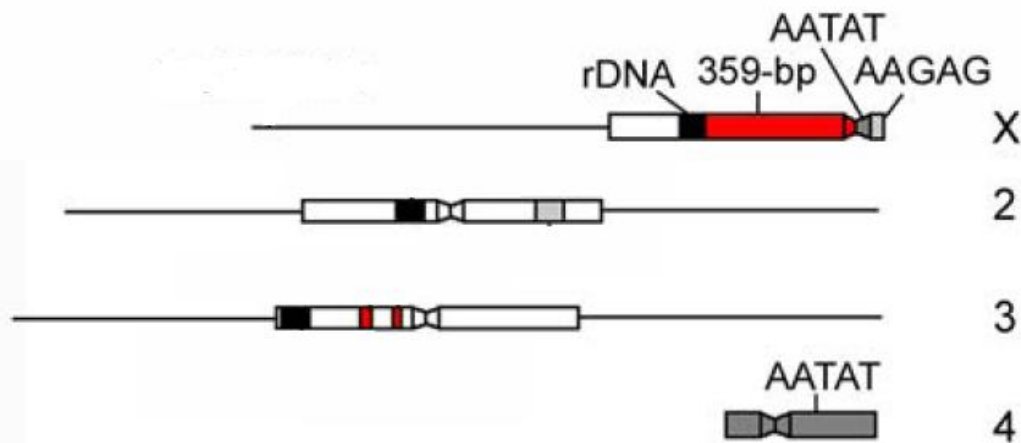


Figure 12. Genomic sequences used as probes for *in situ* hybridization. Schematic representation of satellites used as targets of FISH. Boxes and lines represent heterochromatin and euchromatin, respectively. Constrictions in boxes represent the centromeres. Chromosomal regions are not drawn to scale. The 359-bp satellite block was used for the X chromosome. A small subset of localization on chromosome 3 can be seen with the X probe. The AATAT repeats were used to recognize the 4 chromosome, with a small localization on the X chromosome as well. Each probe had a specific Alexa Fluor attached to the probe for visualization [52].

Ovary dissection and fixation:

The same eight lines from the second NDJ assay were used for cytological analysis. From these excision lines, virgin females of the same *FM7/yw; Δ/Df(3R)AN6; pol* genotype were collected and aged with fresh yeast paste without males for 4 days post eclosion (dpe). The females were then anesthetized and the ovaries were hand dissected using forceps in 1X Robb's Media + 1% Bovine Serum Albumin (BSA). The ovaries were then transferred to 1.0 mL of fixative solution (8% formaldehyde and 1X Fix Buffer) in a 1.5 mL eppendorf tube to fix for 4 minutes.

Immunofluorescent, Fluorescent *in situ* hybridization and confocal microscopy:

Immuno-FISH was performed by a novel combined approach from an adaptation of the described standard protocols [50-52]. After the fixation period, the ovaries were washed with PBST. The ovaries were ruptured to separate the individual ovarioles. The ovarioles were then washed with PBST four times for 15 minutes each wash. The ovaries were dechorionated by rolling between frosted glass slides to make the oocyte permeable for the antibody to enter. The ovaries were again briefly washed three times. The oocytes were then blocked for 1 hour in PBST-NGS (475 μL PBST, 25 μL Normal Goat Serum). After one hour, new PBST-NGS was added, along with the primary antibody, Rat anti-tubulin-α (1:250 dilution). They were incubated at 4°C overnight. The oocytes were washed briefly three times with PBST and once for 15 minutes. The oocytes were once again blocked for 1 hour in PBST-NGS. After the hour, new PBST-NGS and the secondary antibody, Goat anti-rat IgG, tagged with Alex Fluor 647, (1:250 dilution) was

added to the oocytes and incubated at 4°C overnight. The oocytes were washed briefly three times with PBST and then post-fixed in 4% formaldehyde for 30 minutes.

After the fixation period, the ovaries were washed briefly three times in PBST and then were transferred to 2X SSCT (3M Sodium Chloride, 0.3M Sodium Citrate, pH 7.0, 0.1% Tween-20). They were then washed with 2X SSCT three times for 10 minutes each wash. Following the washes, the ovarioles were incubated consecutively in 20%, 40%, and 50% formamide-containing 2X SSCT for 10 minutes each. After the formamide ramp up, the ovarioles were transferred to fresh 2X SSCT containing 50% formamide and incubated at 37 °C for 2 hours. The sample was aspirated as much as possible leaving behind the ovarioles. A quarter of a microliter of each of the X [100ng/μL] and 4 [200ng/μL] chromosome fluorescently-labeled DNA probes were combined with 36 μL of hybridization solution (dextran sulfate, sodium chloride, sodium citrate, and formamide) and added to the ovarioles. The sample was placed at 92°C for 3 minutes to denature, then was placed at 32°C overnight. Then the probe mix was aspirated, and the sample was placed in a formamide ramp down process, incubating for 10 minutes each in 40% and 20% formamide-containing 2X SSCT at room temperature, followed by an additional incubation with just 2X SSCT. After completing the washes, the ovarioles were incubated with 0.5 mL 2X SSCT containing 2.5 μL of 200X DAPI (4',6-Diamidino-2-Phenylindole) for 10 minutes, and then washed 2 times with 2X SSCT for 10 minutes each. Finally, the ovarioles were mounted on slides with Slowfade Gold mounting media and cover slips were sealed with nail polish.

Microscopy was conducted using a Leica TCS SPE II confocal microscope and Leica Application Suite Imaging software. Images were edited with Adobe Photoshop.

While both immunofluorescence and FISH had been performed in prometaphase oocytes in the past separately, they had not been previously combined. With previous FISH protocols, stringent formamide washes were needed to make the chorion permeable to the probes. However, with the chorion removed for the antibodies, wash stringency had to be reduced to not wash away the probes.

DNA Isolation:

The DNA from 30 flies for each P-element excision was extracted following the protocol from the Langley Lab, University of California - Davis (1999). The flies were homogenized in 300 μ L of solution, composed of 20% SDS, 1M Tris (pH 8.0), 0.5M EDTA (pH 8.0) and water. Once homogenized, the solution was incubated for 30 minutes at 65°C. After the incubation time, 21 μ L of 8M potassium acetate (KAc) was added and then incubated again for 30 minutes on ice. After a 10 minute centrifugation at room temperature, the supernatant was collected and transferred to a new tube and the total volume of solution in the eppendorf was brought up to 400 μ L with TE.

The supernatant was extracted twice with an equal volume of phenol, again spinning each extract for 10 minutes. After these two extractions, the supernatant was extracted once, after spinning for 2 minutes, with an equal volume of a 24:1 chloroform:isoamyl alcohol solution. Then, 40 μ L of 3M sodium acetate (pH 5.2) (NaAc) and 800 μ L of 95% ethyl alcohol (EtOH) was added and placed on ice for 10 minutes. After 10 minutes, the solution was spun for 30 minutes.

After the spin, the supernatant was taken off and the pellet was washed with 180 μ L of 70% EtOH and then spun again for 5 minutes. Again the supernatant was taken off

and the pellet was allowed to air dry for approximately 5 minutes. The pellet was then resuspended in 20 μ L of TE and stored at -20°C.

Primers:

Using the software program Primer3, primers were designed to amplify the sequence of DNA centered around the 14th nucleotide of the 5' UTR where the P-element, P{GS:13084}, is inserted into the *ald* gene. The 22 base pair left flanking primer designed was 5'--CATCACTCTCCCTCACTCAAAG--3' and the 20 base pair right flanking primer designed was 5'--CCTCGTTTGGACTTGGAAAG--3'. The primers were ordered from Integrated DNA Technologies, Inc. (Skokie, IL.).

Polymerase Chain Reaction and Gel Electrophoresis:

A master mix, (1X Polymerase Chain Reaction (PCR) buffer, 0.2 mM dNTP mixture, 1.5 mM magnesium chloride (MgCl₂), 0.5 μ M of each primer, 0.5 μ L of *Taq* DNA Polymerase, and distilled water) was prepared and added to 1 μ L [250 ng/ μ L] of the template DNA into PCR tubes. Using a Vapo.protect Mastercycler pro S, the tubes were incubated at 94°C for 2 minutes to denature the template. A Touchdown program was used for 10 cycles, which was composed of a denaturing component for 45 seconds at 94°C, an annealing component for 45 seconds beginning at 60°C and decreasing 1°C per cycle, and finally an extension component for 1 minute at 72°C. After the completion of the Touchdown program for 10 cycles, another 15 cycles of PCR amplification was performed, denaturing for 45 seconds at 94°C, annealing for 45 seconds at 55°C, and extending for 1 minute at 72°C. The extension times varied for specific excisions, since all of the lines did not amplify under the same conditions (i.e., extension time). A 45

second extension time was used for excisions 1, 4, 23, 25, and 30; whereas, a 1 minute extension time was used for excision 15 and a 4.5 minutes for excision 26. A final 4 minute extension incubation time at 72°C was used to finish the PCR amplification process.

Once the PCR was completed, an Ethidium Bromide and agarose gel was prepared for gel electrophoresis. For each excision line, 5 µL of the PCR reaction solution and 1 µL of loading dye was loaded into each well. A New England Bio Labs 2-log DNA ladder was also loaded into a well for comparison purposes. The gel was run for approximately 90 minutes at 100 volts. After the gel electrophoresis was complete, the gel was then viewed under ultraviolet light with the BioSpectrum® Imaging System and software.

DNA Sequencing:

The PCR products were purified using a QIAGEN® QIAquick PCR Purification kit. The purification process was carried out in a conventional tabletop microcentrifuge at room temperature. 500 µL of Buffer PB were added to the 100 µL of the PCR reaction product and mixed. The sample was then applied to the QIAquick column and centrifuged for 1 minute. The column was then washed with 0.75 mL of Buffer PE and centrifuged for 1 minute. The flow-through was discarded and the sample was centrifuged again for 1 minute to eliminate any remaining ethanol residue from the Buffer PE. The DNA was eluted with 50 µL of Buffer EB (10 mM Tris-Cl, pH 8.5) and centrifuged for 1 minute. The samples were then kept at -20°C until needed.

The purified PCR products were quantified by Nanodrop 2000 Spec and then sequenced at the DNA Sequencing Core facility at the Stowers Institute for Medical

Research (Kansas City, MO). DNA Sequences were analyzed using *conseq* software program and aligned with ClustalW2 - Online Alignment software (European Bioinformatics Institute, <http://www.clustal.org/clustal2/>).

Western Blot Analysis:

Males and females for each excision hemizygote, *FM7/yw; ΔDf(3R)AN6; pol*, were set up in yeasted vials for 4 days. On day 4, the females were placed in egg chambers with grape juice agar plates for 3 hours. Thirty eggs were then collected from the agar plates. The eggs were then hand squashed in 30 μL (1 μL/egg) of 3X SDS load buffer and heated at 95°C for 5 minutes. Five microliters of these preparations were ran on precast Bio-Rad® Ready-gels at 200V for 45 minutes, and then transferred to a nitrocellulose membrane using a wet-methanol method transfer cell at 200 mA for 2 hours. After transfer, gels were preserved and stained overnight with Coomassie as a loading control. The blot was blocked with 5% dry milk (PBS + 5% dry milk powder), hybridized overnight with shaking in 5% dry milk with 1:5,000 Rabbit anti-Ald antibody (STI-131) [2], and washed five times for 5 minutes with 10 mL of TBS + 0.1% Tween-20. The blot was hybridized as before with 1:3,000 Goat anti-Rabbit conjugated with Horseradish peroxidase secondary antibody, and washed three times for 5 minutes with 10 mL of TBS + 0.1% Tween-20. It was then visualized with a 1:1 mixture of SuperSignal® West Pico Stable Peroxide Solution and Luminol/Enhancer Soution (Thermo Scientific).

Statistical Analysis:

The statistical significant difference between broods 1 and 2 for the secondary crosses were calculated using the comparison of two nondisjunction rates. The broods were combined into one total sample if the difference between their two nondisjunction rates (Z), at significance level $\alpha=0.05$, was less than or equal to 1.96, as calculated [53].

The confidence intervals for both the genetic and cytological nondisjunction were calculated for a 95% confidence significance. The cytological 95% confidence interval was calculated using a standard binomial confidence interval, whereas, the genetic 95% confidence interval was calculated by a hierarchical-Poisson NDJ model [53].

Calculation of the coefficient of correlation (r) was done using the CORREL function on Microsoft Excel.

Excision 14 (*ald*^{*P*{*GS:13084*}-*excision14*}}):

The excision 14 line was unable to be amplified through the PCR process. A number of other methods were then used to help further classify the line.

PCR was run to see if the ends of the P-element were in fact present in this line. The primers, mentioned above, were used in conjunction with primers designed to sequence the ends of the P-element. The 5' out sequencing primer, 5'---TCGTCCGCACACAACCTTTC---3', and 3' out sequencing primer, 5'---CTCACTCAGACTCAATACGAC---3', were used to identify if the ends were present. PCR products were run on an agarose gel and visualized as above.

The original, *P*{*GS:13084*}, P element contains a *GFP* (Green Fluorescent Protein) protein under the transcriptional control of UAS, which can be expressed by Gal4 protein. Females, *yw; Exc 14/TM3, sb; pol*, were crossed with *yw; P{nosGal4}; pol*

males. The *nosGal4* construct expresses Gal4 protein in the female germline under control of the *nanos* promoter, and can bind to the *UAS* sequence and when heat-shocked, can cause transcription of the *GFP* (Figure 13).

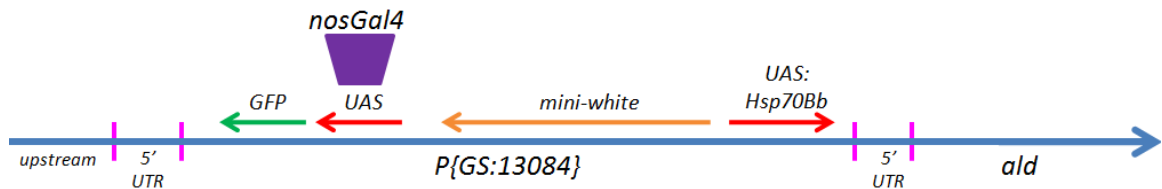


Figure 13. Interaction of *nosGal4* and *UAS* of P{GS:13084} In order to test for components of the P-element inserted into the Excision 14 line, progeny, *yw; Exc 14/TM3, sb; pol*, were crossed with *yw; P{nosGal4}; pol* progeny. *nosGal4* can associate with the *UAS* sequence and when heat-shocked, transcription occurs of the *GFP*. Females, *yw; P{nosGal4}/+; P{GS:13084}^{Al4}/+; pol*, were collected and heated at 37°C for 1 hour. After the incubation period, the females were allowed to recover for another hour. Once recovered, the females were then anesthetized and the ovaries were dissected, fixed, and viewed under the microscope. The figure is a systematic representation of *nosGal4* interacting with the *UAS* sequence in order to drive transcription of the *GFP* in order to test whether or not these components were present in the excision 14 line.

Female, *yw; P{nosGal4}/+; P{GS:13084}^{Al4}/+; pol*, flies were collected and heat shocked at 37°C for 1 hour. After the incubation period, the females were allowed to recover for another hour. Once recovered, ovaries were dissected and fixed as described above. Fixed ovaries were then mounted on slides with Slowfade Gold mounting media and viewed using the Leica[®] confocal microscope in order to look for the presence of Green Fluorescent Protein.

V. RESULTS

Rates of *X* and *4* chromosome nondisjunction were measured for a preliminary series of crosses using excisions of a P-element excision, $ald^{P[GS:13084]}$, to provide progeny of the various alleles of the *ald* gene. Females for each P-element excision, *FM7/yw; ald¹/Δ; pol*, were crossed individually to *ADI* males to measure the frequency of nondisjunction. Table 1 shows the NDJ rates for both the *X* and *4* chromosomes for each of the 24 excision lines. The preliminary X NDJ rates range from 2.3% to 41.0%, whereas the 4 NDJ rates range from 2.1% to 32.9%. The majority of lines have a $\geq 10\%$ NDJ rate for the *X* chromosome, while there is a $\leq 10\%$ NDJ rate for the *4* chromosome for the majority of lines (Figure 14).

From this preliminary cross, 8 excision lines (as seen in Tables 1 and 2) were chosen with well-separated NDJ rates. These excision lines had a range of X NDJ, from approximately 2% to 30%, as well as a range of 4 NDJ, from approximately 3% to 33%.

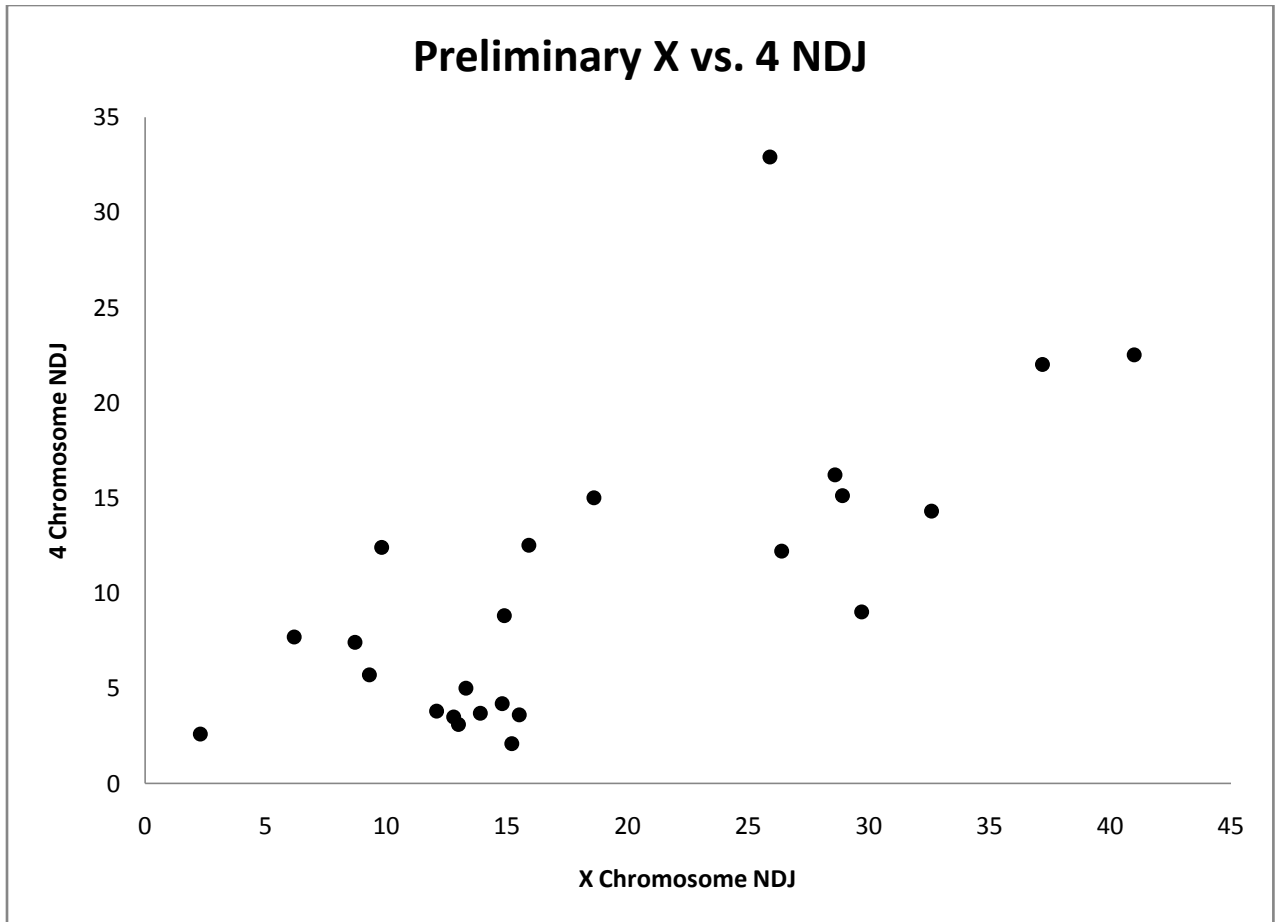


Figure 14. Preliminary X and 4 nondisjunction rate assay The figure shows the wide range of nondisjunction rates for the X and 4 chromosomes for females for each excision line *FM7/yw; ald¹/ald^{P(GS:1-3084)-excision}*; *pol* crossed to *C(1,Y), v f B; C(4)RM, ci ey^R* (AD1) males. The X NDJ rates range from 2.3% to 41.0%, whereas the 4 NDJ rates range from 2.1% to 32.9%, each with varying sample sizes (shown in Table B1).

The selected excision lines were then used in a second nondisjunction assay with larger sample sizes, and assayed cytologically through the use of a combined protocol of Immuno-FISH. Females for each selected P-element excision, *FM7/yw; Δ/Df(3R)AN6; pol*, were crossed individually to AD1 males to measure the genetic X and 4 nondisjunction again. Females of the same genotypes were also aged for 4 days and their oocytes were examined cytologically for chromosome orientation at metaphase I arrest.

N	Genetic X NDJ (%)	Excision	Cytological X NDJ (%)	N
2466	0.7	25	0.0	201
4644	8.2	15	9.8	204
2341	10.4	30	11.7	206
2193	10.9	14	12.6	231
4137	10.9	4	14.7	218
2543	10.9	1	15.2	204
2150	13.8	26	18.0	250
2324	39.8	23	35.5	214

Table 1. X chromosome genetic NDJ and cytological malorientation rates The table shows the genetic nondisjunction rates for the X chromosome for females for each excision line, *FM7/yw*; *ald*^{*P1GS:1-3084*}-*excision*/*Df(3R)AN6*; *pol*, crossed to *ADI* males. The rates are in ascending order with a range of 0.7% to 39.8% nondisjunction. The sample size for each excision includes the total of both brood 1 and 2. The combination of the two broods was justified by calculating the statistical difference between the two broods using a cut-off of $|Z| \leq 1.96$ [53]. The table also shows the cytological nondisjunction rates for the X chromosome for Iummno-FISH prepped 4 dpe, virgin female oocytes for each excision line, *FM7/yw*; *ald*^{*P1GS:1-3084*}-*excision*/*Df(3R)AN6*; *pol*. The rates of chromosome malorientation rate range from 0% to 35.5% for the X chromosome. N represents the sample size for each line.

N	Genetic 4 NDJ (%)	Excision	Cytological 4 NDJ (%)	N
2466	0.6	25	0.0	201
4644	6.4	15	7.8	204
2341	8.3	30	5.8	206
2543	8.3	1	12.4	204
4137	8.8	4	8.7	218
2150	10.4	26	14.0	250
2193	10.5	14	9.5	231
2324	28.6	23	31.3	214

Table 2. 4 chromosome genetic NDJ and cytological malorientation rates The table shows the nondisjunction rates for the 4 chromosome for females for each excision line, *FM7/yw*; *Δ/Df(3R)AN6*; *pol*, crossed to *ADI* males. The rates are in ascending order with a range of 0.6% to 28.6% nondisjunction. The sample size for each excision includes the total of both brood 1 and 2. The combination of the two broods was justified by calculating the statistical difference between the two broods using a cut-off of $|Z| \leq 1.96$ [53]. The table also shows the cytological nondisjunction rates for the 4 chromosome for Iummno-FISH prepped 4 dpe, virgin female oocytes for each excision line, *FM7/yw*; *ald*^{*P1GS:1-3084*}-*excision*/*Df(3R)AN6*; *pol*. The rates of chromosome malorientation rate range from 0% to 31.3% for the 4 chromosome. N represents the sample size for each excision line.

The secondary round of nondisjunction assay crosses showed a range of X NDJ, from a background level of NDJ (0.7%) to a high level of NDJ (39.8%) (Table 1). The *ald*^{Excision25}, the precise excision, had the background level of NDJ, whereas *ald*^{Excision23} showed the highest level of NDJ with 28.6% for the X chromosome. The 8 excisions appear to fall into one of 3 categories, which is different from the previous wide range observed in the preliminary assay (Figure 14 and Table B1). The three categories are the background level (0.7%), the mid-range NDJ levels (~8% to ~14%), and the high NDJ level (~40%). The 4 chromosome NDJ was also analyzed and showed to have a range from a background level of NDJ (0.6%) to a high level of NDJ (28.6%). Again, Excision 25 and Excision 23 were at the ends of the range, respectively. In regards to 4 chromosome NDJ, there are again 3 prevalent groups, similar to the X chromosome: the background level (0.6%), the mid-range NDJ level (~6% to 10%), and the high NDJ level (~29%). The sample size consisted of two broods for each excision line. To ensure that there was no statistical significance between the broods, the Z-score, at $\alpha=0.05$, was calculated for each line. Each excision line had a $|Z| \leq 1.96$, showing no difference between the two broods (as seen in Table B2) which were then pooled.

The 8 excisions line were originally chosen with a wide spread of NDJ rates based on the X chromosome for the *Excision/ald*^l experimental cross. The *ald*^l allele is a point mutant that produces a normal amount of mutant protein [2]. The second experiment used a deletion allele, *Excision/Df(3R)AN6*, which showed a different pattern. The 8 excisions clumped into the 3 categories instead of the wide-spread rates (Figure 15). The higher X chromosome NDJ rate lines were not chosen since they do not survive over a deficiency. This dramatic difference between the preliminary and secondary spreads suggests that the

ald¹ protein is slightly dominant and is having a slightly deleterious effect when compared to a simple deletion of the gene (Figure 15).

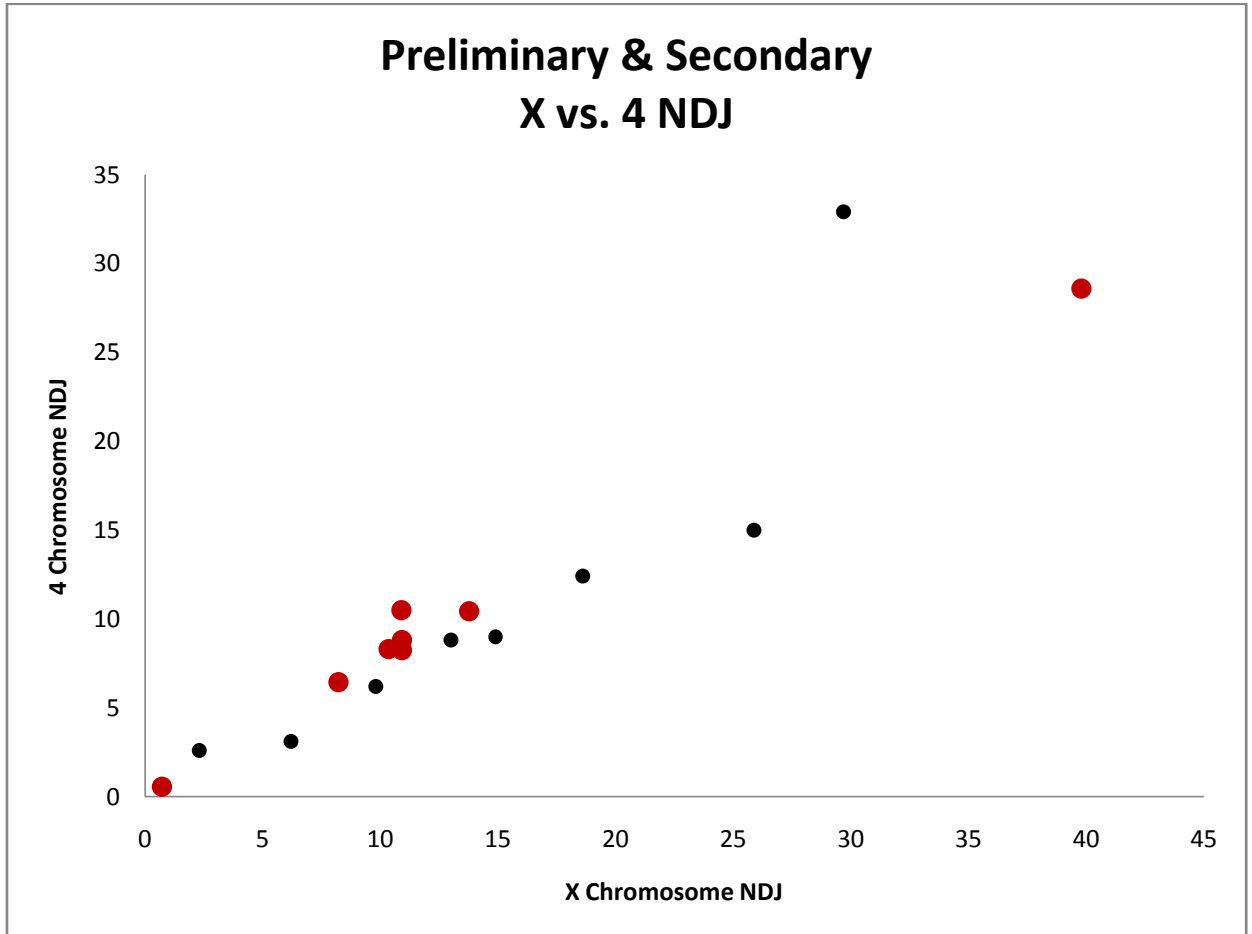


Figure 15. *ald¹* vs. *Df(3R)AN6* nondisjunction assays The black points show the wide range of nondisjunction rates for the *X* and *4* chromosomes for females for each excision line *FM7/yw; ald¹/ald^{P[GS:1-3084]-excision}; pol* crossed to *C(1,Y), v f B; C(4)RM, ci ey^R* (AD1) males during the preliminary cross in which the point mutant, *ald¹*, was used during the experiment. The red points show the clustering of nondisjunction rates for the *X* and *4* chromosomes for females for each excision line *FM7/yw; Df(3R)AN6/ald^{P[GS:1-3084]-excision}; pol* crossed to AD1 males during the preliminary cross in which the small deletion, *Df(3R)AN6*, was used during the experiment. As shown in the figure, the 8 excisions clumped into the 3 categories during the secondary assay (red points) instead of the wide-spread rates that was observed during the preliminary assay (black points). This dramatic difference between the preliminary and secondary spreads suggests that the *ald¹* protein is slightly dominant and is having a slightly deleterious effect when compared to a simple deletion of the gene.

The cytological analysis of each line for the *X* and *4* chromosomes is shown in Tables 1 and 2, respectively. Images of the five possible outcomes of the cytological

analysis when examining the oocytes of 4 dpe virgins, *FM7/yw; Δ/Df(3R)AN6; pol* :
 coorientation, X-only NDJ, 4-only NDJ, $XX \leftrightarrow 44$ NDJ, and $XX44 \leftrightarrow \emptyset$ NDJ; are
 shown in Figure 16, as well as in Appendix C (Figures C1-5).

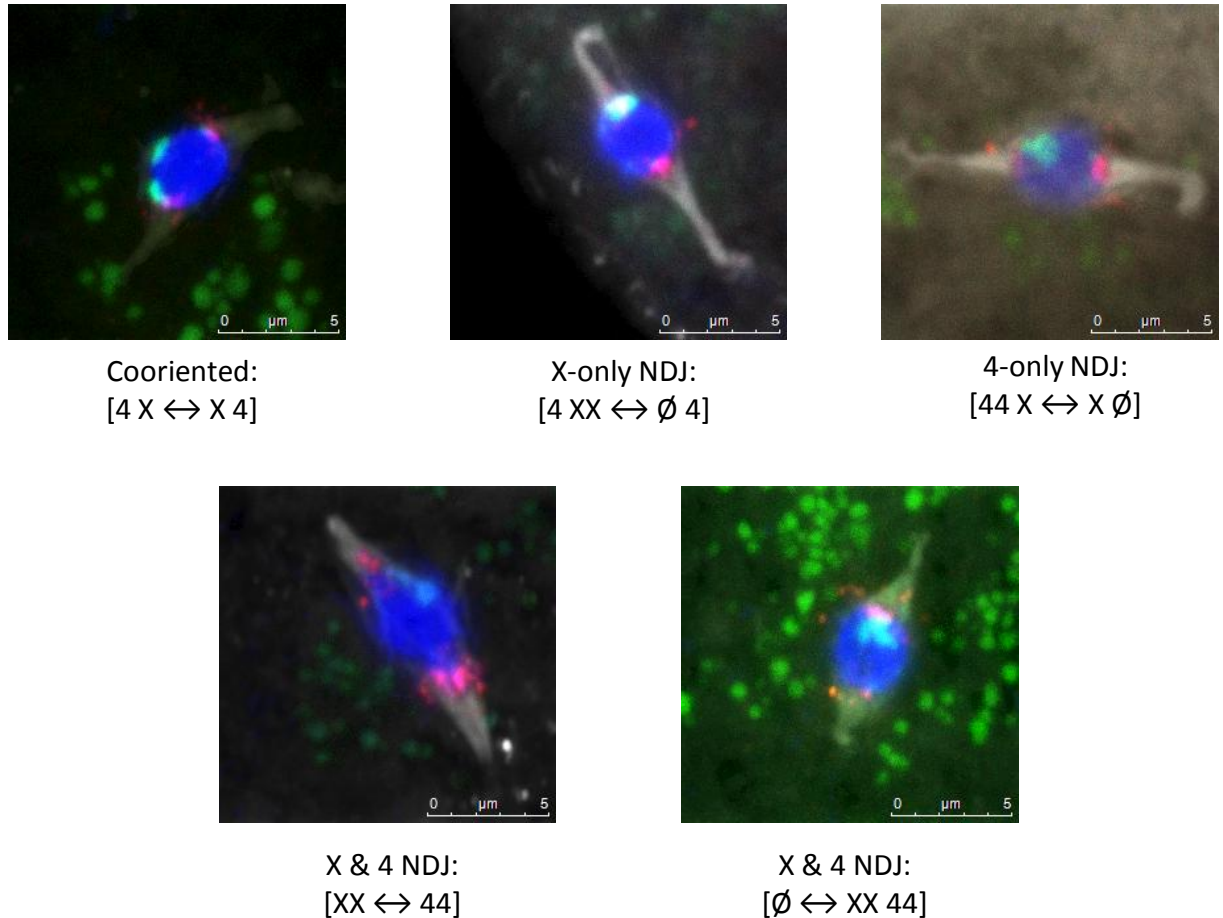


Figure 16. Cytological examination scenarios Four day post eclosion, virgin females, *FM7/yw; Δ/Df(3R)AN6; pol*, hemizygotes for each excision line were fixed, Immuno-FISH probed, and oocytes were scored for X and 4 chromosome coorientation at metaphase I arrest to correlate with the genetic nondisjunction assay. The 359-bp satellite block on the X chromosome, tagged with Alexa Fluor 488 (shown in green) and the AAT-AT-repeating sequence recognizing the 4 chromosome, as well as a small region on the X chromosome, tagged with Alexa Fluor 560 (shown in red) was used as FISH probes to measure chromosome coorientation. The meiotic spindle (shown in gray) was probed through immunofluorescent, using a secondary antibody tagged with Alexa Fluor 647, to detect the tubulin of the spindle. The figure shows the merged images of all 4 fluorescent channels. The cytological examinations showed five scenarios: (1) cooriented chromosomes ($4 X \leftrightarrow X 4$), with both Xs and 4s properly oriented towards opposite poles, (2) X-only NDJ ($4 XX \leftrightarrow 4$), with the Xs oriented towards the same pole and the 4s oriented towards opposite poles, (3) 4-only NDJ ($44 X \leftrightarrow X$), with the 4s oriented towards the same pole and the Xs oriented towards opposite poles, (4) X & 4 NDJ ($XX \leftrightarrow 44$), with the two Xs oriented towards the same pole and the two 4s oriented towards the same pole, but opposite of the Xs, and (5) X & 4 NDJ ($44 XX \leftrightarrow \emptyset$), with both Xs and 4s oriented towards the same pole and none oriented towards the opposite pole. Measurement bar = 5 μ m.

The cytological analysis of X chromosome NDJ showed a similar range of rates as in the genetic assay, from 0% to approximately 36%. These rates, with the exception of Excision 25, were all above 10% with the sample size collected. The mid-range NDJ lines seemed to cluster in the cytological assay as they had previously been shown to do in the genetic assay (Table 1). A similar range was observed for the 4 chromosome as well. It showed a range from 0% to approximately 31%. The lines clustered as they had previously been shown to do in the genetic assay, with slightly higher value for the mid-range group (Table 2).

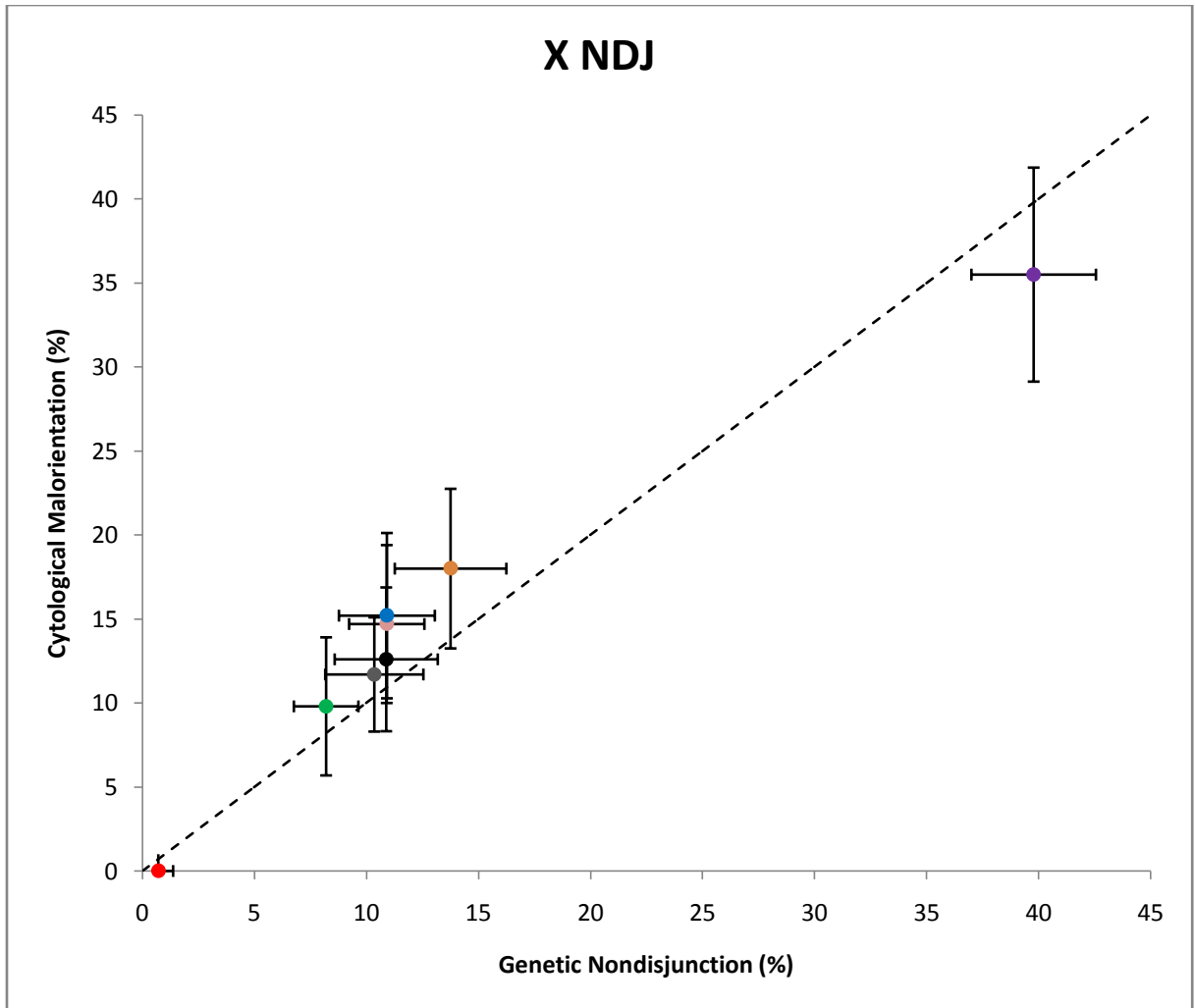


Figure 17. Correlation of genetic and cytological NDJ rates for the X chromosome

Genetic NDJ rates for the *ald* alleles were assayed in *FM7/yw; ΔDf(3R)AN6; pol* hemizygotes and measured by counting progeny (Table 1). Virgin females of the same genotype for each excision line were fixed, Immuno-FISH probed, and oocytes were scored for X chromosome coorientation at metaphase I arrest. Each data point represents one of the 8 excision lines with at least 200 oocytes, corresponding with Table 1. The correlation between genetic NDJ and cytological malorientation was examined and shown to be highly correlated ($r=0.97$). As the genetic NDJ increases, so does the malorientation of the chromosomes in the "lemon" when examined cytologically. The vertical lines represent unique 95% confidence interval error bars for each line, calculated by the standard binomial confidence interval. The horizontal lines represent 95% confidence interval error bars for each line, calculated by the hierarchical-Poisson NDJ model [53]. Error bars can be found in Appendix B (Table B5). Dashed line = unity.

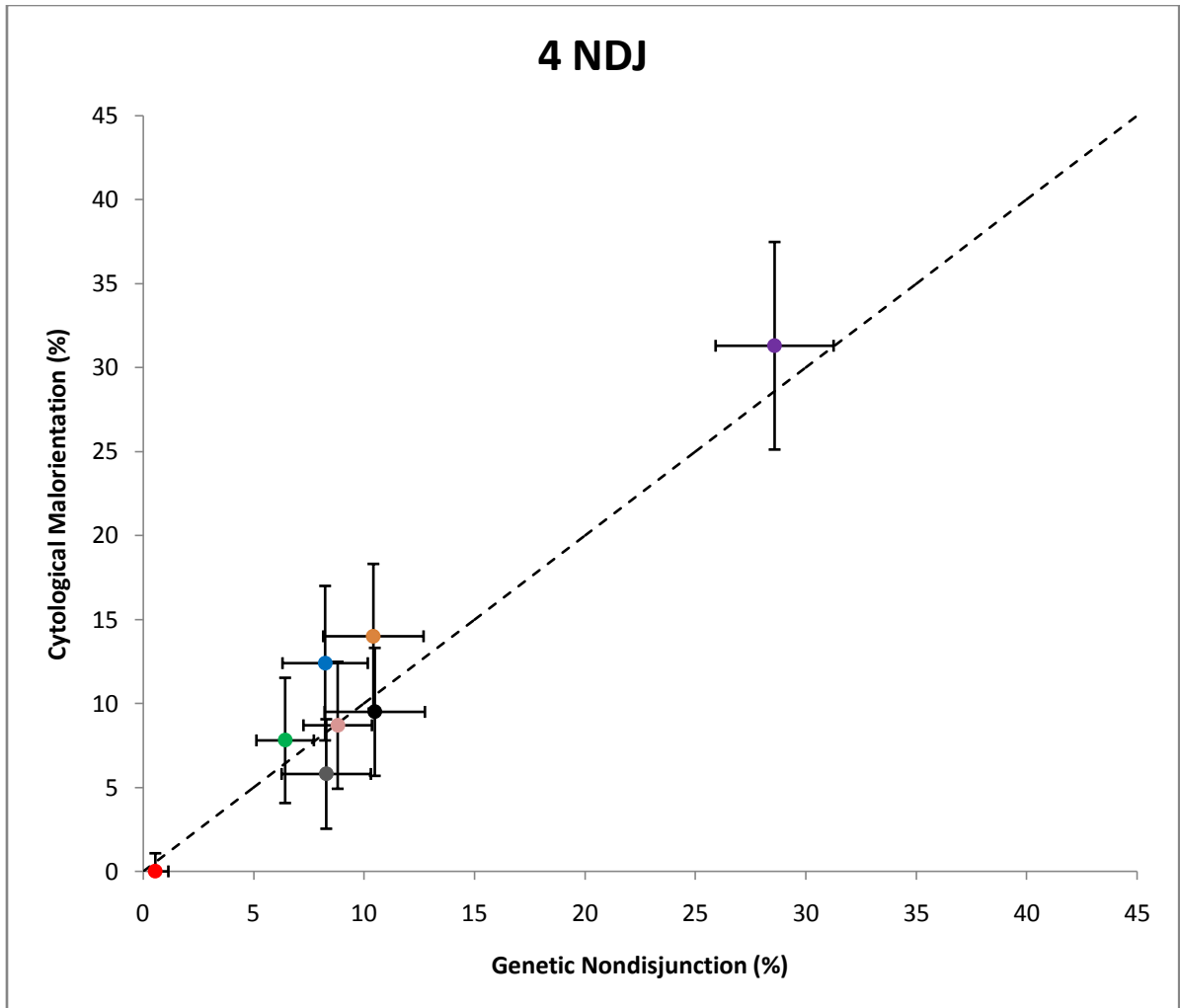


Figure 18. Correlation of genetic and cytological NDJ rates for the 4 chromosome

Genetic NDJ rates for the *ald* alleles were assayed in *FM7/yw; Δ/Df(3R)AN6; pol* hemizygotes and measured by counting progeny (Table 2). Virgin females of the same genotype for each excision line were fixed, Immuno-FISH probed, and oocytes were scored for 4 chromosome coorientation at metaphase I arrest. Each data point represents one of the 8 excision lines with at least 200 oocytes, corresponding with Table 2. The correlation between genetic NDJ and cytological malorientation was examined and shown to be highly correlated ($r=0.97$). As the genetic NDJ increases, so does the malorientation of the chromosomes in the "lemon" when examined cytologically. The vertical lines represent unique 95% confidence interval error bars for each line, calculated by the standard binomial confidence interval. The horizontal lines represent 95% confidence interval error bars for each line, calculated by the hierarchical-Poisson NDJ model [53]. Error bars can be found in Appendix B (Table B5). Dashed line = unity.

As shown in Figures 17 and 18, the correlation between the genetic NDJ and cytological malorientation rates were observed to be highly associated for both the X and 4 chromosomes; $r= 0.97$ and 0.97 , respectively. The 8 lines clustered into 3 groups: the low level NDJ, the mid-range NDJ, and the high NDJ level; instead of the wide range of

values as observed in the *ald*¹ preliminary experiment. As the genetic nondisjunction increased for both the *X* and *4* chromosomes, so did the cytological malorientation of the chromosomes within the "lemon."

When examining the double nondisjunctional progeny in both the genetic and cytological assays, heterologous doubles ($XX \leftrightarrow 44$, with both *Xs* oriented towards one pole and the two *4s* are oriented towards the opposite pole) were much more likely in all lines than the non-heterologous doubles ($XX44 \leftrightarrow \emptyset$, with both *Xs* and *4s* oriented towards one pole and no *X* or *4* oriented towards the opposite pole). The majority of the lines were between approximately 10 and 33 times as likely to result in heterologous doubles than non-heterologous doubles in the genetic assay. This was also observed in the cytological analysis as well, but not to the degree as in the genetic analysis due to the smaller sample size. The lines all were below 10 times as likely, but the heterologous doubles were still more likely than the non-heterologous doubles (Table B3). The percent of doubles for the heterologous nondisjunction category show a direct relationship between the genetic and cytological assays (Table B4 & Figure B1). However, the non-heterologous doubles did not show the same relationship (Table B4 & Figure B2). Most of the lines clumped around 1-2% of the total progeny, with the lone exception of Excision 23 being ~6-7%. This supports the earlier observation of heterologous double events being much more likely than those of the non-heterologous doubles.

The 8 lines were analyzed further through a variety of methods; PCR, DNA sequencing and Western Blot analysis, in order to further classify the characteristics of each one. The Western Blot analysis failed, but is being repeated at a later date. DNA was extracted from each line in order to amplify a 475 base pair centered around the 14

nucleotide of the 5'UTR. Out of the 8 excision lines, 7 ($\Delta 25$, 30, 1, 4, 23, 15 and 26) were able to be amplified through PCR.

From the analysis of the PCR, Excision 25, previously characterized as the precise excision, was shown to be 475 bp, as well as Excision 30. Excisions 1 and 4 were amplified bands of approximately 530 nucleotide bases, while Excision 23 was about a 600 bp band. Excisions 15 and 26 were the two largest bands that were able to be amplified, being approximately 2.6 kb and 4.6 kb, respectively (Figure 19).

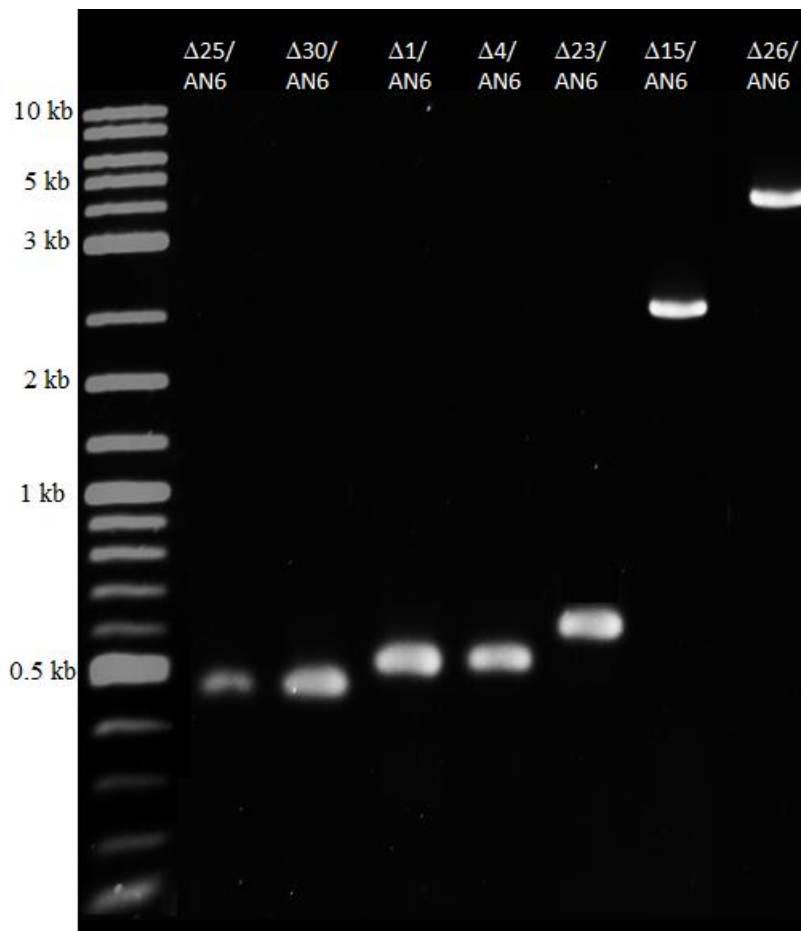


Figure 19. Polymerase Chain Reaction amplification of excision DNA DNA was extracted, using a phenol:chloroform extraction method, from males and females from each excision line, *FM7/yw; $\Delta/Df(3R)AN6; pol$* . A 475 base-pair region was amplified through PCR, centered around the 14th nucleotide of the 5' UTR where the P-element, P{GS:13084}, is inserted into the *ald* gene to analyze each excision line. The left primer: 5'--CATCACTCTCCCTCACTCAAAG--3' and the right primer: 5'--CCTCGTTTGGACTTGGAAAG--3' were used to amplify this region. 7 out of 8 excision lines were amplified, with the lone exception of Excision 14. The 0.1 kb - 10 kb New England Bio Lab ladder was used as a marker control. Excisions 25 & 30 appear to be approximately 475 base pairs (bp), Excisions 1 and 4 are approximately 530bp, and Excision 23 is approximately 600bp. The two large products, Excisions 15 and 26, appear to be approximately 2.6kb and 4.6kb, respectively.

The PCR products were then sequenced and are detailed in Appendix D, as well as the *ald* region with the full P{GS:13084} inserted into the 5'UTR as reference. The majority of these lines, with the exception of Excision 23, were not previously classified through sequencing.

Excisions 25 and 30 are shown to be precise excisions by sequence analysis, but Excision 25 has background levels of NDJ, whereas Excision 30 has about 10% NDJ. The sequences were aligned using ClustalW2 alignment software and can be seen in Appendix D. One difference between Excision 25 and all of the other lines was a single "C" nucleotide just upstream of the insertion site of P-element. The other 7 lines have a "T" in that position, as well as the reference sequence (Flybase.org).

Excision 1 and 4 resulted in two identical sequences, with statistically similar NDJ rates. These lines show a small insertion of 45 nucleotides of the P-element into the 5'UTR. Overlapping reads of the 3' and 5' end sequences of P{GS:13084} incorporate these 45 nucleotides (nt).

Excision 23 was previously sequenced and showed that it left 130 nt from the 5' end. When Excision 23 was sequenced this second time, the same 130 nt were still present. Consistent with the known P element transposition mechanism [54] 8 nt at the insertion site were also duplicated, except in lines 25 and 30, which reverted this duplication. Excisions 25 and 30 therefore have reverted the insertion, although 25 has the previously mentioned T to C change. Excisions 1 and 4 share the same 45 nt of remaining P element sequence, and Excision 23 contains 130 nt of P element sequence.

Excision 15 was shown, from PCR, to be approximately 2.6 kb, which indicates that approximately 2.1 kb of the P{GS:13084} sequence is inserted into the 5' UTR of *ald*.

Sequence reads from PCR primers could not sequence the entire 2.6 kb product; however, reads from the left and right were able to sequence about 750 nt from each direction. The sequence in Appendix D is approximately 1.5 kb, with a portion from the left and a portion of the right ends. These sequences showed the remaining sequence was rearranged. Within Excision 15, a small portion of the 3' end was evident in the sequence. The majority of the left read was part of the *mini-white* gene. The right read begins with another portion of the *mini-white* sequence as well; totaling approximately 900 nt of the *mini-white* sequence within the sequence of Excision 15. The alignment between Excision 15 and the *mini-white* sequence can be seen in Appendix E. Also in Excision 15, is the outward facing *Hsp70Bb* heat-shock promoter. Excision 15 has the entire sequence of the 5' end of the P{GS:13084} 5' sequence; however, a portion of the sequence is duplicated.

Excision 26 has approximately 4.1 kb of the P{GS:13084} sequence inserted into the 5' UTR, since the PCR indicated that the product size was about 4.6 kb. Like Excision 15, sequence reads were unsuccessful to sequence the entire 4.6 kb product; however, reads from the left and right were able to sequence about 750 nt from each direction. The sequence analysis shows that Excision 26 has both the 3' and 5' end sequences inserted into the genome. Like Excision 15, these sequences show some rearrangement of the P element. There are nucleotides within the sequence that does not necessarily match a known portion of the P{GS:13084}, but matches segments of non-coding sections of the 6.83 kb P{GS:13084} sequence. A segment of an untranslated region of the P-element, known as the SV40 3'UTR, is incorporated and duplicated into the Excision 26 line. There is evidence, from the right read, that some of the *mini-white* gene is present within

the Excision 26 sequence. As in Excision 15, the outward facing *Hsp70Bb* promoter is inserted in the sequence, along with the 5' end of the P-element.

Even though Excision 15 and 26 have part of the *mini-white* locus, the flies have white eyes like all of the other lines. Therefore the imprecise excision has rendered the *mini-white* gene nonfunctional in these lines, which under normal functioning circumstances would give the flies peach colored eyes. Both of these lines have the outward facing *Hsp70Bb* promoter, which is known to cause leaky transcription [2]. Parts of the P{GS:13084} sequence is inserted to some degree into each of these lines, with the exceptions being Excisions 25 and 30 (Figure 20). However, it varies from line to line, giving each line an unique NDJ rate. These DNA sequences did not indicate any flanking segments of DNA of the *ald* gene were deleted.

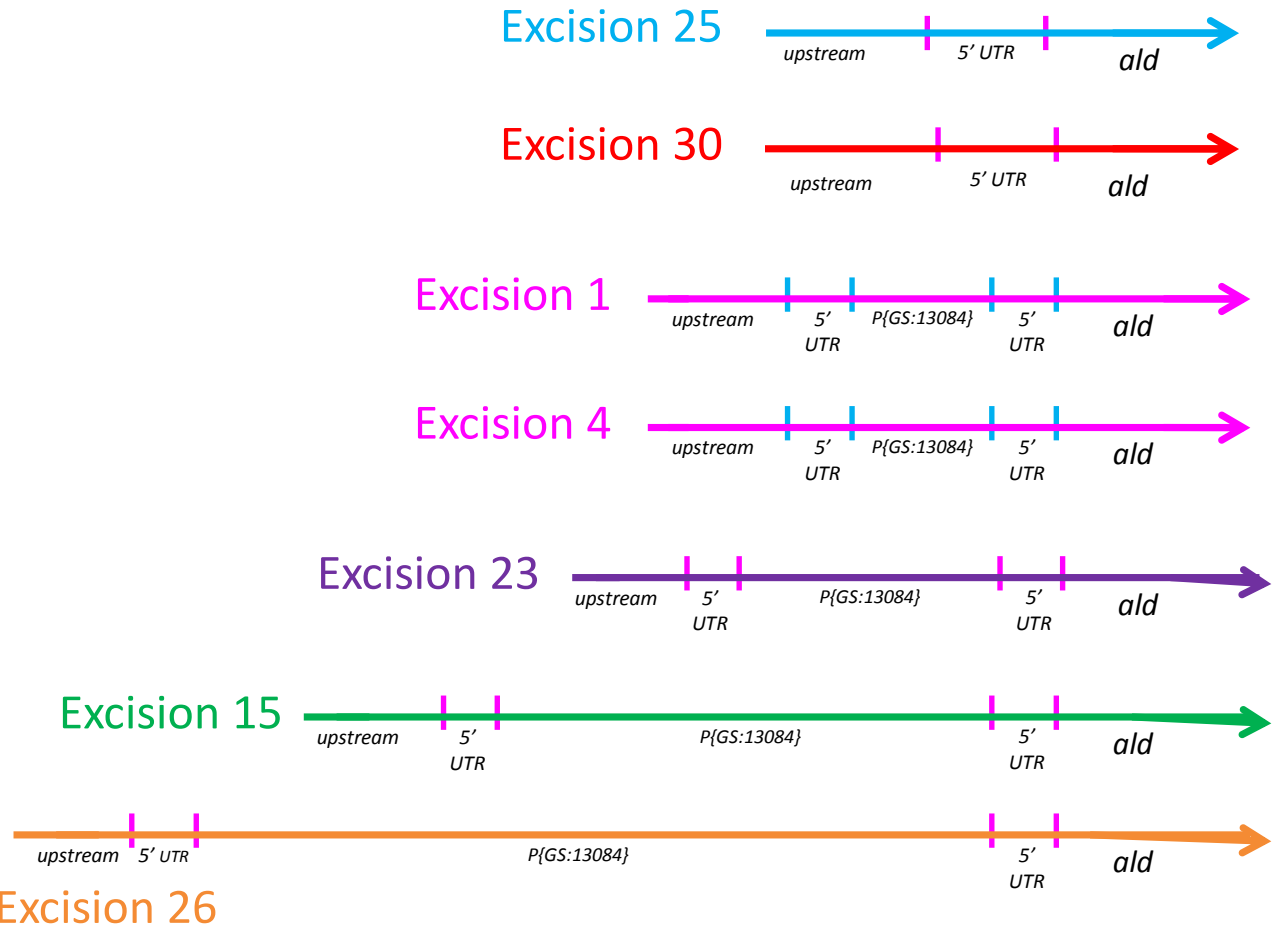


Figure 20. DNA sequence analyses of P{GS:13084} excision lines DNA from each excision line, *FM7/yw; Δ/Df(3R)AN6; pol*, was sequenced in order to examine the amount of the P{GS:13084} sequence that was inserted into the genome. Above shows a systematic representation of the amount of P-element was inserted into each line that was sequence, with the exception of Excision 14 since it was unable to be sequenced. Excisions 25 and 30 were shown to be precise excisions with no remaining P{GS:13084} inserted, Excision 1 and 4 were shown to have the same 45 nucleotides in common inserted into their genome, and Excision 23 was shown to have a 130 nucleotide insertion. Excision 15 and 26 had 2.1 and 4.1 kb inserted into their genomes, respectively. Full sequence analysis shown in Appendix D & E.

Excision 14 could not be amplified by PCR, so a series of other experiments were used to further classify how much, if any, of the 6.83 kb P-element was left within line. Excision 14 progeny have white eyes, indicating that some portion of the *mini-white* is missing. It is not certain how much, if any, of the sequence is present. The failure of the PCR reaction (even with a long extension time) suggests a large amount of the P element is still present, but the good viability of this line also indicates that the *ald* locus must still

be functional. Like the Excision 15, a large portion of the *mini-white* gene could still be present, but given the white eyes in this strain must be nonfunctional (Figure F1).

The 3' and 5' ends were attempted to be amplified to test for their presence. Figure F2 (Appendix F) shows that Excision 14 has the 3' end of the P{GS:13084} is still present, but the amplification was weak and could not be sequenced. The 5' end of the P-element was unable to be amplified through PCR, which suggests the internal primer was absent.

Excision 14 was also analyzed for the ability to produce *GFP*. As shown in Figure F3, the original P element contains a GFP gene at its 3' end, that could be expressed under UAS control when heat shocked. The observation of GFP indicates that the GFP gene in the Excision 14 line and its UAS promoter are intact. It is uncertain exactly how much of the P{GS:13084} is left in the genome since amplification failed, but the minimum elements still present are shown in Figure 21.



Figure 21. Components of the P{GS:13084}-excision 14 *ald* allele A systematic representation of the various components that comprise the 6.83 kb P-element, P{GS:13084}, that is inserted after the 14 nucleotide of the 5' UTR of the *ald* gene. Without any elimination of the components of the P-element, P{GS:13084} has an outward facing heat shock promoter, *Hsp70Bb*, as well as another *Hsp70Bb*, upstream of the Green Fluorescent Protein (*GFP*). The *GFP* is under the control of the *Hsp70Bb* region of the gene. Within the P-element, the *mini-white* gene, if present, which is a {w⁺} allele, gives the flies peach color eyes. Finally, the P-element is flanked by a 5' and 3' region on either end. Through the further classification of Excision 14, the *mini-white* gene has to either be eliminated or reduced to the point of malfunction of the gene since the flies have white eyes. The *GFP* analysis showed that the *GFP* protein, as well as the *UAS*, must still be present in the genome. When examined for the 5' and 3' ends, the 3' end was still present; however, the 5' end did not amplify through PCR.

VI. DISCUSSION

Until recently, it was thought that nondisjunction was caused due to the nonexchange chromosomes being trapped out on the spindle at metaphase I arrest since flies did not undergo congression. Theurkauf and Hawley developed a model in which *D. melanogaster* female meiosis was thought to undergo a form of "anti-congression" where the exchange chromosomes stayed at the metaphase plate while the nonexchange chromosomes were in a balanced configuration on opposite sides of the spindle [1, 37-40]. From this model, the explanation of how nonexchange chromosomes segregated was described since they were believed to enter prometaphase physically paired and then moved directly to opposite sides of the spindle to arrest at metaphase. This model also predicted that nondisjunction would result if both chromosomes moved onto the same arm of the spindle [1].

However, it was discovered that *Drosophila* undergo congression, in which the chromosomes are aligned at the spindle equator with their centromeres oriented towards opposite spindle poles [20]. The fact that all of the chromosomes undergo congression to return to the main compact, "lemon" shaped mass invalidated the old mechanism for NDJ for meiosis I [30]. So the question was raised as to what was the mechanistic basis of meiosis I nondisjunction under this new model? The hypothesis was that meiosis I nondisjunction was a result of the chromosomes being incorrectly cooriented during congression as they arrest in the "lemon" shaped mass at Metaphase I Arrest.

To examine these mechanisms under the new model, an allelic series of *ald* alleles generated from imprecise excision of a P-element, P{GS:13084}, in the 5' UTR from a single source chromosome. These P-element alleles range from precise excisions with

wildtype levels of NDJ to hypomorphic alleles with intermediate levels of NDJ to semi-lethal alleles that appear to have no remaining *ald* function [48]. These mutant alleles are dosage-dependent alleles, which change the amount of protein produced; however, the protein that is produced appears to be wildtype. These *ald* mutants are capable of completing congression, but have a wide range of NDJ rates, making them suitable to study female meiosis. So, a series of crosses were set up to test for *X* and *4* chromosome through a nondisjunction assay and were then compared cytologically to Immuno-FISH probed oocytes arrested at metaphase I for the coorientation of the chromosomes.

Consistent with the predictions of the hypothesis, it was discovered that these *ald* alleles showed a high correlation ($r=0.97$) between nondisjunction rates measured genetically and the misalignment of the chromosomes at metaphase I arrest measured cytologically. As both *X* and *4* chromosome nondisjunction increased so did the cytological malorientation of their chromosomes. Within the lines, nondisjunction was observed from background levels to high levels (~40%). When examining the *X* & *4* nondisjunction doubles, the heterologous doubles ($XX \leftrightarrow 44$, or the two *Xs* separating to the opposite pole of the two *4s*) were as much as 10 times more likely than the non-heterologous doubles ($XX44 \leftrightarrow \emptyset$, or both the *Xs* and *4s* segregating to the same pole). Even though the doubles were a small part of the overall sample size, the trend was observed in both the genetic and cytological assays in all 8 excision lines. The P-element excision lines were sequenced to study how much, if any, of the P{GS:13084} sequence was left within the 5' UTR of the *ald* gene. Two of the lines were identified as precise excisions ($\Delta 25$ & $\Delta 30$), Excisions 1 & 4 were identified as sharing a common sequence with a 45 nt fragment insertion, and Excision 23 left 130 nt from the 5' end of the P-

element sequence. The two largest insertions of sequence was that of Excisions 15 and 26, showing insertions of approximately 2.1 kb and 4.1 kb, respectively, of the P{GS:13084} sequence. Excision 14 was unable to be sequenced like the others, but was shown to have portions of the 3' end, *GFP* and *Hsp70Bb* fragments of the P{GS:13084} sequence inserted into that line's genome.

With the demonstration that chromosome congression takes place in *Drosophila* female meiosis [30] and that chromosomes can cross the spindle mid-zone multiple times to try to coorient themselves with their homolog [41], the model of how nondisjunction occurs was also rendered invalid. The findings support the hypothesis that NDJ is caused by chromosomes congressing to the "lemon" with maloriented chromosomes. The genetic nondisjunction rates for both the *X* and *4* chromosomes were highly correlated with the cytological malorientation rates ($r=0.97$). The sample sizes of the cytological analyses were significantly lower than the nondisjunction assay; however, the confidence intervals were below $\pm 6\%$ as expected for the size of this sample.

From previous research [2], it is known that some of these *ald* excision alleles vary the amount of protein produced, but produce protein that appears to be wildtype. Only Excision 23 was characterized under this research, but showed that Excision 23 produced considerably less protein than another precise excision, Excision 33, when tested. This would suggest the Ald dosage is inversely proportional to the nondisjunction rate. This is shown in the current data. Excision 25 has only background levels of nondisjunction, genetically and cytologically, whereas Excision 23 has high levels of nondisjunction approaching the level of random segregation. The other allele lines could

not be characterized by Western Blot analysis, but will be repeated to examine the amount of *ald* protein produced by each line.

The examination of the double nondisjunctional progeny, of both the heterologous and non-heterologous types, showed a significant difference between the two classes. The heterologous doubles, or the two *Xs* separating to the opposite pole of the two *4s*, were at least 10 times as likely than the non-heterologous doubles, or both the *Xs* and *4s* segregating to the same pole, in the genetic assay. The same trend was observed in the cytological assay, albeit at a lower extent than in the genetic assay, but still showed that this particular type of double nondisjunction was more likely. The heterologous double events showed a 1:1 relationship between the genetic assay and cytological assay, whereas the non-heterologous doubles did not. The $XX44 \leftrightarrow \emptyset$ doubles appeared to clump around 1-2% of the total progeny observed for each line, with the exception of Excision 23 (~6-7%). This may implicate a size constraint, within the "lemon," to package these chromosomes into the main mass. It could potentially be easier for the cell to package the two *Xs* and two *4s* on opposite poles, if double nondisjunction occurred, than the all four of those chromosomes on one side. The non-heterologous double lemons would appear abnormal, or lopsided, unless the autosomes nondisjoin too ($XX44 \leftrightarrow 2233$). However, this particular case with the autosomes nondisjoining too would be lethal and never would survive into adulthood, but could still be observed cytologically. When observing these non-heterologous doubles cytologically, the autosomes were not scored, but the difference between the genetic assay and cytologically assay was slight for the majority of lines. It would have been expected to see a more of a difference between the values, with the cytological numbers higher than those of the genetic assay.

From just this evidence, an actual mechanism cannot be isolated; however, further research into this problem will potentially provide evidence to describe the mechanism behind this finding.

The sequencing data provided insight into the actual components of what was left of the P{GS:13084} sequence in the 5' UTR of the *ald* gene. From previous work, Excision 25 was shown to be a precise excision of the P-element, leaving the 5' UTR uninterrupted, and through the current data was shown again to be a precise excision. Given that line has wildtype levels of nondisjunction, this suggests this line has precisely reverted the P element insertion. Also from previous work, Excision 23 was confirmed to have 130 nt from the 5' end of the P-element inserted into the sequence, along with the expected duplication of 8 nucleotides flanking the insertion site. It inserted 2 nt ("CA") after the 14th nt of the 5' UTR, right before the insertion of any P-element material, and also 6 nt ("ACCCCG"), at the end of the inserted material and before the 5' UTR resumed. These 8 nucleotides were a consequence the P-element transposase insertion mechanism [54]. Excisions 15 and 26 were the largest insertions, 2.1 kb and 4.1 kb, respectively. Both lines have reads from the left and right of the sequences, but due to sequence quality, the lines do not have complete sequences that overlap as in the other lines. Within Excision 15, contain portions of the 3' end and 5' ends of the P-element. A segment of the 5' end was actually duplicated into the sequence as well. Excision 15 contains a large amount of the *mini-white* gene; however, enough of the gene is missing that renders the gene nonfunctional, giving the flies white eyes. Finally, Excision 15 contains the *Hsp70Bb* protein. This protein causes leaky transcription, so since it is in line with *ald* coding sequence, it is most likely causing a small amount of transcription of

wildtype Ald protein, sufficient enough to cause ~10% NDJ. Excision 26, on the other hand, contains more components of the P{GS:13084} sequence. It contains both ends of the P-element, as well as some portion of the *mini-white* gene, but not enough of the gene to give the flies peach colored eyes. It also has a recognized 3' UTR region sequence and within this portion, it duplicates a segment a couple of times. Like Excision 15, Excision 26 also contains the *Hsp70Bb* outward facing heat-shock promoter. These excisions could have potentially died in other scenarios, but since the leaky transcription of some wildtype Ald protein is produced, they survive and only have ~10% NDJ. However, the amount of protein that these lines are producing still needs to be determined through Western Blot analysis. Excisions 15 and 26 still need to have complete sequences. With knowing portions of the sequence from the current data, primers can be used to amplify smaller sections of the DNA within the P-element to combine in order to give the completed sequence of each line.

Excision 30's sequence was a surprising result since a precise excision would be expected to have only background levels of nondisjunction; however, Excision 30 has approximately 10% NDJ. Excision 30 was one of the preliminary excisions that was shown to be lethal over a much larger deletion, *Df(3R)ED5780*. However, it had relatively low NDJ over *ald^l*, and had relatively low NDJ when over the smaller deficiency, *Df(3R)AN6*. Ultimately, the flies survived and were able to reproduce under this smaller deletion. To show ~10% nondisjunction with the precise excision of the P-element from the 14 nt insertion site of the 5' UTR, there has to be other factors involved in Excision 30. One possibility is that the P-element hopped to another area within the genome, but still able to affect the *ald* gene. P-elements are unpredictable and have the

ability to hop from chromosome to chromosome. Further research into this allele will have to be conducted in order to explain this line. First, Excision 30 needs to be crossed with the larger deficiency, *Df(3R)ED5780*, to test to see if the *Exc30/Df(3R)ED5780* survive or not. Another experiment could be to amplify other regions (i.e., further upstream) for the P{GS:13084} sequence.

Excision 14 was unable to be sequenced like the other lines. Through a series of other experiments, certain components were concluded to be part of the Excision 14 line. The presence of the 3' end was a very weak positive result as compared to the control (the P{GS:13084} stock) when doing the PCR. It needs to be replicated in order to confirm the results. One possible way of sequencing Excision 14 would be to try inverse polymerase chain reaction. Unlike the conventional PCR, inverse PCR allows PCR to be carried out even if only one sequence is available from which primers may be designed. Using inverse PCR may be useful in amplifying Excision 14 and ultimately be able to obtain the sequence.

A larger question remains unanswered from this evidence. The fact that these congression defects are setting up chromosome malorientation supports the underlying mechanism of meiosis I nondisjunction under the new model of metaphase I arrest. The mechanisms behind what causes these congression defects remain unclear. Are these congression defects caused by an error when balancing the chromosomes on the spindle or when packing the chromosomes within the "lemon" to arrest at metaphase? Further research including live imaging of the congression process could provide the evidence in order to define a mechanism.

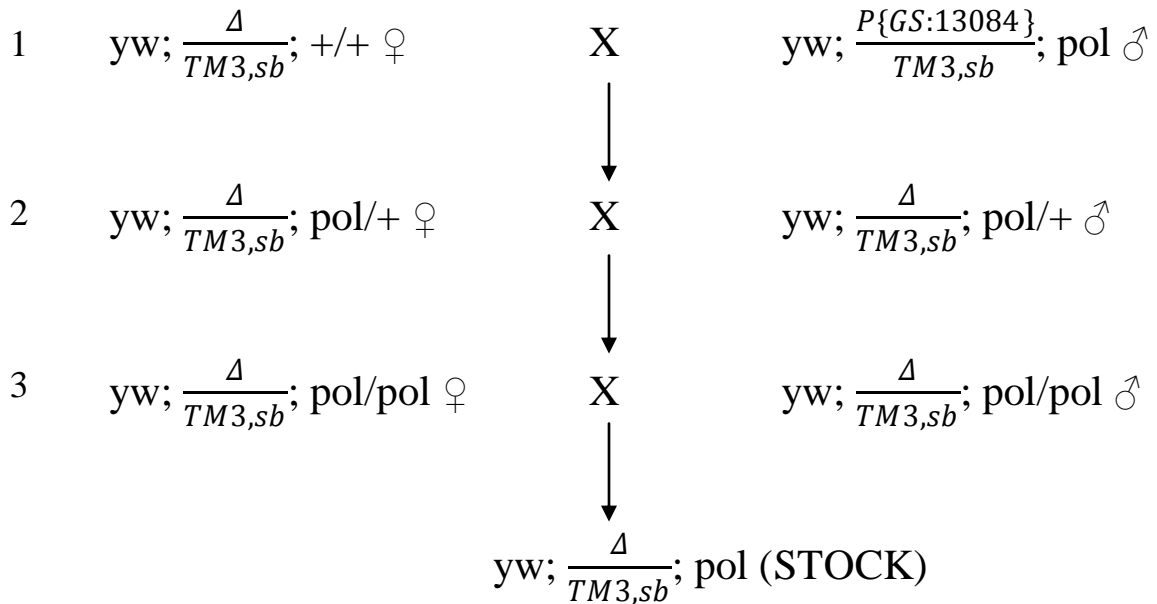
Some limitations of this experiment included the novel cytological approach of combining immunofluorescent localization and fluorescent *in situ* hybridization in *Drosophila* oocytes. Each protocol has been previously done in oocytes separately, but the combination of the two has not been done until now due to the chorion, which blocks antibody penetration. With previous FISH protocols, the stringency of the formamide washes were much higher in order to make the chorion permeable to the probes; however, with the combined protocol, they had to be reduced as to not wash away the antibody or other probes from the oocyte as discovered through numerous attempts to implement the protocol. There is room for further optimization, as there is still a large amount of background fluorescence when taking images on the confocal microscope. Another limitation of this experiment is with the calculation of the confidence intervals for the genetic assay. The confidence interval was calculated using the hierarchical-Poisson NDJ model [53]. However, this model was designed for X-only nondisjunction. Often in research, as in this experiment, X and 4 chromosome nondisjunction are measured simultaneously. So by using this hierarchical-Poisson NDJ model confidence interval calculation, the true confidence interval is underestimated for both chromosomes. This does not affect the overall conclusions based on the data since the intervals are underestimated; however, further research will hopefully provide a similar multinomial calculation for the 4-only and X & 4 double nondisjunction.

In conclusion, the experiment set out to correlate genetic nondisjunction rates with cytological chromosome malorientation rates at metaphase I arrest in an attempt to understand the mechanisms by which meiosis I nondisjunction occurs under the new model of metaphase I arrest. Using a *Drosophila* homolog of the spindle checkpoint

protein, *mps1*, a series of crosses with an allelic series of *ald* mutants with varying nondisjunction rates were set up in order to test whether or not congression defects that cause the chromosomes to misalign as they proceed from prometaphase to the metaphase I "lemon" arrest stage is the ultimate cause of meiosis I nondisjunction. Understanding this process in flies further could potentially lead to a better understanding of nondisjunction in the female germline of humans, in which it commonly causes a range of issues from miscarriages to diseases like Down syndrome, or Trisomy 21. This *mps1* gene is widely conserved and, like flies, humans have a homolog of this gene. Accurate segregation of the chromosomes is a dosage-sensitive system and the better understanding of how the fly system responds to changes in the amount of this protein is important in further understanding this process. Further research in meiosis I and mechanisms by which nondisjunction occurs could potentially provide a better understanding and ultimately aid in the prevention of diseases such as Down syndrome.

VII. APPENDIX A - Fly Crosses & Visible Markers

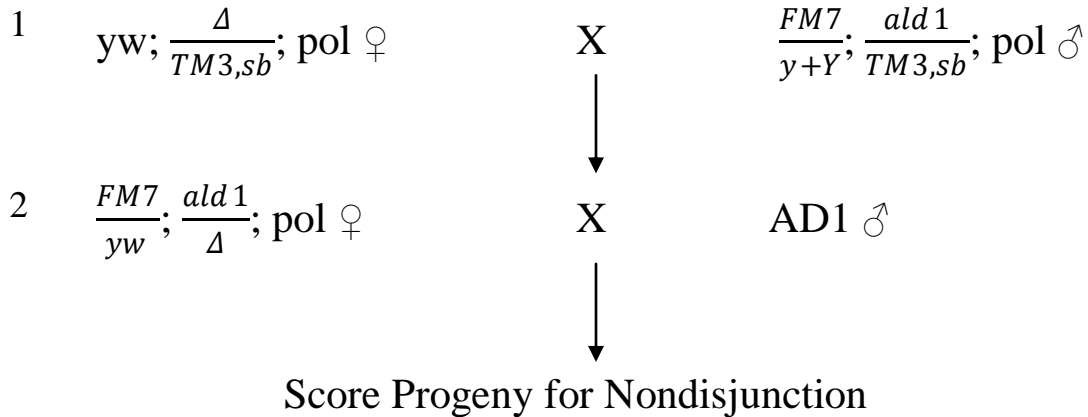
Stock Fly Crosses



Δ = each excision

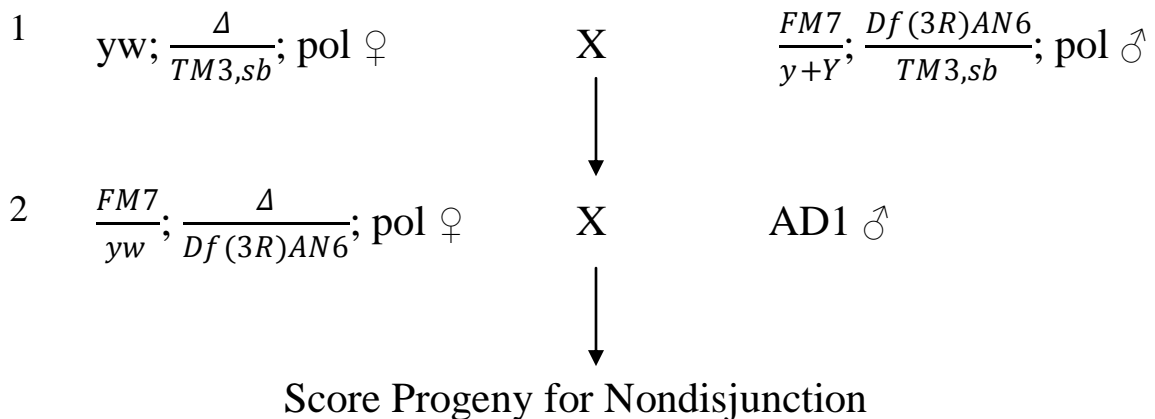
A series of fly crosses using different excisions of the P-element allele $ald^{P\{GS:13084\}}$, was done to test progeny of the various alleles of the *ald* gene. These excisions were generated in a previous study [48] and had been maintained by Dr. William Gilliland. In cross 1, the excision stocks for each line were crossed with the homozygous *poliert* P-element stock. Hemizygous *poliert*, white eyed males and females were collected. These progeny were able to be differentiated through eye color, since progeny with a copy of the P{GS:13084} allele have orange eyes. Cross 2 and 3 were sibmated each generation in order to make each line homozygous for the chromosome 4 marker *poliert* (*pol*) in order to test for 4 chromosome nondisjunction. These flies will have white eyes from the *white* (*w*) allele, but also the eye surface will be glazed and shiny, like glass, without individual eye facets, which can be differentiated from others that will have compound eyes with individual eye facets.

Preliminary Fly Crosses



Once the $yw; \Delta/TM3, sb; pol$ stock for each line was created (as previously shown), females were crossed to $FM7/y+Y; ald^1/TM3, Sb; pol$ males (which have brown bodies, white shiny eyes, and short bristles) (cross 1), picking up $FM7/yw; ald^1/\Delta; pol$ virgin females for each excision. $FM7$ is a balancer chromosome, and when heterozygous with a normal sequence X, will prevent the X chromosomes from recombining [50]. These $FM7/yw; ald^1/\Delta; pol$ females were differentiated from other progeny by their bristles. These white eyed females were Sb^+ , or had long straight bristles, whereas other progeny were Sb^- , or had short bristles. These females from the cross were then crossed with the males of the tester stock, $AD1$, (cross 2) and their progeny were scored for nondisjunction.

Secondary Fly Crosses



Once the $yw; \Delta/TM3, sb; pol$ stock for each line was created (as previously shown), females were crossed to $FM7/y+Y; Df(3R)AN6/TM3, Sb; pol$ males (cross 1), picking up $FM7/yw; Df(3R)AN6/\Delta; pol$ virgin females for each excision. These $FM7/yw; Df(3R)AN6/\Delta; pol$ females were differentiated from other progeny as previously described. These females from the cross were then crossed with the males of the tester stock, $AD1$, (cross 2) and their progeny were scored for nondisjunction.

X Outcomes

	$FM7$ or yw	\emptyset	$FM7/yw$
$\widehat{X}Y,$ $v f B$	$FM7/attached-X Y, v f B$ or $yw/attached-X Y v f B$ ♀	$attached-X Y, v f B/\emptyset$ ♂ Brown body, vermilion eye color, forked bristles, Bar eyes males ($y^+ w^+ v^- f^- B^-$)	Do not survive into adulthood
\emptyset	$FM7/\emptyset$ or yw/\emptyset ♂ Yellow body, white eye males ($y^- w^- v^+ f^+ B^+$)	Do not survive into adulthood	$FM7/yw$ ♀ Yellow body, white eye females ($y^- w^- v^+ f^+ B^+$)

Figure A1. X chromosome progeny outcomes A systematic representation of the potential outcomes for the progeny of the nondisjunction assay for the X chromosome. The female's potential gametes are shown along the top, with 3 possibilities: one of the two achiasmate Xs, no X, or both Xs into the same gamete. The AD1 tester stock male's gametes are listed vertically on the side. With the AD1 cross, visible markers are attached within this genome to both the X and 4 in order to provide a phenotypic difference between the progeny if nondisjunction occurred in the female germline. The top and bottom left boxes show the normal progeny, whereas the *attached X-Y, v f B* and *FM7/yw* progeny are X nondisjunctional progeny. Two progeny classes (00 and XXX) do not survive into adulthood.

4 Outcomes

	<i>pol</i>	\emptyset	<i>pol/pol</i>
 <i>C(4)RM, ci ey^R</i>	<i>C(4)RM, ci ey^R / pol</i> Normal compound eye, with separated facets (<i>ci⁺ ey^{R+} pol⁺</i>)	<i>C(4)RM, ci ey^R / \emptyset</i> Wing vein interrupted, eye will range from being reduced to completely missing (<i>ci ey^{R-} pol⁺</i>)	Do not survive into adulthood
\emptyset	<i>pol / \emptyset</i> <i>minute*</i> Eye surface is glazed over and shiny like glass (<i>pol</i>)	Do not survive into adulthood	<i>pol / pol</i> Eye surface is glazed over and shiny like glass (<i>pol</i>)

Figure A2. Chromosome 4 progeny outcomes A systematic representation of the potential outcomes for the progeny of the nondisjunction assay for the 4 chromosome. The female's potential gametes are shown along the top, with 3 possibilities: one of the two achiasmate 4s, no 4, or both 4s into the same gamete. The AD1 tester stock male's gametes are listed vertically on the side. With the AD1 cross, visible markers are attached within this genome to both the X and 4 in order to provide a phenotypic difference between the progeny if nondisjunction occurred in the female germline. The *C(4)RM, ci ey^R* is a compound chromosome which has two 4 chromosomes attached to form one chromosome. The *C(4)RM/pol* class are the normal progeny with wildtype eyes, whereas the homozygous *pol/pol* class arose from nondisjunction in the maternal germline. The 4-haploid *minute* category, *pol/ \emptyset* , have a single copy of chromosome 4. This chromosome contains important rDNA genes, and reduces the amount of protein the fly can make by 50%. The flies are very sick, with shorter and thinner bristles than normal. Their eyes are *pol* because they are hemizygous for that mutant chromosome. Because their survival is highly variable, they need to be identified and excluded from analysis. Two progeny classes ($\emptyset\emptyset$ and *C(4)RM/pol/pol*) do not survive into adulthood.

Visible Markers

X-Linked Markers:

yellow (y): The body color is golden brown (Wildtype body color is coffee brown).

white (w): The eye color is white (Wildtype eyes are brick red in color).

Bar (B): This is a dominant gene that affects the shape of the eye:

Wildtypes (+/+) have oval eyes

Hemizygotes (B/+) have kidney bean eyes

Homozygote females (B/B) (and B/Y males) have narrow slit-shaped eyes

vermillion (v): The eye color is a bright orange-red

forked (f): The bristles along the back are shorter, twisted and split (Wildtype bristles are long and straight)

4-Linked Markers:

poliert (pol): The eye surface texture is glazed over and shiny without any individual facets (Wildtype eyes are compound eyes with individual facets).

cubitus interruptus (ci): A vein on the wing, the cubitus vein, is either noncontiguous or missing. (Wildtype cubitus vein is continuous).

eyeless, Russian allele (ey^R): The eye is round instead of typically being oval and smaller. With this allele, the penetrance can vary ranging from the eye being smaller than normal to completely absent.

Nondisjunctional Assay Progeny

Normal Progeny:

Normal Male (X 4): yw or $yw B$

Normal Female (X 4): $yw/v f B$ or $FM7 yw B/ v f B$

4-Only Nondisjunctional Progeny:

Null-4 Male (X Ø): $yw; ci ey^R$ or $yw B; ci ey^R$

Null-4 Female (X Ø): $B; ci ey^R$

Diplo-4 Male (X 44): $yw; pol$ or $yw B; pol$

Diplo-4 Female (X 44): $B; pol$

X-Only Nondisjunctional Progeny:

Null-X Male (Ø 4): $v f B$

Diplo-X Female (XX 4): $yw B$

X and 4 Double Nondisjunctional Progeny:

Null-X Diplo-4 Male (Ø 44): $v f B; pol$

Diplo-X Null-4 Female (XX Ø): $yw B; ci ey^R$

Null-X Null-4 Male (Ø Ø): $v f B; ci ey^R$

Diplo-X Diplo-4 Female (XX 44): $yw B; pol$

VIII. APPENDIX B: Supplementary Data

A			B		
<i>Excision</i>	<i>X NDJ (%)</i>	<i>Sample Size</i>	<i>Excisions</i>	<i>4 NDJ (%)</i>	<i>Sample Size</i>
*25	2.3	344	21	2.1	1292
*30	6.2	1157	*25	2.6	344
2	8.7	1172	*26	3.1	1058
38	9.3	1427	34	3.5	313
*1	9.8	266	17	3.6	982
22	12.1	943	31	3.7	374
34	12.8	313	22	3.8	943
*26	13.0	1058	18	4.2	1097
5	13.3	813	5	5.0	813
31	13.9	374	38	5.7	1427
18	14.8	1097	2	7.4	1172
*15	14.9	308	*30	7.7	1157
21	15.2	1292	*15	8.8	308
17	15.5	982	*23	9.0	619
20	15.9	893	35	12.2	492
*14	18.6	506	*1	12.4	266
*4	25.9	85	20	12.5	893
35	26.4	492	11	14.3	926
36	28.6	748	*14	15.0	506
13	28.9	166	13	15.1	166
*23	29.7	619	36	16.2	748
11	32.6	926	29	22.0	468
29	37.2	468	6	22.5	356
6	41.0	356	*4	32.9	85

Table B1. Preliminary nondisjunction assay of excision lines "A" shows the nondisjunction rates for the X chromosome for females for each excision line *FM7/yw; ald¹/ald^{P(GS:1-3084)-excision}; pol* crossed to *C(1,Y), v f B; C(4)RM, ci ey^R* (AD1) males. The rates are in ascending order with a range of 2.3% to 41.0% nondisjunction of varying sample sizes. "B" shows the nondisjunction rates for the 4 chromosome for females for each excision line *FM7/yw; ald¹/Δ; pol* crossed to *C(1,Y), v f B; C(4)RM, ci ey^R* males. The rates are in ascending order with a range of 2.1% to 32.9% nondisjunction of varying sample sizes. The excision lines, noted by an asterisk (*) and bolded, were chosen to further examine their NDJ rates in a secondary round of crosses with a larger sample size and to be compared cytologically as well.

Excision	Z Score for X	Z Score for 4
	B1: B2	B1: B2
<i>1</i>	0.272	0.112
<i>4</i>	1.872	1.96
<i>14</i>	0.583	0.404
<i>15</i>	0.084	1.96
<i>23</i>	0.161	0.604
<i>25</i>	1.303	0.732
<i>26</i>	1.005	1.707
<i>30</i>	1.555	1.96

Table B2. Statistical significance between broods Genetic NDJ rates for the *ald* alleles were assayed in *FM7/yw; Δ/Df(3R)AN6; pol* hemizygotes and measured by counting progeny. After day 5, the females and males were transferred to a new vial, or brooded, to increase the sampling total. The sample sizes in Tables 2 and 3 are a result of the addition of the two broods. The statistical difference between the nondisjunction rates were tested between broods 1 and 2 to ensure that there was no difference. The sampling difference was calculated using a cut-off of $|Z| \leq 1.96$ at $\alpha=.05$ [53]. Examining the data, there was no statistical difference between broods 1 and 2 for any line. The values range from 0.084 to 1.96; however, all fall within the range of showing no statistical difference between the two broods.

Excision	Genetic Analysis		Ratio	Cytological Analysis		Ratio
	XX 44	XX44 0		XX 44	XX44 0	
1	33	1	33	9	3	3
4	55	2	27.5	10	1	10
14	35	6	5.8	10	2	5
15	37	4	9.2	5	2	2.5
23	143	45	3.2	19	13	1.5
25	5	0	0	0	0	0
26	36	3	12	15	8	1.9
30	24	2	12	6	2	3

Table B3. Heterologous and Non-heterologous doubles Genetic NDJ rates for the *ald* alleles were assayed in *FM7/yw; Δ/Df(3R)AN6; pol* hemizygotes and measured by counting progeny. Virgin females of the same genotype for each excision line were fixed, Immuno-FISH probed, and oocytes were scored for chromosome coorientation at metaphase I arrest. The double nondisjunction progeny, $XX \leftrightarrow 44$ and $XX44 \leftrightarrow \emptyset$, were counted in both the genetic and cytological assay, raw numbers shown above. The heterologous doubles, $XX \leftrightarrow 44$, were much more likely than the non-heterologous doubles, $XX44 \leftrightarrow \emptyset$. In the lines, the heterologous doubles were seen to be at least 10 times more likely. Even though the cytological ratios are not as high as the genetic ratios, the trend seemed to be consistent with the heterologous doubles being the more likely case when looking at the double nondisjunctional progeny within that sample size.

Genetic % Heterologous	Cytological % Heterologous	Excision	Genetic % Non-Heterologous	Cytological % Non-Heterologous
2.60	4.41	1	0.16	1.47
2.66	4.59	4	0.19	0.46
3.19	4.33	14	1.09	0.87
1.59	2.45	15	0.34	0.98
12.31	8.88	23	7.75	6.07
0.41	0.00	25	0.00	0.00
3.35	6.00	26	0.56	3.20
2.05	2.91	30	0.34	0.97

Table B4. Percent Heterologous and Non-heterologous doubles Genetic NDJ rates for the *ald* alleles were assayed in *FM7/yw; Δ/Df(3R)AN6; pol* hemizygotes and measured by counting progeny. Virgin females of the same genotype for each excision line were fixed, Immuno-FISH probed, and oocytes were scored for chromosome coorientation at metaphase I arrest. The double nondisjunction progeny, $XX \leftrightarrow 44$ and $XX44 \leftrightarrow \emptyset$, were counted in both the genetic and cytological assay, raw numbers shown above in Table 5. The heterologous doubles, $XX \leftrightarrow 44$, were much more likely than the non-heterologous doubles, $XX44 \leftrightarrow \emptyset$. In the lines, the heterologous doubles were compared as a percent of the total progeny for the genetic assay and cytologically. Within an acceptable amount of error, the results show a direct correlation between the genetic and cytological % heterologous doubles. On the other hand, the non-heterologous doubles do not seem to follow that same trend. Once again, showing that heterologous doubles are much more likely than the non-heterologous doubles.

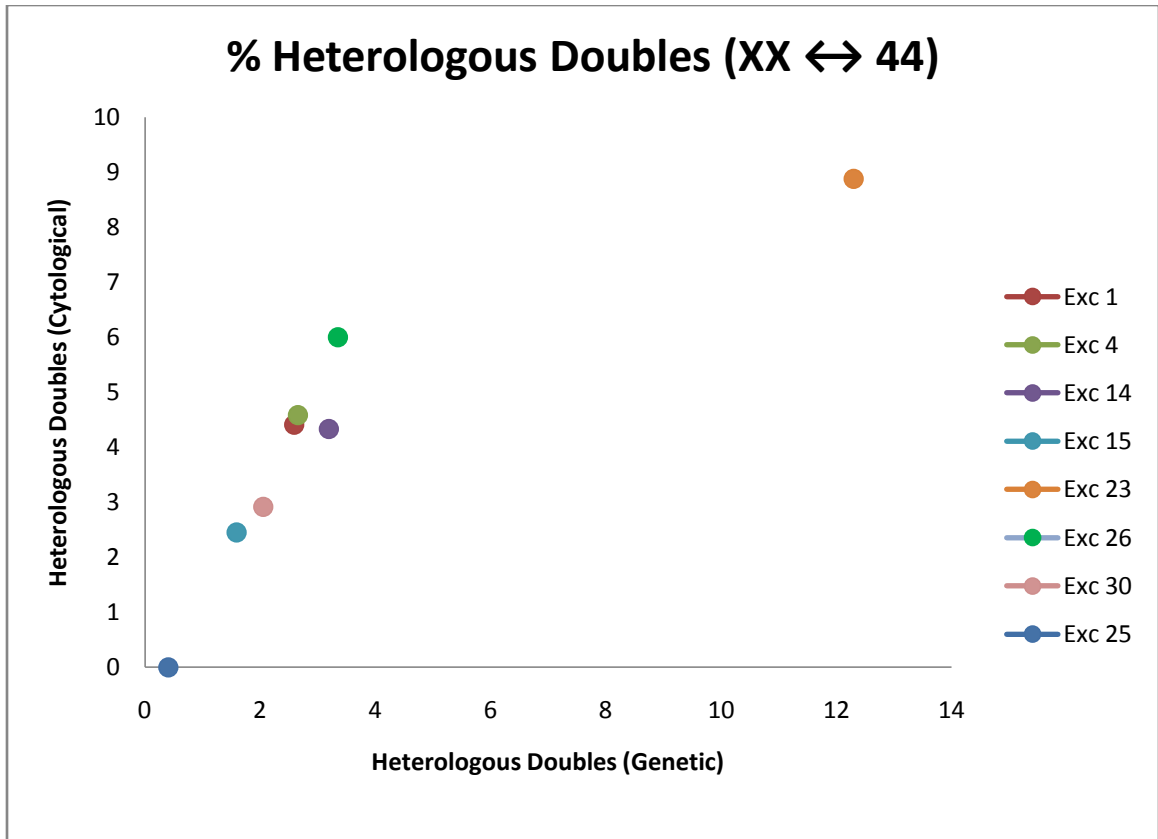


Figure B1. Percent Heterologous doubles Genetic NDJ rates for the *ald* alleles were assayed in *FM7/yw; Δ/Df(3R)AN6; pol* hemizygotes and measured by counting progeny. Virgin females of the same genotype for each excision line were fixed, Immuno-FISH probed, and oocytes were scored for chromosome coorientation at metaphase I arrest. The double nondisjunction progeny, $XX \leftrightarrow 44$, were scored in both the genetic and cytological assay. The percent doubles of the total progeny for the genetic and cytological assays appear to be directly correlated within reasonable error.

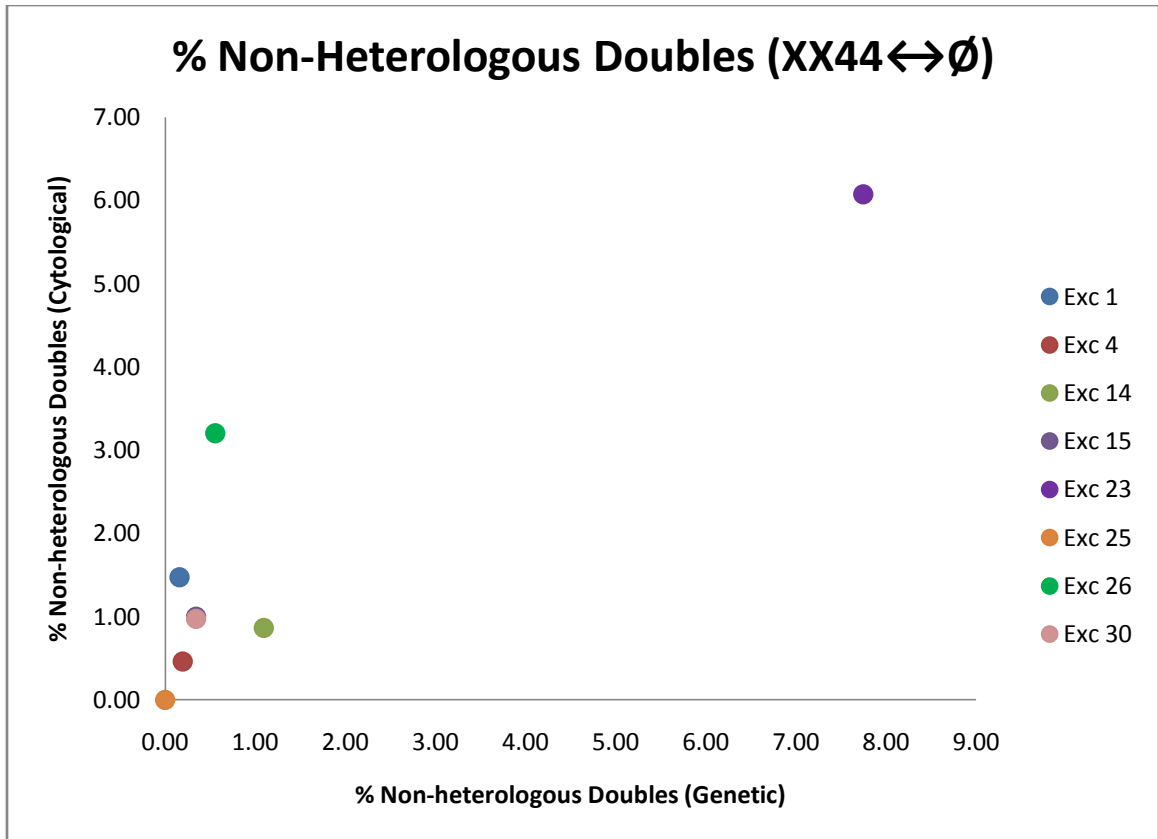


Figure B2. Percent Non-heterologous doubles Genetic NDJ rates for the *ald* alleles were assayed in *FM7/yw; ΔDf(3R)AN6; pol* hemizygotes and measured by counting progeny. Virgin females of the same genotype for each excision line were fixed, Immuno-FISH probed, and oocytes were scored for chromosome coorientation at metaphase I arrest. The double nondisjunction progeny, $XX44 \leftrightarrow \emptyset$, were counted in both the genetic and cytological assay. The percent doubles of the total progeny for the genetic and cytological assays appear to not be as correlated as the heterologous doubles. Most of the lines appear to have 1-2% of non-heterologous doubles, with the exception being Excision 23 having roughly 6%. This shows that non-heterologous double events are again much less likely to occur than the heterologous doubles.

A. GENETIC NDJ					
<i>Excision</i>	X NDJ		<i>Excision</i>	4 NDJ	
	95% Confidence Interval (%)	Error Bars (%)		95% Confidence Interval (%)	Error Bars (%)
1	4.27	±2.14	1	3.86	±1.93
4	3.35	±1.68	4	3.1	±1.55
14	4.6	±2.3	14	4.54	±2.27
15	2.87	±1.44	15	2.61	±1.30
23	5.56	±2.78	23	5.34	±2.67
25	1.33	±0.66	25	1.17	±0.59
26	4.98	±2.49	26	4.54	±2.27
30	4.38	±2.19	30	4.03	±2.02

B. CYTOLOGICAL NDJ					
<i>Excision</i>	X NDJ		<i>Excision</i>	4 NDJ	
	95% Confidence Interval (%)	Error Bars (%)		95% Confidence Interval (%)	Error Bars (%)
1	9.84	±4.92	1	9.2	±4.6
4	9.39	±4.70	4	7.55	±3.78
14	8.56	±4.28	14	7.61	±3.81
15	8.22	±4.11	15	7.46	±3.73
23	12.73	±6.37	23	12.35	±6.18
25	2	±1.0	25	2	±1.0
26	9.5	±4.75	26	8.61	±4.31
30	8.79	±3.4	30	6.52	±3.26

Table B5. 95% Confidence Intervals for genetic and cytological assays Genetic NDJ rates for the *ald* alleles were assayed in *FM7/yw; Δ/Df(3R)AN6; pol* hemizygotes and measured by counting progeny. Virgin females of the same genotype for each excision line were fixed, Immuno-FISH probed, and oocytes were scored for chromosome coorientation at metaphase I arrest. For each genetically assayed line, 95% confidence interval error bars were calculated by the standard binomial confidence interval. For each cytologically assayed line, 95% confidence interval error bars were calculated by the hierarchical-Poisson NDJ model [53]. The genetically assayed showed a confidence interval for all lines of $\leq \pm 2.78\%$ for the X chromosome and $\leq \pm 2.27\%$ for the 4 chromosome. The cytologically assayed showed higher confidence intervals for both the X and 4 chromosomes; however the sample size difference was significant, with the genetic assay of ≥ 2000 and the cytological assay of approximately 200. Most of the lines, for both the X and 4 chromosomes, showed a $\leq \pm 5\%$ confidence interval with the exception of Excision 23, which showed a confidence interval of approximately $\pm 6\%$

IX. APPENDIX C: Cytology Images

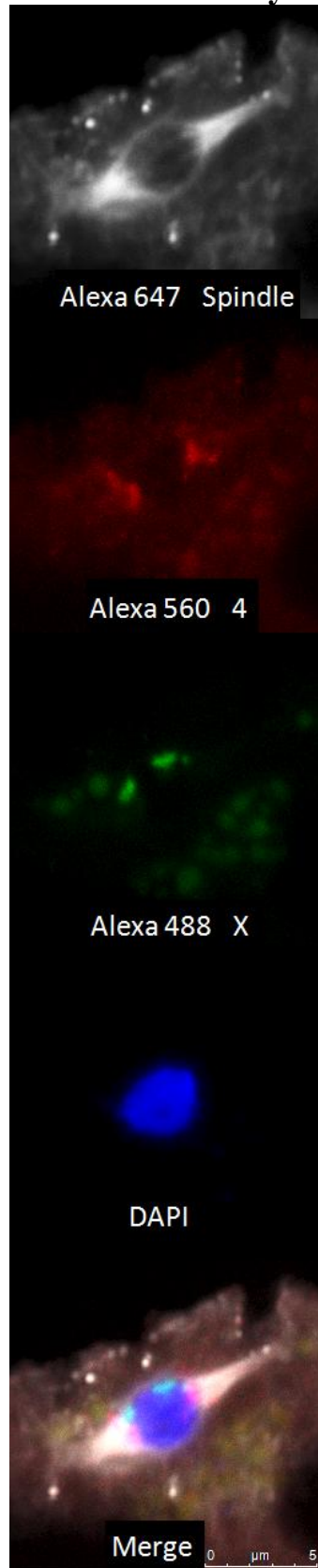


Figure C1. Cytological coorientation of X and 4 chromosomes Four day post-eclosion, virgin females, *FM7/yw; $\Delta/Df(3R)AN6; pol$* ; were fixed, Immuno-FISH probed and stained with DAPI. Approximately 200 oocytes were scored for each line for the coorientation of the X and 4 chromosomes within the "lemon" at metaphase I arrest. The 359-bp satellite block on the X chromosome, tagged with Alexa Fluor 488 (shown in green) and the AAT-AT-repeating sequence recognizing the 4 chromosome, as well as a small region on the X chromosome, tagged with Alexa Fluor 560 (shown in red) was used as FISH probes to measure chromosome coorientation. The meiotic spindle (shown in gray) was probed through immunofluorescent, using a secondary antibody tagged with Alexa Fluor 647, to detect the tubulin of the spindle. The nuclear DNA was stained with DAPI. Panels (from top left to bottom center): Meiotic spindle, 4 chromosome, X chromosome, nuclear DNA, and the merge of all four channels with micrometer ruler) This shows that both the X and 4 chromosomes are cooriented (aligned) properly to opposite poles on the spindle.

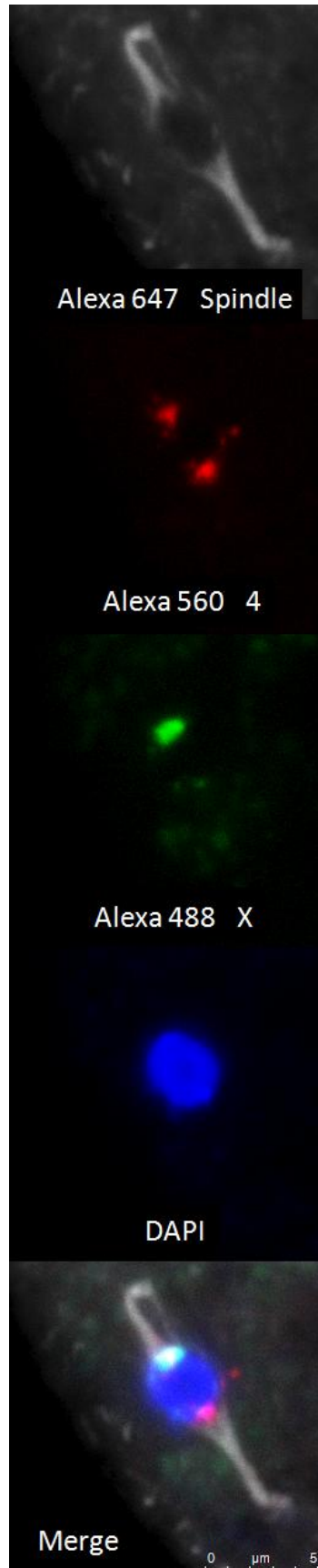


Figure C2. Cytological X-only NDJ Four day post-eclosion, virgin females, *FM7/yw; Δ/Df(3R)AN6; pol*; were fixed, Immuno-FISH probed and stained with DAPI. Approximately 200 oocytes were scored for each line for the coorientation of the X and 4 chromosomes within the "lemon" at metaphase I arrest. The 359-bp satellite block on the X chromosome, tagged with Alexa Fluor 488 (shown in green) and the AAT-AT-repeating sequence recognizing the 4 chromosome, as well as a small region on the X chromosome, tagged with Alexa Fluor 560 (shown in red) was used as FISH probes to measure chromosome coorientation. The meiotic spindle (shown in gray) was probed through immunofluorescent, using a secondary antibody tagged with Alexa Fluor 647, to detect the tubulin of the spindle. The nuclear DNA was stained with DAPI. Panels (from top left to bottom center): Meiotic spindle, 4 chromosome, X chromosome, nuclear DNA, and the merge of all four channels with micrometer ruler) This shows that the 4 chromosomes are cooriented properly to opposite poles on the spindle. The two X chromosomes are aligned to the same pole within the "lemon," which would proceed through meiosis resulting in an aneuploid gamete with regards to the X chromosome.

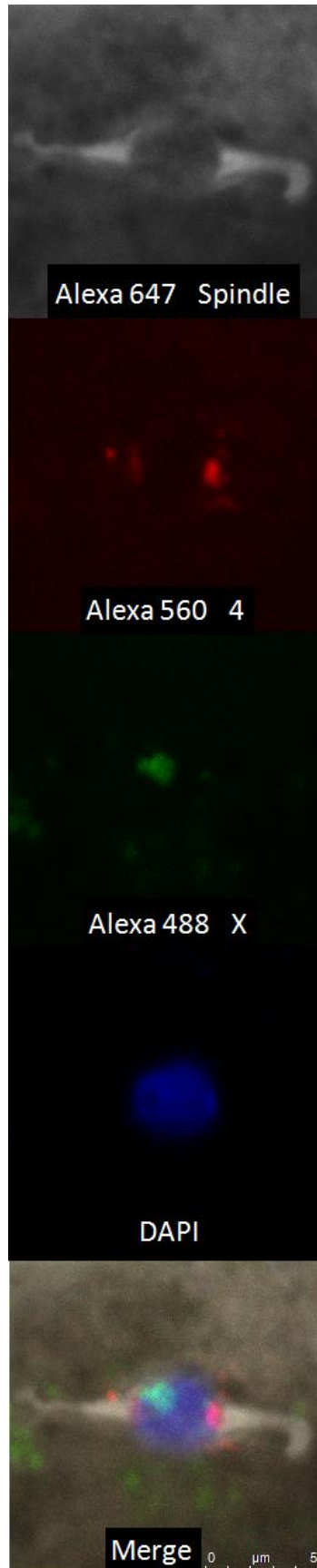


Figure C3. Cytological 4-only NDJ Four day post-eclosion, virgin females, *FM7/yw; Δ/Df(3R)AN6; pol*; were fixed, Immuno-FISH probed and stained with DAPI. Approximately 200 oocytes were scored for each line for the coorientation of the X and 4 chromosomes within the "lemon" at metaphase I arrest. The 359-bp satellite block on the X chromosome, tagged with Alexa Fluor 488 (shown in green) and the AAT-AT-repeating sequence recognizing the 4 chromosome, as well as a small region on the X chromosome, tagged with Alexa Fluor 560 (shown in red) was used as FISH probes to measure chromosome coorientation. The meiotic spindle (shown in gray) was probed through immunofluorescent, using a secondary antibody tagged with Alexa Fluor 647, to detect the tubulin of the spindle. The nuclear DNA was stained with DAPI. Panels (from top left to bottom center): Meiotic spindle, 4 chromosome, X chromosome, nuclear DNA, and the merge of all four channels with micrometer ruler) This shows that the X chromosomes are cooriented properly to opposite poles on the spindle. The two 4 chromosomes are aligned to the same pole within the "lemon," which would proceed through meiosis resulting in an aneuploid gamete with regards to the 4 chromosome.

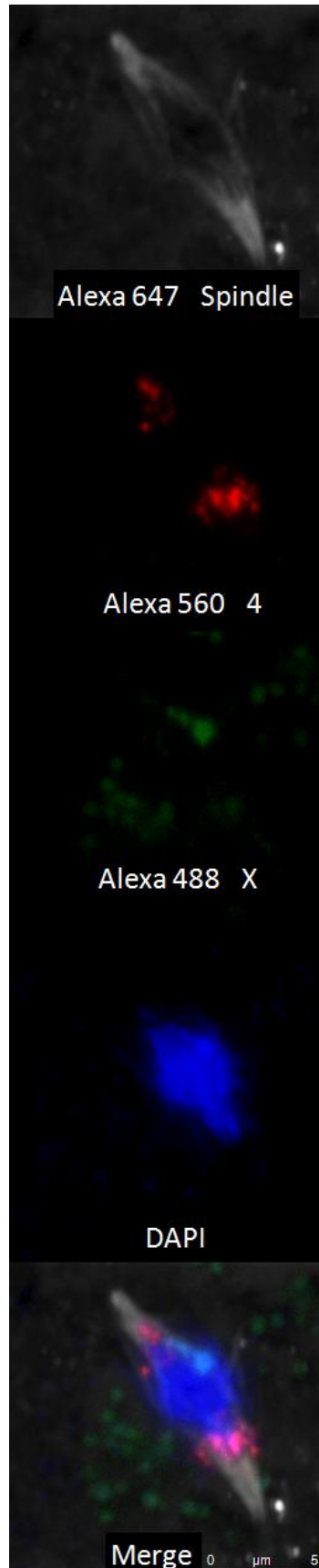


Figure C4. Cytological heterologous segregation double NDJ Four day post-eclosion, virgin females, *FM7/yw; Δ/Df(3R)AN6; pol;* were fixed, Immuno-FISH probed and stained with DAPI. Approximately 200 oocytes were scored for the coorientation of the *X* and *4* chromosomes within the "lemon" at metaphase I arrest. The 359-bp satellite block on the *X* chromosome, tagged with Alexa Fluor 488 (shown in green) and the AAT-AT-repeating sequence recognizing the *4* chromosome, as well as a small region on the *X* chromosome, tagged with Alexa Fluor 560 (shown in red) was used as FISH probes to measure chromosome coorientation. The meiotic spindle (shown in gray) was probed through immunofluorescent, using a secondary antibody tagged with Alexa Fluor 647, to detect the tubulin of the spindle. The nuclear DNA was stained with DAPI.

Panels (from top left to bottom center): Meiotic spindle, *4* chromosome, *X* chromosome, nuclear DNA, and the merge of all four channels with micrometer ruler). The two *X* chromosomes are aligned at on pole, whereas the two *4* chromosomes are at the opposite pole. This resulted from double nondisjunction of the heterologous *X* & *4* chromosomes ($XX \leftrightarrow 44$), and would proceed through meiosis to create gametes with 2 *X* chromosomes (and no *4s*) and vice versa with the *4* chromosomes. When double nondisjunction occurred in the lines, the heterologous segregation doubles were shown to be at least 1.5 times as likely non-heterologous segregation doubles to as much 10 times the number of non-heterologous doubles.

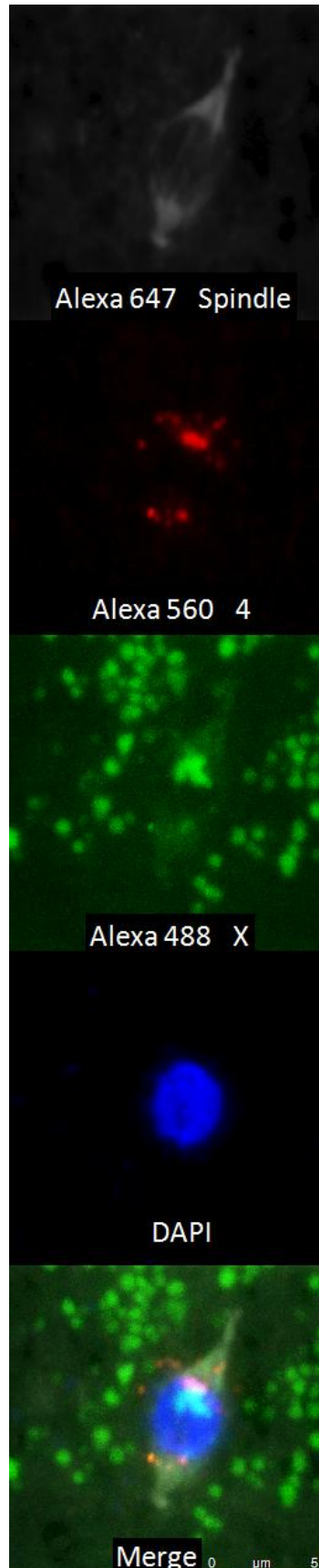


Figure C5. Cytological non-heterologous double NDJ

Four day post-eclosion, virgin females, *FM7/yw; Δ/Df(3R)AN6; pol*; were fixed, Immuno-FISH probed and stained with DAPI.

Approximately 200 oocytes were scored for each line for the coorientation of the *X* and *4* chromosomes within the "lemon" at metaphase I arrest. The 359-bp satellite block on the *X* chromosome, tagged with Alexa Fluor 488 (shown in green) and the AAT-AT-repeating sequence recognizing the *4* chromosome, as well as a small region on the *X* chromosome, tagged with Alexa Fluor 560 (shown in red) was used as FISH probes to measure chromosome coorientation.

The meiotic spindle (shown in gray) was probed through immunofluorescent, using a secondary antibody tagged with Alexa Fluor 647, to detect the tubulin of the spindle. The nuclear DNA was stained with DAPI. Panels (from top left to bottom center):

Meiotic spindle, *4* chromosome, *X* chromosome, nuclear DNA, and the merge of all four channels with micrometer ruler) The two *X* chromosomes and two *4* chromosomes are aligned at the same pole, with no *X* or *4* chromosome on the other pole. This resulted from

double nondisjunction of the *X* & *4* chromosomes ($XX44 \leftrightarrow \emptyset$), and would proceed through meiosis to create gametes with 2 *X* & *4* chromosomes and the other would have neither an *X* or *4*.

When double nondisjunction occurred in the lines, the heterologous segregation doubles were shown to be at least 1.5 times as likely non-heterologous segregation doubles to as much 10 times the number of non-heterologous

doubles.

X. APPENDIX D: Consensus DNA Sequences of P{GS:13084} Excisions

Excision 25

CTCACTCAAAGAGTGTGCTTTTATATTTGCTTGTTGTCAACACTAAATTATAATTTAGG
TAGTTTTCAATATTTCTTAATTTAAAATATTTAAACATTTATTTAAATCCTCATTTTCGT
TTAATTATTTTAAAACCTTAGCCTTCGGCTACTTAAGTTTTATTAACTATTTAAAGGCTTC
ATTCAGCGCGCTTTGGATGTTTTAAATTTTGAACCTTTGGTCACACTTGAATAAAAAACA
AATTTAAACCCCGCATTTGATTTGCAATTGGATATTTAACTATTTGTCTGGGCAGAATAA
ATCGGGTTGCAAGATGACCACGCCTGTGCCCCGCCGCACCAAGGACATGATGGCACTGG
GACTGGACTCCGACTCCGAGGACGACTTTAACACGCCATAACCGACCACGACAAGCGGCG
GCGGGAGAACGAAAACAGCAGCCGGTGGCGTCTTTCCAAG

Excision 30

CCTCACTCAAAGAGTGTGCTTTTATATTTGCTTGTTGTCAACACTAAATTATAATTTAG
GTAGTTTTCAATATTTCTTAATTTAAAATATTTAAACATTTATTTAAATCCTCATTTTCG
TTTAATTATTTTAAAACCTTAGCCTTCGGCTACTTAAGTTTTATTAACTATTTAAAGGCTT
CATTCAGCGCGCTTTGGATGTTTTAAATTTTGAACCTTTGGTCACACTTGAATAAAAAAT
AAATTTAAACCCCGCATTTGATTTGCAATTGGATATTTAACTATTTGTCTGGGCAGAATA
AATCGGGTTGCAAGATGACCACGCCTGTGCCCCGCCGCACCAAGGACATGATGGCACTG
GGACTGGACTCCGACTCCGAGGACGACTTTAACACGCCATAACCGACCACGACAAGCGGC
GCGGGAGAACGAAAACAGCAGCCGGTGGCGTCTTTCCA

Excision 1

CTCACTCAAAGAGTGTGCTTTTATATTTGCTTGTTGTCAACACTAAATTATAATTTAGG
TAGTTTTCAATATTTCTTAATTTAAAATATTTAAACATTTATTTAAATCCTCATTTTCGT
TTAATTATTTTAAAACCTTAGCCTTCGGCTACTTAAGTTTTATTAACTATTTAAAGGCTTC
ATTCAGCGCGCTTTGGATGTTTTAAATTTTGAACCTTTGGTCACACTTGAATAAAAAATA
AATTTAAACCCCGCACATGATGAAATAACATGAAATAACATAATATGTTATTTTCATCAT
GACCCCGCATTTGATTTGCAATTGGATATTTAACTATTTGTCTGGGCAGAATAAATCGGG
TTGCAAGATGACCACGCCTGTGCCCCGCCGCACCAAGGACATGATGGCACTGGGACTGG
ACTCCGACTCCGAGGACGACTTTAACACGCCATAACCGACCACGACAAGCGGCGGCGGGA
GAACGAAAACAGCAGCCGGTGGCGTCTTTCC

Excision 4

CTCACTCAAAGAGTGTGCTTTTATATTTGCTTGTTGTCAACACTAAATTATAATTTAGG
TAGTTTTCAATATTTCTTAATTTAAAATATTTAAACATTTATTTAAATCCTCATTTTCGT
TTAATTATTTTAAAACCTTAGCCTTCGGCTACTTAAGTTTTATTAACTATTTAAAGGCTTC
ATTCAGCGCGCTTTGGATGTTTTAAATTTTGAACCTTTGGTCACACTTGAATAAAAAATA
AATTTAAACCCCGCACATGATGAAATAACATGAAATAACATAATATGTTATTTTCATCAT
GACCCCGCATTTGATTTGCAATTGGATATTTAACTATTTGTCTGGGCAGAATAAATCGGG
TTGCAAGATGACCACGCCTGTGCCCCGCCGCACCAAGGACATGATGGCACTGGGACTGG
ACTCCGACTCCGAGGACGACTTTAACACGCCATAACCGACCACGACAAGCGGCGGCGGGA
GAACGAAAACAGCAGCCGGTGGCGTCTTTCCA

Excision 23

TCACTCAAAGAGTGTGCTTTTATATTTGCTTGTGTCAACACTAAATTATAATTTAGGT
AGTTTTCAATATTTCTTAATTTAAAATATTTAAACATTTATTTAAATCCTCATTTCGTT
TAATTATTTTAAAACCTTAGCCTTCGGCTACTTAAGTTTTATTA ACTATTTAAAGGCTTCA
TTCAGCGCGCTTTGGATGTTTTAAATTTTGAACCTTTGGTCACACTTGAATAAAAAATAA
ATTTAAACCCCGCACATGATGAAATAACATAACTCAGACTCAATACGACACTCAGAATA
CTATTCCTTTTACTCGCACTTATTGCAAGCATAACGTTAAGTGGATGTCTCTTGCCGACG
GGACCACCTTATGTTATTTTCATCATGACCCCGCATTTGATTTGCAATTGGATATTTAAC
TATTTGTGCGGCAGAATAAATCGGGTTGCAAGATGACCACGCCTGTGCCCGCCGCACC
AAGGACATGATGGCACTGGGACTGGACTCCGACTCCGAGGACGACTTTAACACGCCATA
CCGACCACGACAAGCGGCGGGGAGAACGAAAACAGCAGCCGGTGGCGTCTTTCCA

Excision 15 - Left End

TAAATTATAATTTAGGTAGTTTTCAATATTTCTTAATTTAAAATATTTAAACATTTATTT
AAATCCTCATTTCGTTTAATTATTTTAAAACCTTAGCCTTCGGCTACTTAAGTTTTATT
AACTATTTAAAGGCTTCATTCAGCGCGCTTTGGATGTTTTAAATTTTGAACCTTTGGTCAC
ACTTGAATAAAAAATAAATTTAAACCCCGCACATGATGAAATAACAGCAAATAAACAAG
CGCAGCTGAACAAGCTAAACAATCTGCAGTAAAGTGCAAGTTAAAGTGAATCAATTTAA
AGTAACCAGCAACCAAGTAAATCAACTGCAACTACTGAAATCTGCCAAGAAGTAATTAT
TGAATACAAGAAGAGA ACTCTGAATAGGGAATTGGGAATTCGCCACCATGAGTAAAGG
AGAAGA ACTTTTTACTGGAGTTGTCCCAATTCTTGTTGAATTAGATGGTGTGTTAATG
GGCACAAATTTTCTGTGTCAGTGGAGAGGGTGAAGGTGATGCAACATACGGAAAACCTTACC
CTTAAATTTATTTGCACTACTGGAAA ACTACCTGTTCCATGGCCAACACTTGTCACTAC
TTTCACTTATGGTGTTC AATGCTTTTTCAAGATACCCAGATCATATGAAACGGCATGACT
TTTTCAAGAGTGCCATGCCC GAAGGTTATGTACAGGAAAGAACTATATTTTTTCAAAGAT
GACGGGA ACTACAAGACACGTGCTGAAGTCAAGTTTGAAGGTGATACCCTTGTTAATAG
AATCGAGTTAAAAGGTATTGATTTTAAAGAAGATGGAAACATTCTTGGACACAAATTGG
AATACA ACTATAACTCACACAATGTATACATCATGGCAGACAAACAAAAGAATGGAATC

Excision 15 - Right End

TTTTGCTCAGAAGAAATGCCATCTAGTGATGATGAGGCTACTGCTGACTCTCAACATTC
TACTCCTCCAAAAAAGAAGAGAAAGGTAGAAGACCCCAAGGACTTTCTTTCAGAATTGC
TAAGTTTTTTGAGTCATGCTGTGTTTAGTAATAGA ACTCTTGCTTGCTTTGCTATTTAC
ACCACAAAGGAAAAAGCTGCACTGCTATAACAAGAAAATTTATGGAAAAATATTTGATGTA
TAGTGCTTGACTAGAGATCATAATCAGCCATACCACATTTGTAGAGGTTTTACTTGCT
TTAAAAAACCTCCCACACCTCCCCCTGAACCTGAAACATAAAATGAATGCAATTGTTGT
TGTTAACTTGTTTATTGCAGCTTATAATGGTTACAAATAAAGCAATAGCATCACAAATT
TCACAAATAAAGCATTTTTTTTCACTGCATTCTAGTTGTGGTTTGTCCAAACTCATCAAT
GTATCTTATCATGTCTGGATCTGCGGCCGCGGCTCGACCTGCAGCCAAGCTTTGCGTAC
TCGCAAAATTATTTAAAATAAAACTTTAAAATAAATTTCTGCTAATTAATATTATGAGTT
AATTCAAACCCACGGACATGCTAAGGGTTAATCAACAATCATATCGCTGTCTCACTCA
GACTCAATACGACACTCAGAATACTATTCCTTTCACTCGCACTTATTGCAAGCATAACGT
TAAGTGGATGTCTCTTGCCGACGGGACCACCTTATGTTATTTTCATCATGCTCAGAATAC
TATTCCTTTCACTCGCACTTATTGCAAGCATAACGTTAAGTGGATGTCTCTTGCCGACGG
GACCACCTTATGTTATTTTCATCATGACCCCGCATTTGATTTGCAATTGGATATTTAACT
ATTTGTGCGGCAGAATAAATCGGGTTGCAAGATGACCACGCCTGTGCCCGCCGCACCA

AGGACATGATGGCACTGGGACTCCGACTCCGAGGACGACTTTAACACGCCATACCGACC
ACGACAAGCGGCGG

Excision 26 - Left End

AATATTTCTTAATTTAAAATATTAACATTTATTTAAATCCTCATTTCGTTTAATTAT
TTTAAACTTAGCCTTCGGCTACTTAAGTTTTATTAACTATTAAGGCTTCATTCAGCG
CGCTTTGGATGTTTTAAATTTTGAACCTTGGTCACACTTGAATAAAAAATAAATTTAAA
CCCCGCACATGATGAAATAACATAAGGTGGTCCCGTCGATAGCCGAAGCTTACCGAAGT
ATACACTTAAATTCAGTGCACGTTTGCTTGTGAGAGGAAAGGTTGTGTGCGGACGAAT
TTTTTTTTGAAAACATTAACCCCTTACGTGGAATAAAAAAAATGAACTAGTCGAATTC
CCAATTCCTATTCAGAGTTCTCTTCTTGTATTCAATAATTACTTCTTGGCAGATTTCA
GTAGTTGCAGTTGATTTACTTGGTTGCTGGTTACTTTTAATTGATTCACTTAACTTGC
ACTTTACTGCAGATTGTTTAGCTTGTTCAGCTGCGCTTGTATTTGCTTAGCTTTTCG
TTAGCGACGTGTTCACTTTGCTTGTGTAATTGAATTGTGCTCCGTAGACGAAGCGCC
TCTATTTATACTCCGGCGCTCGCTAGAGTCTCCGCTCGGAGGACAGTACTCCGCTCGGA
GGACAGTACTCCGCTCGGAGGACAGTACTCCGCTCGGAGGACAGTACTCCGCTCGGAGG
ACAGTACTCCGACCTGCAGGCATGCAAGCTTGGATCTGCGGCCGCGGTCTAGAAGGCCT
AATTCTAGTATGTATGTAAGTTAATAAAACCCATTTTTTGC GGAAAGTAGATAAAAAAA
CATTTTTTTTTTTTTT

Excision 26 - Right End

CTCTTGCTTGCTTTGCTATTTACACACAAAGGAAAAAGCTGCACTGCTATAACAAGAAAA
TTATGGAAAAATATTTTGATGTATAGTGCCTTGACTAGAGATCATAATCAGCCATACCA
CATTTGTAGAGGTTTTACTTGCTTTAAAAAACCTCCCACACCTCCCCCTGAACCTGAAA
CATAAAATGAATGCAATTGTTGTTGTTAACTTGTTTATTGCAGCTTATAATGGTTACAA
ATAAAGCAATAGCATCACAAATTTACAAATAAAGCATTTTTTTTCACTGCATTCTAGTT
GTGGTTTGTCCAAACTCATCAATGTATCTTATCATGTCTGGATCTGCGGCCGCGGCTCG
ACCTGCAGCCAAGCTTTGGGTACTCGCAAATTATTAATAAATAAACTTTAAAAATAATT
TCGTCTAATTAATATTTATGAGTTAATTCAAACCCACGGACATGCTAAGGGTTAATCAA
CAATCATATCGCTGTCTCACTCAGACTCAATACGACACTCAGAATACTATTCTTTTAC
TCGCACTTATTGCAAGCATAACGTTAAGTGGATGTCTCTTGCCGACGGGACCACCTTATG
TTATTTTCATCATGACCCCGCATTTGATTTGCAATTGGATATTTAACTATTTGTCGGGCA
GAATAAATCGGGTTGCA

**ald region with P{GS:13084} inserted after the 14th
nucleotide of the 5'UTR**

gtggcagctctgtgatgaccatgaaaaacaagacaaccctaaaatgtaacaataaaacttactgtagaat
ttgaatatctaattttatatttaagccattcttacttttaaatcattttgatgtattttatacatcactc
tccctcactcaaagagtgtgcttttatatgttctgtgtcaacactaaattataattaggtagttttca
atatttcttaatttaaaatattaacattttatttaaatcctcattttcgtttaatttttaaaacttagc
cttcggctacttaagttttattaactattaaggttccattcagcgcgctttggatgttttaattttgaa
ctttggtcacacttgaataaaaaatAAATTTAAACCCCG

CATGATGAAATAACATAAGGTGGTCCCGTCGGCAAGAGACATCCACTTAACGTATGCTTGCAATAAGTGCG
AGTGAAAGGAATAGTATTCTGAGTGTCTGATTGAGTCTGAGTGAGACAGCGATATGATTGTTGATTAACCC
TTAGCATGTCCGTGGGGTTTTGAATTAACCTATAATATTAATTAGACGAAATTATTTTTaaagttttat
taataattttgtagtacgcaaagcttggctgcaggtcgaGCGCGCCGCAAgatccgatccagacatgata

agatacattgatgagtttggacaaaccacaactagaatgcagtgaaaaaatgctttatattgtgaaatttg
tgatgctattgctttatattgtaccattataagctgcaataaacaagttaacaacaacaattgcattcatt
ttatgtttcagggttcagggggagggtgtgggaggttttttaagcaagtaaaacctctacaaatgtggatg
gctgattatgatctctagtcaggcactatacatcaaatattccttattaaccctttacaaattaaaaag
ctaaaggtacacaatttttgagcatagttattaatagcagacactctatgcctgtgtggagtaagaaaaa
cagtatgttatgattataactgttatgcctacttataaagggttacagaatatttttccataattttctgt
atagcagtgagctttttcctttgtgggtgtaaataagcaagcaagagttctattactaaacacagca
tgactcaaaaaacttagcaattctgaaggaaagtccttgggggtcttctacctttctctcttttttggagg
agtagaatgttgagagtcagcagtagcctcatcatcactagatggcatttcttctgagcaaaacagggttt
cctcattaaaggcattccaccactgctcccattcatcagttccataggttggaaatctaaaatacacaaaaca
attagaatcagtagttaaacaacattatacacttaaaaaattttatatttaccttagagctttaaatctctgt
aggtagttgtccaattatgtcacaccacagaagtaagggtccttcacaagatcctctagaggtaccctc
GACTCTAGATTATTTGTATAGTTCATCCATGCCATGTGTAAATCCAGCAGCTGTTACAAAACCTCAAGAAGGA
CCATGTGGTCTCTCTTTTCGTTGGGATCTTTTCGAAAGGGCAGATTGTGTGGACAGGTAATGGTTGTCTGGT
AAAAGGACAGGGCCATCGCCAATTGGAGTATTTTGTGATAATGGTCTGCTAGTTGAACGCTTCCATCTTC
AATGTTGTGTCTAATTTTGAAGTTAACTTTGATTCCATTCTTTTGTGTTGTCTGCCATGATGTATACATTGT
GTGAGTTATAGTTGTATTCCAATTTGTGTCCAAGAATGTTTCCATCTTCTTTAAAATCAATACCTTTTAAAC
TCGATTCTATTAACAAGGGTATCACCTTCAAACCTTGACTTCAGCACGTGTCTTGTAGTTCCCGTCATCTTT
GAAAAATATAGTTCTTTTCTGTACATAACCTTTCGGGCATGGCACTCTTGAAAAAGTCATGCCGTTTCATAT
GATCTGGGTATCTTGAAAAGCATTGAACACCATAAGTGAAAGTAGTGACAAGTGTTGGCCATGGAACAGGT
AGTTTTCCAGTAGTGCAAATAAATTTAAGGGTAAGTTTTCCGTATGTTGCATCACCTTACCCTCTCCACT
GACAGAAAATTTGTGCCATTAACATCACCATCTAATTCACAAGAATTGGGACAACCTCCAGTGAAAAGTT
CTTCTCCTTTACTCATGGTGGCGGAATTCcaattccctattcagagttctcttcttctgtattcaataatta
cttcttggcagatttcagtagttgcagttgatttacttgggttgcgtggttacttttaattgattcactttaa
cttgcactttactgcagattgtttagcttgttcagctgcgcttgtttatattgcttagctttcgttagcgga
cgtgttcactttgcttgtttgaattgaattgtcgctccgtagacgaagcgcctctatttataactccggcgc
tcgctagagctctccgctcggaggacagtagctccgctcggaggacagtagctccgctcggaggacagtagctcc
gctcggaggacagtagctccgctcggaggacagtagctccgacctgcaggcatgCCTGCATctacacaaggaa
caaacactggatgtcactttcagttcaaattgtaacgctaatcactccgaacaggtcacaaaAAATTACCT
TAAAAAGTCATAATATTAATTAAGATAAATATAGCTGTGAGGGAAATATATACAAAATATATTGGAGCAAA
TAAATTTGATACATACAAATATTTTACTAATTTCTATTGAGACGAAATGAACCACCTCGGAACCATTTGAGC
GAaccgaatcgcgcggaactaacgacagtcgctccaaggtcgtcgaacaaaagggtgaatgtgttgcggaga
gcggttgggagacagcgaagagcaactacgaaacgtgggtgtgggtggagggtgaattatgaagagggcgcgc
gatttgaagagtatgtatataaaaaatataatcccggtgttttatgtagegataaaacaggtttttgatgtaa
ggtagtcaggtgtgtgaagtcttttgggttagaagacaaaatccaaagtctacttgtggggatgttcgaagggg
aaatacttgtattctataggtcatalcttgtttttattggcacaataataattacattagctttttgagggg
ggcaataaacagtaaacacgatggtaataatggtaaaaaaaaaaaaaaacaagcagttatttcggatatagtc
ggctactccttgcgtcgggcccgaagtcttagagccagatagtcgagcaccgggaagctcacgatgagaat
ggccagaccacagtagtccagcggcagatcggcggcgggagaagttaagcgtctccaggatgaccttgcgg
aactggggcacgtgggtgttcgacgatgtgcagctaatttcgcccggctccacgtccgcccattgggttaatc
agcagaccctcgttggcgtaacggaacctagagaggtacgacaacctttgaggtatactggcaccgagcc
cgagttcaagaagaagccgccaagagcaggaatggtagataaccggcggacccacagacagcgcctatcg
aggctcagaggagctggcgcaggatattagatatccgaaggacggttgacacattggccaccagagtgaccagc
gccaggcagttgaagaagtgcagcactccggcccgcagtcgatcatcgataggcaatcgccgtgaagac
cagtgccactgtgagaaaaagcgggcaattcggcaatcgtttggccagaaagtatgtgtcacagcgataaa
gtcgacttcgggacctccctcataaaaaactggcagctctgaggtgaacacctaaatcgaatcgattcattag
aaagttagtaaattattgaaatgcaaatgtattctaaacatgacttacatttatcgtggcaaaagcgtttt
gaaaggtcatgttgggtcaggaagaggaagatggctccggtgatattcatcacaccctacttgcgtgagttgt
tggcccaaaaagatgaggccaatcaagatggcaacctctgcaaatataaaatggttactcgcactctcattaa
tattcgcgagttaaatgaaatttatttctctgcaaaactataaactatacatctcattgaaaaaaact
aagaaggtgtggaatcaggcaattctatctaaaatctagcgaatttgtttccaagaattgtaagcgttat
atcatttgtttccactggaaccactcaccgttgtctgaataagtcgcacttttacgaggagtgGTTCTCTTG
AGCACCCGACAGCCAGGATCGCCACAGGACCGCCCGGAACTGCATGAACCaggtggcctttaggtgtaccc
attctccggctgctccagtggtcttctccagatttttgggtggccaacaactgctccatataccggggtactt
tgctaattggcaaaaattgtcgccatatacttggcgatccgatcacgggactcgatctcccgctccgggcacaac
ggccaacacctgtacgtaaaagTCCGCCGATTGTAGTTGGTAGGACACTGGGCACCCACGCTGGATAGGA
GTTGAGATGTAATGTAATGCTAGATACCCTTAATAAACACATCGAACTCACTAGGAAAAGAAGTCGACGGC

TTCGCTGGGAGTGCCCAAGAAAGCTACCCTGCCCTCGGCCATCAGAAGGATCTTGTCAAAGAGCTCAAACA
GCTCGGAAGACGGCTGATGAATGGTCAGGATGACGGTCTTGCCCTTCTGCGACAGCTTCTTCAGCACCTGG
ACGACGCTGTGGGCGGTAAATGAGTCCAGTCCGGAGGTGGGCTCATCGCAGATCAGAAGCGGGCGGATCGGT
TAGTGCCTCGGAGGCGAATGCCAGACGCTTCTTTCTCCGCCGGACAGACCTTTACCctgcccgggacac
cgatgatcgtgtgctgacatttggctgagcgaagctcctggatcacctgatccacgcggggccactcgctgc
cgataggtcagatgtcgtggcatccgcacatggccttggaaaatcaggtgttccctggccggttagggagcc
gataaagaggtcatcctgctggacataggegcacctggcctgcatctccttggcgtccacaggttggccat
tgagcagTCGCATCCCGGATGGCGATACTTGGATGCCCTGCGGCGATCGAAAGGCAAGGGCATTTCAGCAGG
GTCGTCTTTCCGGCACCGGAAGTGCATCACGGCCAAAAGTTCCGCCGGATAGGCCACGCCGCAAActga
gtttcaaattggtaattggaccctttattaagatttcacacagatcagccgactgccaatagaaaactcacc
gttcttgagcaaatgtttcctgggcccgggtatgtgctcgctcggttcagaaatagtcgcccgtgtccgggtga
ccagctgcccgcctccggagcccggctgattgaccgCCCCAAAGATGTCCATATTGTGCCAGGCATAGGTG
AGGTTCTCGGCTAGTTGGCCGCTCCCTGAACCCGGAGTCTCCGGCGGACTGGGTGGCAGGAGCGTGCCGTA
GTTTTTGGCCTGCCGAAGCCCTGGTTAATGCAGCTCTGCGAAGCGTCCGCTGTACCCTGCAATGATAGG
GGATCTCAAATATCAACTACAAGCGTTATGCTCATCTAACCCGAACAAAACGAAGTATCCTACGAAGTAG
GTTTATACTTTTATTTATTTTTTGTGCATAGCTTAAAATATCTGGTTGTTATATTTTTTGTAAAAAGAAT
GTAGTCGAAAATGAATGCCTTTAGATGTCTTGATCATGATATGATCTTAAAAATTGTCTTATATAGCGAGC
ACAGCTACCAGAATAATCTGTTTCGTGTCACTATTTGTTTGTGCGATTGCGGTTTTGGGATTTTTTGTGGGTC
GCAGTTCTCACGCCGAGACAATTTGATGTTGCAATCGCAGTTCCCTATAGATCAAGTGAACCTAAGATGTA
TGCACATGTACTACTCACATTGTTTCAGATGCTCGGCAGATGGGTGTTTGTGCTCCCGCAATTAATAGCT
CCTGATCCTCTTGGCCATTGCCGGGATTTTTCACACTTTCCCTGCTTACCCACCCAAAACCAATCACCA
CCCCAATCACTCAAAAAACAAACAAAAATAAGAAGCGAGAGGAGTTTTGGCACAGCACTTTGTGTTAATT
GATGGCGTAAACCGCTTGGAGCTTCGTACAGAAACCGCTGACAAAGTGCAACTGAAGGCGGACATTGACGC
TAGGTAACGCTACAAACGGTGGCGAAAGAGATAGCGGACGCGAGCGGCGAAAGAGACGGCGATATTTCTGTG
GACAGAGAAGGAGGCAACAGCgctgactttgagtggaaatgtcattttgagtgagaggtaatcgaaagaac
ctggtacatcaaatacccttggatcgaagtaaatttaaaactgatcagataagttcaatgatatccagtg
agtaaaaaaaaaaaatgtttttttatctactttccgcaaaaatgggttttattaacttacatacacta
gaattAGGCCTTCTAGACCGCGGCCGAGATCCAAGCTTGCATGCCTGCAGGTCCGAGTACTGTCTCCCGA
GCGGAGTACTGTCTCCGAGCGGAGTACTGTCTCCGAGCGGAGTACTGTCTCCGAGCGGAGTACTGTCT
TCCGAGCGGAGACTCTAGCGAGCGCCGGAGTATAAATAGAGGCGCTTCGTCTACGGAGCGACAATTC AATT
CAAACAAGCAAAGTGAACACGTGCTAAGCGAAAGCTAAGCAAATAAACAAGCGCAGCTGAACAAGCTAAA
CAATCTGCAGTAAAGTGCAAGTTAAAGTGAATCAATTAAGTAACCAGCAACCAAGTAAATCAACTGCAA
CTACTGAAATCTGCCAAGAAGTAATTATTGAATACAAGAAGAGAAGTCTGAATAGGGAATTGGGAATTCGA
CTAGTTTCATTTTTTTTTTATTCCACGTAAGGGTTAATGTTTTTCAAAAAAAAAATTCGTCCGCACACAACCTT
TCCTCTCAACAAGCAAACGTGCACTGAATTTAAGTGTATACTTCGGTAAGCTTCGGCTTTTCGACGGGACCA
CCTTATGTTATTTTCATCATG

CATTTGATTTGCAATTGGATATTTAACTATTTGTGCGGCAGAATAAATCGGGTTGCAAGATGACCACGCCT
GTGCCCCGCCGACCAAGGACATGATGGCACTGGGACTGGACTCCGACTCCGAGGACGACTTTAACACGCC
ATACCGACCACGACAAGCGGGCGGGGAGAACGAAAACAGCAGCCGGTGGCGTCTTTCCAAGTCCAACGA
GGGGCAAGGAGAACGAACCGCATCCCCTGCCATAAATATGCTgtaagaactgggacagcaatgtccagta
tcgcatgacatctcctgttctccatacataagtcctcctgag

XI. APPENDIX E: DNA Sequence Analyses of P{GS:13084} Excisions

Alignment Data [Exc 1, 4, 23, 30, and 25]

```
Exc1      TCACTCAAAGAGTGTGCTTTTATATTTGCTTGTTGTCAACACTAAATT
Exc4      TCACTCAAAGAGTGTGCTTTTATATTTGCTTGTTGTCAACACTAAATT
Exc23     TCACTCAAAGAGTGTGCTTTTATATTTGCTTGTTGTCAACACTAAATT
Exc30     TCACTCAAAGAGTGTGCTTTTATATTTGCTTGTTGTCAACACTAAATT
Exc25     TCACTCAAAGAGTGTGCTTTTATATTTGCTTGTTGTCAACACTAAATT
ald       TCACTCAAAGAGTGTGCTTTTATATTTGCTTGTTGTCAACACTAAATT
*****

Exc1      ATAATTTAGGTAGTTTTCAATATTTCTTAATTTAAAATATTTAAACATTTATTTAAATCCT
Exc4      ATAATTTAGGTAGTTTTCAATATTTCTTAATTTAAAATATTTAAACATTTATTTAAATCCT
Exc23     ATAATTTAGGTAGTTTTCAATATTTCTTAATTTAAAATATTTAAACATTTATTTAAATCCT
Exc30     ATAATTTAGGTAGTTTTCAATATTTCTTAATTTAAAATATTTAAACATTTATTTAAATCCT
Exc25     ATAATTTAGGTAGTTTTCAATATTTCTTAATTTAAAATATTTAAACATTTATTTAAATCCT
ald       ATAATTTAGGTAGTTTTCAATATTTCTTAATTTAAAATATTTAAACATTTATTTAAATCCT
*****

Exc1      CATTTTCGTTTAATTATTTTAAAACCTTAGCCTTCGGCTACTTAAGTTTTATTAACTATTA
Exc4      CATTTTCGTTTAATTATTTTAAAACCTTAGCCTTCGGCTACTTAAGTTTTATTAACTATTA
Exc23     CATTTTCGTTTAATTATTTTAAAACCTTAGCCTTCGGCTACTTAAGTTTTATTAACTATTA
Exc30     CATTTTCGTTTAATTATTTTAAAACCTTAGCCTTCGGCTACTTAAGTTTTATTAACTATTA
Exc25     CATTTTCGTTTAATTATTTTAAAACCTTAGCCTTCGGCTACTTAAGTTTTATTAACTATTA
ald       CATTTTCGTTTAATTATTTTAAAACCTTAGCCTTCGGCTACTTAAGTTTTATTAACTATTA
*****

Exc1      AAGGCTTCATTCAGCGCGCTTTGGATGTTTTAAATTTTGAACCTTTGGTCACACTTGAATA
Exc4      AAGGCTTCATTCAGCGCGCTTTGGATGTTTTAAATTTTGAACCTTTGGTCACACTTGAATA
Exc23     AAGGCTTCATTCAGCGCGCTTTGGATGTTTTAAATTTTGAACCTTTGGTCACACTTGAATA
Exc30     AAGGCTTCATTCAGCGCGCTTTGGATGTTTTAAATTTTGAACCTTTGGTCACACTTGAATA
Exc25     AAGGCTTCATTCAGCGCGCTTTGGATGTTTTAAATTTTGAACCTTTGGTCACACTTGAATA
ald       AAGGCTTCATTCAGCGCGCTTTGGATGTTTTAAATTTTGAACCTTTGGTCACACTTGAATA
*****

Exc1      AAAAATAAATTTAAACCCCGCACATGATGAAATAACATGA-----AATA--ACA--
Exc4      AAAAATAAATTTAAACCCCGCACATGATGAAATAACATGA-----AATA--ACA--
Exc23     AAAAATAAATTTAAACCCCGCACATGATGAAATAACATAA ACTCAGACTCAATACGACACT
Exc30     AAAAATAAATTTAAACCCCGCA-----
Exc25     AAAAACAAATTTAAACCCCGCA-----
ald       AAAAATAAATTTAAACCCCGCA-----
*****

Exc1      -----TAA-----
Exc4      -----TAA-----
Exc23     CAGAATACTATTCTTTCACTCGCACTTATTGCAAGCATACGTTAAGTGGATGTCTCTTG
Exc30     -----
Exc25     -----
ald       -----
```

```

Exc1      -----TATGTTATTTTCATCATGACCCCGCATTTGATTTGCAATTGGATAT
Exc4      -----TATGTTATTTTCATCATGACCCCGCATTTGATTTGCAATTGGATAT
Exc23     CCGACGGGACCACCTTATGTTATTTTCATCATGACCCCGCATTTGATTTGCAATTGGATAT
Exc30     -----CATTTGATTTGCAATTGGATAT
Exc25     -----CATTTGATTTGCAATTGGATAT
ald       -----CATTTGATTTGCAATTGGATAT
                                     *****

Exc1      TTAACTATTTGTCTGGGCAGAATAAATCGGGTTGCAAGATGACCACGCCTGTGCCCCGCCG
Exc4      TTAACTATTTGTCTGGGCAGAATAAATCGGGTTGCAAGATGACCACGCCTGTGCCCCGCCG
Exc23     TTAACTATTTGTCTGGGCAGAATAAATCGGGTTGCAAGATGACCACGCCTGTGCCCCGCCG
Exc30     TTAACTATTTGTCTGGGCAGAATAAATCGGGTTGCAAGATGACCACGCCTGTGCCCCGCCG
Exc25     TTAACTATTTGTCTGGGCAGAATAAATCGGGTTGCAAGATGACCACGCCTGTGCCCCGCCG
ald       TTAACTATTTGTCTGGGCAGAATAAATCGGGTTGCAAGATGACCACGCCTGTGCCCCGCCG
                                     *****

Exc1      CACCAAGGACATGATGGCACTGGGACTGGACTCCGACTCCGAGGACGACTTTAACACGCC
Exc4      CACCAAGGACATGATGGCACTGGGACTGGACTCCGACTCCGAGGACGACTTTAACACGCC
Exc23     CACCAAGGACATGATGGCACTGGGACTGGACTCCGACTCCGAGGACGACTTTAACACGCC
Exc30     CACCAAGGACATGATGGCACTGGGACTGGACTCCGACTCCGAGGACGACTTTAACACGCC
Exc25     CACCAAGGACATGATGGCACTGGGACTGGACTCCGACTCCGAGGACGACTTTAACACGCC
ald       CACCAAGGACATGATGGCACTGGGACTGGACTCCGACTCCGAGGACGACTTTAACACGCC
                                     *****

Exc1      ATACCGACCACGACAAGCGGCGGGGAGAACGAAAACAGCAGCCGGTGGCGTCTTTCC
Exc4      ATACCGACCACGACAAGCGGCGGGGAGAACGAAAACAGCAGCCGGTGGCGTCTTTCC
Exc23     ATACCGACCACGACAAGCGGCGGGGAGAACGAAAACAGCAGCCGGTGGCGTCTTTCC
Exc30     ATACCGACCACGACAAGCGGCGGGGAGAACGAAAACAGCAGCCGGTGGCGTCTTTCC
Exc25     ATACCGACCACGACAAGCGGCGGGGAGAACGAAAACAGCAGCCGGTGGCGTCTTTCC
ald       ATACCGACCACGACAAGCGGCGGGGAGAACGAAAACAGCAGCCGGTGGCGTCTTTCC
                                     *****

```

Alignment Data
[Exc 15 & P-element 3' end]

```

Exc15     CGCGCTTTGGATGTTTTAAATTTTGAACCTTTGGTCACACTTGAATAAAAAATA
Pel-3'    CGCGCTTTGGATGTTTTAAATTTTGAACCTTTGGTCACACTTGAATAAAAAATA
          *****

Exc15     AATTTAAACCCCGCACATGATGAAATAACA-----
Pel-3'    AATTTAAACCCCGCA--TGATGAAATAACATAAGGTGGTCCCCTCGAAAGCCGAAGCTTA
          *****

Exc15     -----
Pel-3'    CCGAAGTATACACTTAAATTCAGTGCACGTTTGGCTTGGTGGAGAGAAAGGTTGTGTGCGG

```


Alignment Data
 [Exc 15 & P-element *mini-white* gene]

```

mini-white (2541 base-pairs into the gene)
mini-white      GCAAATAAACAAGCGCAGCTGAACAAGCTAAACAATCTG
Exc15           GCAAATAAACAAGCGCAGCTGAACAAGCTAAACAATCTG
                *****

mini-white      CAGTAAAGTGCAAGTTAAAGTGAATCAATTA AAAAGTAACCAGCAACCAAGTAAATCAACT
Exc15           CAGTAAAGTGCAAGTTAAAGTGAATCAATTA AAAAGTAACCAGCAACCAAGTAAATCAACT
                *****

mini-white      GCAACTACTGAAATCTGCCAAGAAGTAATTATTGAATACAAGAAGAGA ACTCTGAATAGG
Exc15           GCAACTACTGAAATCTGCCAAGAAGTAATTATTGAATACAAGAAGAGA ACTCTGAATAGG
                *****

mini-white      GAATTGGGAATTCGCCACCATGAGTAAAGGAGAAGA ACTTTTCACTGGAGTTGTCCCAA
Exc15           GAATTGGGAATTCGCCACCATGAGTAAAGGAGAAGA ACTTTTCACTGGAGTTGTCCCAA
                *****

mini-white      TTCTTGTTGAATTAGATGGTGATGTTAATGGGCACAAATTTTCTGT CAGTGGAGAGGGTG
Exc15           TTCTTGTTGAATTAGATGGTGATGTTAATGGGCACAAATTTTCTGT CAGTGGAGAGGGTG
                *****

mini-white      AAGGTGATGCAACATACGGA AA ACTTACCCTTAAATTTATTTGCACTACTGGAAACTAC
Exc15           AAGGTGATGCAACATACGGA AA ACTTACCCTTAAATTTATTTGCACTACTGGAAACTAC
                *****

mini-white      CTGTTCCATGGCCAACACTTGTCACTACTTTCACTTATGGTGTTCAATGCTTTTCAAGAT
Exc15           CTGTTCCATGGCCAACACTTGTCACTACTTTCACTTATGGTGTTCAATGCTTTTCAAGAT
                *****

mini-white      ACCCAGATCATATGAAACGGCATGACTTTTTCAAGAGTGCCATGCCCGAAGGTTATGTAC
Exc15           ACCCAGATCATATGAAACGGCATGACTTTTTCAAGAGTGCCATGCCCGAAGGTTATGTAC
                *****

mini-white      AGGAAAGA ACTATATTTTTCAAAGATGACGGGA ACTACAAGACACGTGCTGAAGTCAAGT
Exc15           AGGAAAGA ACTATATTTTTCAAAGATGACGGGA ACTACAAGACACGTGCTGAAGTCAAGT
                *****

mini-white      TTGAAGGTGATACCCTTGTTAATAGAATCGAGTTAAAAGGTATTGATTTTAAAGAAGATG
Exc15           TTGAAGGTGATACCCTTGTTAATAGAATCGAGTTAAAAGGTATTGATTTTAAAGAAGATG
                *****

mini-white      GAAACATTCTTGACACAAATTGGAATACA ACTATAACTCACACAATGTATACATCATGG
Exc15           GAAACATTCTTGACACAAATTGGAATACA ACTATAACTCACACAATGTATACATCATGG
                *****

mini-white      CAGACAAACAAAAGAATGGAATCAAAGCTAACTTCAA AATTAGACACAACATTGAAGATG
Exc15           CAGACAAACAAAAGAATGGAATCAAAGCTAACTTCAA AATTAGACACAACATTGAAGATG
                *****

mini-white      GAAGCGTTCAACTAGCAGACCATTATCAACAAAATACTCCAATTGGCGATGGCCCTGTCC
Exc15           -----
  
```

```

mini-white      TTTTACCAGACAACCATTACCTGTCCACACAATCTGCCCTTTCGAAAGATCCCAACGAAA
Exc15          -----

mini-white      AGAGAGACCACATGGTCCTTCTTGAGTTTGTAACAGCTGCTGGGATTACACATGGCATGG
Exc15          -----

mini-white      ATGAACTATACAAATAATCTAGAGTCGAGGGTACCTCTAGAGGATCTTTGTGAAGGAACC
Exc15          -----

mini-white      TTACTTCTGTGGTGTGACATAATTGGACAAACTACCTACAGAGATTTAAAGCTCTAAGGT
Exc15          -----

mini-white      AAATATAAAATTTTTAAGTGTATAATGTGTTAAACTACTGATTCTAATTGTTTGTGTATT
Exc15          -----

mini-white      TTAGATTCCAACCTATGGAECTGATGAATGGGAGCAGTGGTGAATGCCTTTAATGAGGA
Exc15          -----

mini-white      AACCTGTTTTGCTCAGAAGAAATGCCATCTAGTGATGATGAGGCTACTGCTGACTCTCA
Exc15      -----TTTTGCTCAGAAGAAATGCCATCTAGTGATGATGAGGCTACTGCTGACTCTCA
                *****

mini-white      ACATTCTACTCCTCCAAAAAAGAAGAGAAAGGTAGAAGACCCCAAGGACTTTCCTTCAGA
Exc15      ACATTCTACTCCTCCAAAAAAGAAGAGAAAGGTAGAAGACCCCAAGGACTTTCCTTCAGA
                *****

mini-white      ATTGCTAAGTTTTTTGAGTCATGCTGTGTTTAGTAATAGAACTCTTGCTTGCTTTGCTAT
Exc15      ATTGCTAAGTTTTTTGAGTCATGCTGTGTTTAGTAATAGAACTCTTGCTTGCTTTGCTAT
                *****

mini-white      TTACACCACAAAGGAAAAAGCTGCACTGCTATAACAAGAAAATTATGGAAAAATATTCTGT
Exc15      TTACACCACAAAGGAAAAAGCTGCACTGCTATAACAAGAAAATTATGGAAAAATATT---T
                *****

```

Alignment Data
[Exc 15 & P-element Outward facing *Hsp70Bb*]

```

OutHsp70      TTAATAAGGAATATTTGATGTATAGTGCCTTGACTAGAGATCATAATCAGCCATAC
Exc15          TTATGGAAAAATATTTGATGTATAGTGCCTTGACTAGAGATCATAATCAGCCATAC
                ***      *      *****

OutHsp70      CACATTTGTAGAGGTTTTACTTGCTTTAAAAAACCTCCACACCTCCCCCTGAACCTGAA
Exc15          CACATTTGTAGAGGTTTTACTTGCTTTAAAAAACCTCCACACCTCCCCCTGAACCTGAA
                *****

```

OutHsp70 ACATAAAATGAATGCAATTGTTGTTGTTAACTTGTTTATTGCAGCTTATAATGGTTACAA
Exc15 ACATAAAATGAATGCAATTGTTGTTGTTAACTTGTTTATTGCAGCTTATAATGGTTACAA

OutHsp70 ATAAAGCAATAGCATCACAAATTTACAAATAAAGCATTTTTTTTCCTGCATTCTAGTTG
Exc15 ATAAAGCAATAGCATCACAAATTTACAAATAAAGCATTTTTTTTCCTGCATTCTAGTTG

OutHsp70 TGGTTTGTCCAAACTCATCAATGTATCTTATCATGTCTGGATCGGATCTTGCGGCCGCG-
Exc15 TGGTTTGTCCAAACTCATCAATGTATCTTATCATGTCTGGATC-----TGCAGGCCGCGG

OutHsp70 CTCGACCTGCAGCCAAGCTTTGCGTACTCGCAAATTATTAATAAATAAACTTTAAAAATA
Exc15 CTCGACCTGCAGCCAAGCTTTGCGTACTCGCAAATTATTAATAAATAAACTTTAAAAATA

Alignment Data
[Exc 15 & P-element 5' end]

Pel5' CCCACGGACATGCTAAGGGTTAATCAACAATCATATCGCTGTCTCACTC
Exc15 CCCACGGACATGCTAAGGGTTAATCAACAATCATATCGCTGTCTCACTC

Pel5' AGACTCAATACGACACTCAGAATACTATTCTTTCACTCGCACTTATTGCAAGCATAACGT
Exc15 AGACTCAATACGACACTCAGAATACTATTCTTTCACTCGCACTTATTGCAAGCATAACGT

Pel5' TAAGTGGATGTCTCTTGCCGACGGGACCACCTTATGTTATTTTCATCATGCTC-----
Exc15 TAAGTGGATGTCTCTTGCCGACGGGACCACCTTATGTTATTTTCATCATGCTCAGAATACT

Pel5' -----
Exc15 ATTCCTTTCACTCGCACTTATTGCAAGCATAACGTTAAGTGGATGTCTCTTGCCGACGGGA

Pel5' -----ATTTGATTTGCAATTGGATATTTAACTATT
Exc15 CCACCTTATGTTATTTTCATCATGACCCCGCATTGATTTGCAATTGGATATTTAACTATT

Pel5' TGTCGGGCAGAATAAATCGGGTTGCAAGATGACCACGCCTGTGCCCCGCCGCACCAAGGA
Exc15 TGTCGGGCAGAATAAATCGGGTTGCAAGATGACCACGCCTGTGCCCCGCCGCACCAAGGA

Pel5' CATGATGGCACTGGGACTGGACTCCGACTCCGAGGACGACTTTAACACGCCATACCGACC
Exc15 CATGATGGCACTGGG-----ACTCCGACTCCGAGGACGACTTTAACACGCCATACCGACC

Pel5' ACGACAAGCGGCGGGGAGAACGAAAACAGCAGCCGGTGGCGTCTTTCCAAGTCCAAAC
Exc15 ACGACAAGCGGCGG-----

Alignment Data
[Exc 26 & P-element 3' end]

```
Pe13'      TTTATTAACTATTAAAGGCTTCATTTCAGCGCGCTTTGGATGT
Exc26      TTTATTAACTATTAAAGGCTTCATTTCAGCGCGCTTTGGATGT
          *****

Pe13'      TTTAAATTTTGAACCTTTGGTCACACTTGAATAAAAAATAAATTTAAACCCCGCA--TGAT
Exc26      TTTAAATTTTGAACCTTTGGTCACACTTGAATAAAAAATAAATTTAAACCCCGCACATGAT
          *****

Pe13'      GAAATAACATAAGGTGGTCCCGTCGAAAGCCGAAGCTTACCGAAGTATACACTTAAATTC
Exc26      GAAATAACATAAGGTGGTCCCGTCGATAGCCGAAGCTTACCGAAGTATACACTTAAATTC
          *****

Pe13'      AGTGCACGTTTGCTTGTTGAGAGGAAAGGTTGTGTGCGGACGAATTTTTTTTTGAAAACA
Exc26      AGTGCACGTTTGCTTGTTGAGAGGAAAGGTTGTGTGCGGACGAATTTTTTTTTGAAAACA
          *****

Pe13'      TTAACCCTTACGTGGAATAAAAAAAAATGAAACTAGTCGAATTCCCAATTCCTATTCAG
Exc26      TTAACCCTTACGTGGAATAAAAAAAAATGAAACTAGTCGAATTCCCAATTCCTATTCAG
          *****

Pe13'      AGTTCTCTTCTTGTATTCAATAATTACTTCTTGGCAGATTTTCAGTAGTTGCAG
Exc26      AGTTCTCTTCTTGTATTCAATAATTACTTCTTGGCAGATTTTCAGTAGTTGCAG
          *****
```

Alignment Data
[Exc 26 & P-element SV40 3'UTR]

```
SV40      CAGTACTCCGCTCGGAGGACAGTACTC
Exc26      CAGTACTCCGCTCGGAGGACAGTACTC
          *****

SV40      CGACCTGCAGGCATGCAAGCTTGGATCTGCGGCCGCGGTCTAGAAGGCCTAATTCTAGTA
Exc26      CGACCTGCAGGCATGCAAGCTTGGATCTGCGGCCGCGGTCTAGAAGGCCTAATTCTAGTA
          *****

SV40      TGTATGTAAGTTAATAAAAACCCATTTTTGCGGAAAGTAGATAAAAAAACATTTTTTTTT
Exc26      TGTATGTAAGTTAATAAAAACCCATTTTTGCGGAAAGTAGATAAAAAAACATTTTTTTTT
          *****

SV40      TTT
Exc26      TTT
          ***
```

Alignment Data
[Exc 26 & P-element Outward facing *Hsp70Bb*]

```
outHsp70      TTTGATGTATAGTGCCTTGACTAGAGATCATAATCAGCCATACCACA
Exc26         TTTGATGTATAGTGCCTTGACTAGAGATCATAATCAGCCATACCACA
*****

outHsp70      TTTGTAGAGGTTTTACTTGCTTTAAAAAACCTCCCACACCTCCCCCTGAACCTGAAACAT
Exc26         TTTGTAGAGGTTTTACTTGCTTTAAAAAACCTCCCACACCTCCCCCTGAACCTGAAACAT
*****

outHsp70      AAAATGAATGCAATTGTTGTTGTTAACTTGTTTATTGCAGCTTATAATGGTTACAAATAA
Exc26         AAAATGAATGCAATTGTTGTTGTTAACTTGTTTATTGCAGCTTATAATGGTTACAAATAA
*****

outHsp70      AGCAATAGCATCACAAATTTACAAATAAAGCATTTTTTTTTCACTGCATTCTAGTTGTGGT
Exc26         AGCAATAGCATCACAAATTTACAAATAAAGCATTTTTTTTTCACTGCATTCTAGTTGTGGT
*****

outHsp70      TTGTCCAAACTCATCAATGTATCTTATCATGTCTGGATCGGATCTTGCGGCCGCG-CTCG
Exc26         TTGTCCAAACTCATCAATGTATCTTATCATGTCTGGATC-----TGCGGCCGCGGCTCG
*****

outHsp70      ACCTGCAGCCAAGCTTTGCGTACTCGCAAATTATTA AAAAATAAAAACCTTTAAAAATAATTT
Exc26         ACCTGCAGCCAAGCTTTGGGTACTCGCAAATTATTA AAAAATAAAAACCTTTAAAAATAATTT
*****

outHsp70      CGTCTAATTAATATTATGAG
Exc26         CGTCTAATTAATATTATGAG
*****
```

XII. APPENDIX F: Excision 14



Figure F1. Absence of the *mini-white* gene of the P{GS:13084} allele Within the P-element, the *mini-white* gene, if present, which is a $\{w^+\}$ allele, gives the flies peach color eyes. When the different excision lines were created by imprecise P-element excision, all of the various lines had white eyes. This indicates that either the *mini-white* gene has either been hit to some degree as to make the gene nonfunctional or has been completely removed from the sequence. Without direct sequencing, Excision 14 may have portions of the *mini-white* gene still present in the 5'UTR or it may not have any of the sequence left in the genome.

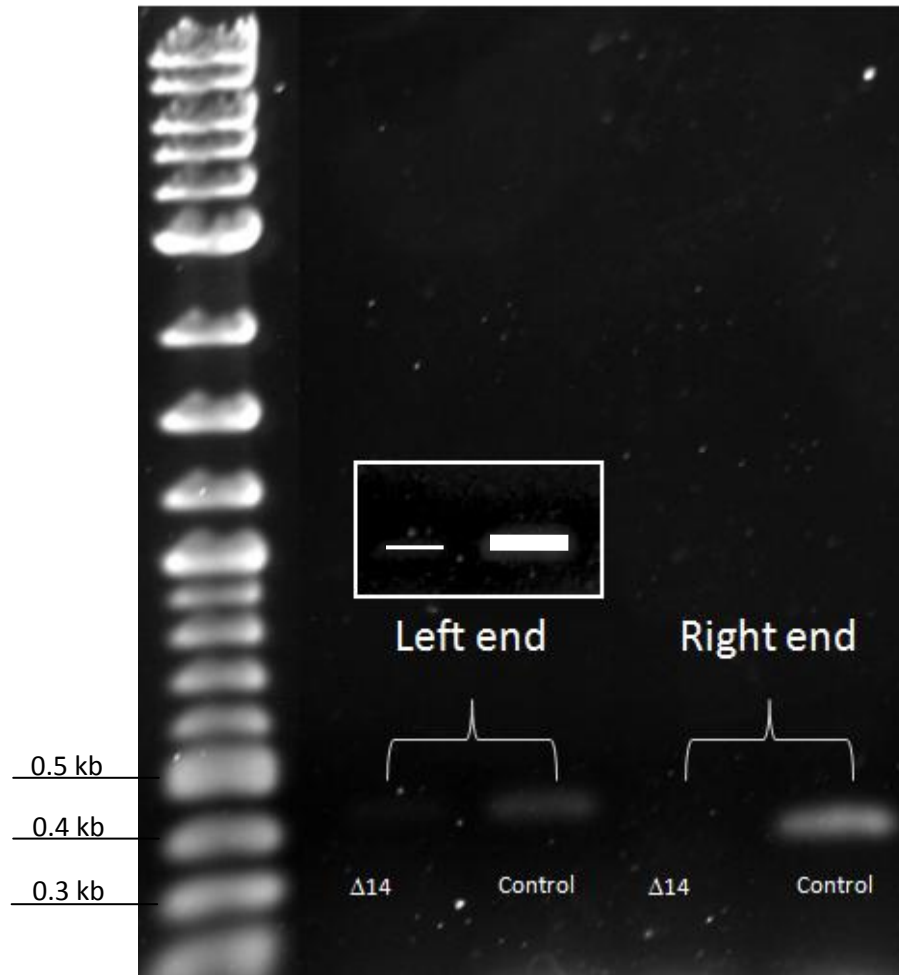


Figure F2. P{GS:13084} 5' and 3' ends PCR amplification DNA was extracted, using a phenol:chloroform extraction method, from males and females from, *FM7/yw; Δ14/Df(3R)AN6; pol* and the control, *yw; P{GS:13084}/AN6;pol*. The presence of the 3' end was tested through PCR amplification using the primers: 5'--CATCACTCTCCCTCACTCAAAG--3' and 5'--- CTCACTCAGACTCAATACGAC---3'; the presence of the 5' end was tested using the primers: 5'--CCTCGTTTGGACTTGAAAG--3' and 5'--- TCGTCCGCACACAACCTTTC---3'. The P-element, P{GS:13084}, was used as a positive control. Excision 14 appears to have the 3' (left) end of the P-element still present in the genome, albeit a faint positive band as shown. The box represents a dramatization of the difference between amplifications of the left end of the P-element in Excision 14 line and the control to show the weak positive outcome. On the other hand, the 5' (right) end did not amplify, indicating that the 5' end of the P{GS:13084} is not present in the 5'UTR of the *ald* gene.

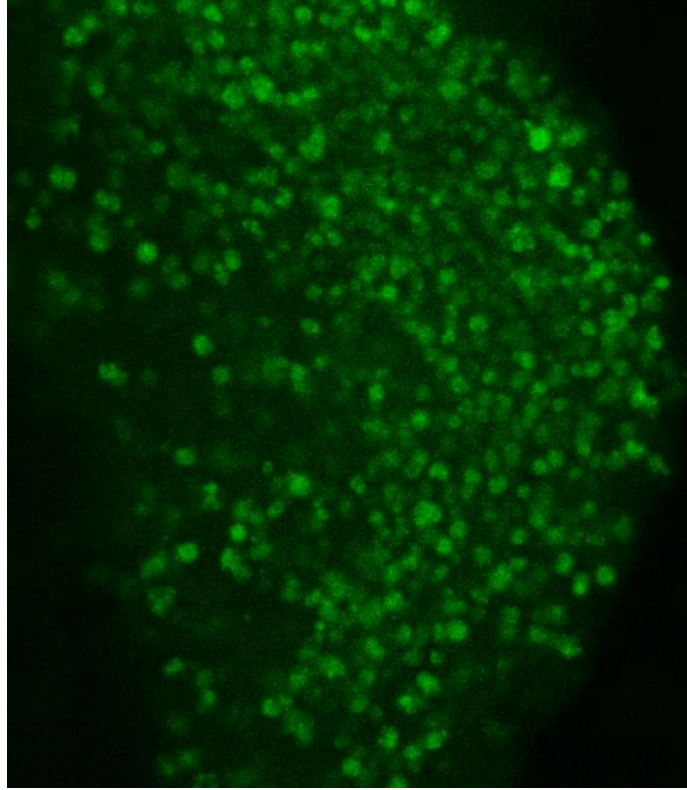


Figure F3. Heat-shocked GFP analysis of Excision 14 Females, *yw; P{nosGal4}/+; P{GS:13084}^{Δ14}/+; pol*, were collected, heated at 37°C for 1 hour, and allowed to recover for another hour. After recovery, the females were dissected, fixed and view with the confocal microscopy for the presence of *GFP*. Since the *GFP* gene is under the control of the *Hsp70Bb*, the *P{nosGal4}* can associate with the promoter and turn on transcription of the gene. The presence of Green Fluorescent Protein in the excision 14 line was evident in the stage 8-10 oocyte when viewed with the confocal microscope, indicating that the *GFP* gene portion is still present in the genome of the excision 14 line.

XIII. APPENDIX G: Raw Data

Progeny:	yw ♂	ypol minute ♀	B ♀	Bpol minute ♀	yw; ci ey ^R ♂	B; ci ey ^R ♀	yw; pol ♂	B; pol ♀	vfB ♂	vfBpol minute ♂	yw ♀	ypol minute ♀	vfB; pol ♂	yw; ci ey ^R ♀	vfB; ci ey ^R ♂	yw; pol ♀
	Oocyte:	X 4	X 4	X 4	X 0	X 0	X 44	X 44	0 4	0 4	XX 4	0 44	XX 0	0 0	XX 44	
Excisions	Normal Progeny				4-NDJ Only Progeny				X-NDJ Only Progeny				X & 4 Double NDJ Progeny			
1	105	0	114	0	3	3	9	6	1	0	6	0	1	2	1	2
2	547	38	441	22	3	1	14	16	30	3	40	4	3	1	0	1
4	26	2	31	3	0	0	1	5	0	0	0	0	0	0	0	11
5	313	3	363	4	5	11	4	9	18	5	30	4	6	0	0	0
6	91	3	85	3	4	7	15	8	21	0	29	0	12	2	0	9
11	299	11	265	18	3	11	20	26	59	17	56	7	15	19	1	1
13	63	6	46	2	2	0	2	5	5	2	11	1	3	5	0	0
14	148	5	216	0	1	10	17	20	19	0	14	1	2	3	2	7
15	120	7	135	3	1	1	0	5	7	2	6	0	2	1	2	5
17	421	7	392	7	3	1	5	8	33	2	34	2	3	5	0	1
18	474	10	437	8	2	4	10	8	44	4	26	3	7	4	0	0
20	333	0	362	3	16	7	13	20	24	0	19	0	7	3	5	13
21	568	11	511	16	1	2	6	8	41	3	52	1	2	1	1	1
22	406	16	397	12	3	8	7	8	26	3	26	1	1	3	0	1
23	187	5	228	1	2	8	1	9	38	0	36	0	9	7	2	0
25	120	6	207	0	3	1	3	2	2	0	2	0	0	0	0	0
26	452	11	449	6	2	3	8	6	23	1	39	2	5	0	1	1
29	147	17	120	2	6	4	11	6	27	2	22	0	16	5	7	10
30	475	23	481	13	9	19	3	26	26	6	30	2	8	7	0	1
31	159	1	159	4	0	2	1	1	8	0	13	0	4	1	0	0
34	136	5	132	8	0	0	1	4	7	0	11	1	0	0	3	0
35	168	0	168	0	6	7	8	5	20	0	28	0	5	1	4	7
36	231	2	238	0	12	10	21	22	42	0	37	1	6	9	5	8
38	680	22	568	16	6	10	18	13	20	6	29	5	8	5	2	2

Table G1. Raw counts for preliminary ald¹ cross The table shows the raw progeny counts from scoring the cross between females for each excision line FM7/yw; ald1/aldP{GS:1-3084}-excision; pol and to attached-XY, vfB; C(4)RM, ci ey^R (AD1) males.

Progeny:	y w ♂	y w pol minute ♂	B ♀	B pol minute ♀	y w; ci ey ^R ♂	B; ci ey ^R ♀	y w; pol ♂	B; pol ♀	v f B ♂	y f B pol minute ♂	y w ♀	y w pol minute ♂	v f B; pol ♂	y w; ci ey ^R ♀	v f B; ci ey ^R ♂	y w; pol ♀
	X 4	X 4	X 4	X 4	X 0	X 44	X 44	X 44	0 4	0 4	XX 4	XX 4	0 44	XX 0	0 0	XX 44
Excisions	Normal Progeny				4-NDI Only Progeny				X-NDI Only Progeny				X & 4 Double NDI Progeny			
1	1093	43	1149	36	14	41	36	63	71	2	42	1	23	10	1	0
4	1697	43	1929	76	36	60	61	115	90	6	92	7	28	27	1	1
14	879	44	1026	22	29	44	40	49	47	12	38	4	18	17	5	1
15	2019	43	2196	114	37	52	51	90	75	16	83	8	19	18	1	3
23	601	37	691	28	85	98	98	174	200	42	189	6	72	71	25	20
25	1041	1	1412	2	1	1	2	0	2	0	2	0	3	2	0	0
26	887	66	941	26	19	43	40	61	63	4	57	9	24	12	1	2
30	940	24	1120	43	19	30	46	58	62	9	40	5	12	12	0	2

Table G2. Raw counts for secondary Df(3R)/AN6 cross The table shows the raw progeny counts from scoring the cross between females for each excision line FM7/yw; Df(3R)/AN6/aldP{GS:1-3084}-excision; pol and to attached-XY, v f B; C(4)RM, ci ey^R (AD1) males.

XIV. Literature Cited

1. Theurkauf, W.E. and R.S. Hawley, *Meiotic spindle assembly in Drosophila females: behavior of nonexchange chromosomes and the effects of mutations in the nod kinesin-like protein*. J Cell Biol, 1992. **116**(5): p. 1167-80.
2. Gilliland, W.D., et al., *The multiple roles of mps1 in Drosophila female meiosis*. PLoS Genet, 2007. **3**(7): p. e113.
3. Hassold, T. and P. Hunt, *To err (meiotically) is human: the genesis of human aneuploidy*. Nat Rev Genet, 2001. **2**(4): p. 280-91.
4. Oliver, T.R., et al., *New insights into human nondisjunction of chromosome 21 in oocytes*. PLoS Genet, 2008. **4**(3): p. e1000033.
5. Page, S.L. and R.S. Hawley, *Chromosome choreography: the meiotic ballet*. Science, 2003. **301**(5634): p. 785-9.
6. Hawley, R.S., K.S. McKim, and T. Arbel, *Meiotic segregation in Drosophila melanogaster females: molecules, mechanisms, and myths*. Annu Rev Genet, 1993. **27**: p. 281-317.
7. Ashburner, M., K.G. Golic, and R.S. Hawley, *Drosophila : a laboratory handbook*. 2nd ed. 2005, Cold Spring Harbor, N.Y.: Cold Spring Harbor Laboratory Press. xxviii, 1409 p.
8. Lee, B. and A. Amon, *Meiosis: how to create a specialized cell cycle*. Curr Opin Cell Biol, 2001. **13**(6): p. 770-7.
9. Lee, B.H. and A. Amon, *Polo kinase--meiotic cell cycle coordinator*. Cell Cycle, 2003. **2**(5): p. 400-2.
10. Marston, A.L. and A. Amon, *Meiosis: cell-cycle controls shuffle and deal*. Nat Rev Mol Cell Biol, 2004. **5**(12): p. 983-97.
11. McKim, K.S., J.K. Jang, and E.A. Manheim, *Meiotic recombination and chromosome segregation in Drosophila females*. Annu Rev Genet, 2002. **36**: p. 205-32.
12. Uhlmann, F., *Chromosome cohesion and segregation in mitosis and meiosis*. Curr Opin Cell Biol, 2001. **13**(6): p. 754-61.
13. Lamb, N.E., S.L. Sherman, and T.J. Hassold, *Effect of meiotic recombination on the production of aneuploid gametes in humans*. Cytogenet Genome Res, 2005. **111**(3-4): p. 250-5.

14. Sekelsky, J.J., et al., *The Drosophila meiotic recombination gene mei-9 encodes a homologue of the yeast excision repair protein Rad1*. Genetics, 1995. **141**(2): p. 619-27.
15. Zitron, A.E. and R.S. Hawley, *The genetic analysis of distributive segregation in Drosophila melanogaster. I. Isolation and characterization of Aberrant X segregation (Axs), a mutation defective in chromosome partner choice*. Genetics, 1989. **122**(4): p. 801-21.
16. Hawley, R.S., et al., *There are two mechanisms of achiasmate segregation in Drosophila females, one of which requires heterochromatic homology*. Dev Genet, 1992. **13**(6): p. 440-67.
17. Hawley, R.S. and W.E. Theurkauf, *Requiem for distributive segregation: achiasmate segregation in Drosophila females*. Trends Genet, 1993. **9**(9): p. 310-7.
18. Whyte, W.L., et al., *The genetic analysis of achiasmate segregation in Drosophila melanogaster. III. The wild-type product of the Axs gene is required for the meiotic segregation of achiasmate homologs*. Genetics, 1993. **134**(3): p. 825-35.
19. Zhang, P. and R.S. Hawley, *The genetic analysis of distributive segregation in Drosophila melanogaster. II. Further genetic analysis of the nod locus*. Genetics, 1990. **125**(1): p. 115-27.
20. Kops, G.J., A.T. Saurin, and P. Meraldi, *Finding the middle ground: how kinetochores power chromosome congression*. Cell Mol Life Sci, 2010. **67**(13): p. 2145-61.
21. Matthies, H.J., et al., *Mutations in the alpha-tubulin 67C gene specifically impair achiasmate segregation in Drosophila melanogaster*. J Cell Biol, 1999. **147**(6): p. 1137-44.
22. Cui, W., et al., *Drosophila Nod protein binds preferentially to the plus ends of microtubules and promotes microtubule polymerization in vitro*. Mol Biol Cell, 2005. **16**(11): p. 5400-9.
23. Brunet, S., et al., *Kinetochore fibers are not involved in the formation of the first meiotic spindle in mouse oocytes, but control the exit from the first meiotic M phase*. J Cell Biol, 1999. **146**(1): p. 1-12.
24. Wignall, S.M. and A.M. Villeneuve, *Lateral microtubule bundles promote chromosome alignment during acentrosomal oocyte meiosis*. Nat Cell Biol, 2009. **11**(7): p. 839-44.
25. Hodges, C.A., et al., *Experimental evidence that changes in oocyte growth influence meiotic chromosome segregation*. Hum Reprod, 2002. **17**(5): p. 1171-80.
26. Wargacki, M.M., et al., *Kip3, the yeast kinesin-8, is required for clustering of kinetochores at metaphase*. Cell Cycle, 2010. **9**(13).

27. Gardner, M.K., et al., *Chromosome congression by Kinesin-5 motor-mediated disassembly of longer kinetochore microtubules*. Cell, 2008. **135**(5): p. 894-906.
28. Gardner, M.K., D.J. Odde, and K. Bloom, *Kinesin-8 molecular motors: putting the brakes on chromosome oscillations*. Trends Cell Biol, 2008. **18**(7): p. 307-10.
29. Savoian, M.S. and D.M. Glover, *Drosophila Klp67A binds prophase kinetochores to subsequently regulate congression and spindle length*. J Cell Sci, 2010. **123**(Pt 5): p. 767-76.
30. Gilliland, W.D., et al., *Congression of achiasmate chromosomes to the metaphase plate in Drosophila melanogaster oocytes*. Dev Biol, 2009. **325**(1): p. 122-8.
31. King, R.C., *Ovarian development in Drosophila melanogaster*. 1970, New York,: Academic Press. x, 227 p.
32. Spradling, A.C., *Developmental genetics of oogenesis*. In: Bate, M. and A.M. Arias, editors. *The development of Drosophila melanogaster*. 1994, Cold Spring Harbor, N.Y.: Cold Spring Harbor Laboratory Press. 1-71 p.
33. Xiang, Y., et al., *The inhibition of polo kinase by matrimony maintains G2 arrest in the meiotic cell cycle*. PLoS Biol, 2007. **5**(12): p. e323.
34. Von Stetina, J.R., et al., *alpha-Endosulfine is a conserved protein required for oocyte meiotic maturation in Drosophila*. Development, 2008. **135**(22): p. 3697-706.
35. Sullivan, W., M. Ashburner, and R.S. Hawley, *Drosophila protocols*. 2000, Cold Spring Harbor, N.Y.: Cold Spring Harbor Laboratory Press. xiv, 697 p.
36. Orr-Weaver, T.L., *Meiosis in Drosophila: seeing is believing*. Proc Natl Acad Sci U S A, 1995. **92**(23): p. 10443-9.
37. Lindsley, D.L. and L. Sandler, *The genetic analysis of meiosis in female Drosophila melanogaster*. Philos Trans R Soc Lond B Biol Sci, 1977. **277**(955): p. 295-312.
38. Afshar, K., et al., *DNA binding and meiotic chromosomal localization of the Drosophila nod kinesin-like protein*. Cell, 1995. **81**(1): p. 129-38.
39. Puro, J., and S. Nokkala, *Meiotic segregation of chromosomes in Drosophila melanogaster oocytes: a cytological approach*. Chromosoma, 1977. **63**: p. 273-8.
40. Dernburg, A.F., J.W. Sedat, and R.S. Hawley, *Direct evidence of a role for heterochromatin in meiotic chromosome segregation*. Cell, 1996. **86**(1): p. 135-46.
41. Hughes, S.E., et al., *Heterochromatic threads connect oscillating chromosomes during prometaphase I in Drosophila oocytes*. PLoS Genet, 2009. **5**(1): p. e1000348.

42. O'Tousa, J., *Meiotic chromosome behavior influenced by mutation-altered disjunction in Drosophila melanogaster females*. Genetics, 1982. **102**(3): p. 503-24.
43. Fischer, M.G., et al., *The mitotic arrest in response to hypoxia and of polar bodies during early embryogenesis requires Drosophila Mps1*. Curr Biol, 2004. **14**(22): p. 2019-24.
44. Fisk, H.A., C.P. Mattison, and M. Winey, *A field guide to the Mps1 family of protein kinases*. Cell Cycle, 2004. **3**(4): p. 439-42.
45. Kulukian, A., J.S. Han, and D.W. Cleveland, *Unattached kinetochores catalyze production of an anaphase inhibitor that requires a Mad2 template to prime Cdc20 for BubR1 binding*. Dev Cell, 2009. **16**(1): p. 105-17.
46. Malmanche, N., et al., *Drosophila BubR1 is essential for meiotic sister-chromatid cohesion and maintenance of synaptonemal complex*. Curr Biol, 2007. **17**(17): p. 1489-97.
47. Gilliland, W.D., et al., *Hypoxia transiently sequesters mps1 and polo to collagenase-sensitive filaments in Drosophila prometaphase oocytes*. PLoS One, 2009. **4**(10): p. e7544.
48. Gilliland, W.D., S.M. Wayson, and R.S. Hawley, *The meiotic defects of mutants in the Drosophila mps1 gene reveal a critical role of Mps1 in the segregation of achiasmate homologs*. Curr Biol, 2005. **15**(7): p. 672-7.
49. Toba, G., et al., *The gene search system. A method for efficient detection and rapid molecular identification of genes in Drosophila melanogaster*. Genetics, 1999. **151**(2): p. 725-37.
50. Xiang, Y. and R.S. Hawley, *The mechanism of secondary nondisjunction in Drosophila melanogaster females*. Genetics, 2006. **174**(1): p. 67-78.
51. Dernburg AF (2000) *In Situ hybridization to somatic chromosomes*. Sullivan W, Ashburner M, Hawley RS, eds (2000) *Drosophila protocols*. Cold Spring Harbor (New York): Cold Spring Harbor Laboratory Press. pp 25–55.
52. Ferree, P.M. and D.A. Barbash, *Species-specific heterochromatin prevents mitotic chromosome segregation to cause hybrid lethality in Drosophila*. PLoS Biol, 2009. **7**(10): p. e1000234.
53. Zeng, Y., et al., *Statistical analysis of nondisjunction assays in Drosophila*. Genetics, 2010. **186**(2): p. 505-13.
54. O'Hare, K. and G.M. Rubin, *Structures of P transposable elements and their sites of insertion and excision in the Drosophila melanogaster genome*. Cell, 1983. **34**(1): p. 25-35.